Characterisation of articular cartilage by micro-beam Raman spectroscopy

MARK FIELDS

June 2016

A thesis presented to the University College London in partial fulfilment of the requirements for the degree of Doctor of Philosophy

Department of Chemistry

University College London

Declaration

I, Mark Fields confirm that the work presented in this thesis is my own. Where information has been derived from other sources, I confirm that this has been indicated in the thesis.

Abstract

The Raman spectrum of cartilage contains detailed information on the composition and structural state of the biochemical components of the tissue. The advantage of Raman spectroscopy over traditional methods of chemical analysis such as chemical assay and histology, is the ability to interrogate tissue composition of samples without the need for addition of markers and sample manipulation.

This work first presents reference spectra for collagen and proteoglycan that are the main contributors to the Raman signal of cartilage tissue. Further work involving D_2O/H_2O exchange investigated the exchangeable hydrogen atoms that contribute to the spectrum.

Micro-Raman spectroscopic mapping was used to examine the distribution of proteoglycan, as a function of depth within tissue samples, from the cartilage surface to the cartilage-bone interface, comparing data for specimens obtained from a young (9 years old) and a more mature individual (62 years old). We showed that the proteoglycan increases as a function of depth and was greater in the tissue from the younger specimen, using peaks from the reference spectrum of proteoglycan to demonstrate this.

We then examined the thermal degradation of cartilage using *in situ* Raman spectroscopy during heating. Previous data had been interpreted in terms of a denaturation event. Our results indicate, that protonation of carboxylic acid groups occurs in freeze-dried samples of articular cartilage and collagen heated to 120°C. Thermogravimetric analysis also revealed hydrous component remaining in freeze-dried cartilage. They provide a new interpretation of the structural changes that occur during heating.

Contents

List of figures

List of tables

Glossary of abbreviations and terms

A.C.	Articular cartilage
CBI	Cartilage-bone interface
CCD	Charge-coupled device
Collagen^{f}	Collagen extracted from human articular
CS	Chondroitin sulphate
CSU	Cartilage surface
C4S	Chondroitin-4-sulphate
C6S	Chondroitin-6-sulphate
DSC	Differential scanning calorimetry
ECM	Extracellular matrix
E.I.C	Electric ion current
GAG	Glycosaminoglycan
GdHCl	Guanidine hydrochloride
HA	Hyaluronan
KS	Keratan sulphate
N.A.	Numerical aperture
RH	Relative humidity

OA	Osteoarthritis
MS	Mass spectrometry
TGA	Thermogravimetric analysis

Terms

kDa	Kilodaltons
Mins	Minutes
xg	Acceleration caused by gravity
ν	Stretching (mode)
δ	Deformation (bending)
γw	Wagging
γr	Rocking
γt	Twisting
as	Asymmetric
s	Symmetric

Acknowledgements

I would like to thank Professor Paul F. McMillan for his academic tutelage and his teaching in the field of spectroscopy. I would like to thank Dr. Jayesh Dudhia for his teachings in the field of cartilage and his assistance with some of the experimental work.

I thank Dr Steven Firth (UCL) and Mr. Rafiqul (RVC), who were of technical support and encouragement during parts of the research. I also thank my colleagues from the McMillan group for their support. As well as Dr. Chris Howard and Dr. Brownsword for the provision of the Raman mapping equipment.

The completion of this thesis was facilitated by encouragement of my family and friends. Thanks to my immediate family, whom despite the distance, were never far away. To the Gray, Reynolds and Lewis families. To Dr. Chris Reynolds, Dr. Rachael Hazael and Martin Lopez for help with the documentation of this thesis. To all my friends of EM, RVC, and UCL.

1.1 Molecular vibrations in complex molecules

By vibrational modes, this means changes in the bond distances and/or angles of molecules. A vibrational mode is said to represent a synchronised change in bond angle or bond distances in parts of a molecule, and the associated energies of these changes in a molecule cause frequency shifts in scattered light (Schrader, 2007). Normal vibrational modes represent an independent synchronous motion of atoms or groups of atoms that may be induced without causing excitation in other normal modes of the same molecule. Hence they are isolated in their energy from other normal modes of vibrations within a similar molecule. They are also isolated in their appearance in Raman and Infra-red (IR) spectra- they occur within specific frequency ranges. These normal modes of vibration are used to show the presence of different functional groups in molecules under analysis. For example, the Raman spectra of molecules containing a carbonyl group show a distinct band at 1600-1700 cm^{-1} in their spectra as a result of the vibrational mode of this functional group. Thus normal vibrational modes are useful tool for structural analysis of unknown compounds and the intensity of the peaks that they produce in a spectrum can be used to infer the quantification of the associated molecular group(s).

Normal vibrational modes in spectra of molecules are assigned to functional groups with libraries of spectra that show empirical data. For example those by Bellamy and Di Li-Vien (Bellamy, 1958; D Li-Ven, 1991) for simple organic molecules and Anthony Tu (Tu, 1982) for biological molecules. For the researcher interested in investigating structure of a particular sample the scientific literature can be used to provide empirical data for the components of which a sample is made up from.

1.2 Vibrational spectroscopies in biological applications

Raman and IR spectroscopy can be used to investigate the molecular composition of samples, which in turn can be used to make inferences of pathological changes in tissues (Hanlon, et al., 2000; Haka, et al., 2005; Kast, et al., 2014).

IR spectroscopy is an analytical technique that involves the probing of molecular structure by passing light from the IR region of the electromagnetic spectrum. The bonds of molecules are found to absorb light of this region in the spectrum. An absorption spectrum can therefore be used to reveal the structure of a sample under investigation.

Raman spectroscopy involves monochromatic light in the visible region of the electromagnetic spectrum, which is scattered from molecules with a change in energy compared to the incident energy. This technique involves the analysis of inelastically scattered light to detect the structure of molecules interacting with the incident light. There must be a change in the polarizability of the molecular group involved in a vibration for a peak to occur in a Raman spectrum.

Until recently IR spectroscopy remained the most prevalent technique for routine analysis of chemicals. However, now Raman spectroscopy is increasingly being developed for use in biological applications because of the low signal contribution from molecular water, which is ubiquitous in biological samples. The technique is also becoming more sensitive with improvements to the detectors used. In the 1960's Raman spectroscopy experiments were carried out on simple biomolecules such as sugars (Bansil, et al., 1978; Barrett and Peticolas, 1979), collagens (Frushour and Koenig, 1975) and more recently complex systems and tissues (Haka, et al., 2005; Esmonde-White, et al., 2009; Bonnier, et al.,

2011; Gamsjaeger, et al., 2014). It can be used to detect cancers (Haka, et al., 2005) and pathology of other diseases from detectable changes in the composition of tissue samples, for example, in brain tumours (Ji, et al., 2013).

1.3 Raman spectroscopy for pathological studies and disease diagnosis

In pathology there is a significant need to investigate the structure and molecular changes in tissue samples. Histopathology is usually used for this, where sections of tissue are stained with dyes to show the presence/absence of molecules. For example, Safranin-O is used as a stain for proteoglycan molecules in articular cartilage tissue sections. The loss of these molecules can be revealed by staining and this technique is used to show the onset of osteoarthritis in biopsy samples. This technique is applied in laboratory experiments as well as on biopsies for clinical examinations. There are drawbacks to the use of histopathology: it is invasive and there is error due to inter-sample variability. Raman spectroscopy is a novel application in this field (Esmonde-White, et al., 2011), it enables analysis of cartilage tissue non-invasively. This research project aims to develop further the application of this technology, for the interest of clinical and for basic research.

Previously, in this research group, Raman spectroscopy was used to investigate changes in the composition of articular cartilage samples of different disease grade (according to Mankin scoring (Mankin and Thrasher, 1975))(Draper, 2009). This study demonstrated that a peak at 1063 cm^{-1} (symmetric stretch of sulphate vibrational mode) could be used to detect the decreasing amount of aggrecan, associated with disease grade in articular cartilage. This lead to a patent for the characterization of osteoarthritis in cartilage samples and consequently the Raman technique may be applied to patients during *in vivo* studies *via* an arthroscopic probe (Nunn, et al., 2013). These studies focused on samples of

specific disease grade as opposed to the samples studied in this thesis, which were of unaffected (healthy) tissue.

1.4 Overview of work described in this thesis

The work described in this thesis focused on the use of Raman spectroscopy to investigate the microstructure of articular cartilage and the characterization of its major molecular components. Chapter 2 of this thesis describes the experimental methods used, including sample preparation, details of the Raman spectroscopic analysis and data reduction techniques.

The intensity and profile of Raman peaks provide indications of the relative amounts of chemical species present in the sample, as well as their bonding environments (Schrader, 2007). The first aim of this research was to study the Raman spectra of the major collagen and proteoglycan constituents of human articular cartilage (Chapter 3). Firstly, we extracted the soluble and insoluble components of articular cartilage. The soluble component was taken as proteoglycan (which is mostly aggrecan) and the insoluble component taken as collagen (mostly collagen type II). This enabled us to characterize the Raman signal from these principal components of articular cartilage.

One particular aspect of this work was to examine the features related to the stretching vibrations of sulphate units ($-OSO_3^-$) contained within the glycosaminoglycan (GAG) component of proteoglycan. This feature is being developed as a marker to diagnose early stage cartilage disease (Draper, 2009; Dudhia, et al., 2010; Nunn, et al., 2013). Investigations of articular cartilage in D_2O and H_2O were also performed; the former to investigate bands which resort from exchangeable hydrogen bonds in the spectrum of cartilage and the latter to investigate the changes in the spectrum as a function of hydration.

Articular cartilage is known to be inhomogeneous in both its internal morphology and the distribution of its molecular components throughout the tissue (Muir, et al., 1970; Ghadially, 1983). In particular, there is a varying distribution of the collagen and aggrecan (the main proteoglycan in cartilage) with depth from the synovial surface to the cartilage-bone interface cross-section. Chapter 4 shows data pertaining to the distribution of proteoglycan in articular cartilage by acquiring spectra systematically along this depth. For this work tissue sections like those sliced for histopathology were assessed for compositional changes with a Raman mapping instrument. This was carried out for two samples of different age groups, a younger specimen (9 years old) and a more mature specimen (62 years old).

Chapter 5 describes high temperature studies of articular cartilage and collagen. Evidence from freeze-dried collagen samples suggests that there is an irreversible change in structure upon heating to 150-200°C)(Miles and Ghelashvili, 1999). We were able, through the use of Raman spectroscopy, to demonstrate the process of peptide bond dissociation in collagen of dehydrated articular cartilage in this temperature range. We also observed evidence for the presence of remnant water within the freeze-dried cartilage. Chapter 6, finally, describes a study of articular cartilage tissue at high and low levels of hydration.

1.5 Articular cartilage and its constitution

Three types of cartilage are typically described, hyaline, elastic and fibrocartilage. Articular cartilage is an example of hyaline cartilage that constitutes a tissue of around 1-10 mm in thickness, which is found at the extremities of the bones where they meet within a synovial capsule (Hall, 2005). Its main function is to provide a frictionless interface between

the bones and to dissipate load during locomotion. It comprises a solid extracellular matrix (ECM) and a fluid (water) phase. Chondrocytes are the only type of cell found in articular cartilage and they are responsible for the production and homeostasis of the ECM. Table 1.1 shows the nature and relative abundance of the main constituents of articular cartilage tissue.

Table 1.1 The main components of articular cartilage

Component of Articular Cartilage (A.C.)	Dry weight of A.C. (%)	Volume of A.C. (%)	Reference
Water		60-80	(Mow, et al., 1992)
Collagen Type II Collagen type IX and XI, X	40-90 <2%		(Muir, et al., 1970)
Proteoglycan aggregates	10-30		(Muir, et al., 1970)
Chondrocytes		5%	(Mow, et al., 1992)

1.5.1 The role of water in articular cartilage tissue

By volume, water is always the most significant component and it plays a central role in the biomechanical properties of articular cartilage. Water absorption into the tissue is influenced mainly by proteoglycan molecules which are trapped within the collagen fibre framework of the ECM. The most abundant proteoglycan of articular cartilage is aggrecan (Hardingham, et al., 1986). This proteoglycan contains poly-anionic GAG molecules which draw in salt ions from the synovial fluid and this results in a high osmotic pressure in the interstices of the ECM. The compartmentalisation of the ionic content in the tissue ECM results in a Gibbs-Donnan equilibrium (Donnan, 1924), which is responsible for the high swelling pressure of articular cartilage.

Collagen fibres have a less pronounced association with water. When the tissue is load-

bearing, water is exuded out of the interstices of the ECM, and in turn, the affinity for the GAG molecules to water increases (due to an increasing osmotic pressure) (Mow, et al., 1992). The high osmotic pressure causes the tissue to return to its original shape when the cartilage is unloaded and the high tensile property of collagen resists the expansion of the ECM. Hence water is predominantly associated with aggrecan molecules or found in the interstices of the ECM as a bulk component.

In the final study reported in this thesis we investigate hydration of articular cartilage by Raman spectroscopy. In Raman spectroscopy, the stretching vibrational modes that undergo hydrogen bonding with water appear at a lower frequency compared to stretching modes that are not involved in hydrogen bonding (Zhang, et al., 2011), this is because of a reduction in the force constant between a given bond upon engagement of hydrogen bonding to water. Whereas bending modes appear at higher frequency when involved in hydrogen bonding compared to non-hydrogen bonded bending modes, since there is a decrease in effective mass of a hydrogen bonded atom. Also, the microenvironment of the functional groups that produce these vibrational modes may change upon hydration, causing vibrational modes to appear different in the Raman spectra. Hence Raman spectroscopy provides structural information pertaining to association of molecular groups with water.

1.5.2 Collagen

The family of collagen macromolecules contains a triple-helical polypeptide structure, based on a similar primary sequence (Vanderrest and Garrone, 1991). Collagens are trimeric proteins formed from the combination of one or more gene products, to form homo- or hetero- trimers. The common feature of the collagen primary sequence in all collagen gene products is the repetition of a Gly–X-Y sequence, where X and Y are either Pro or Hyp (Miller,

1976).

The collagen in articular cartilage is mainly collagen type II, which is a fibrillar collagen made of homotrimer of α(II) chains (Eyre, 2002). Fibrillar collagens form from the cleavage of the N- and C- propeptides to produce a tropocollagen molecule, the most basic unit of the collagen that occurs in the polymerised form. Tropocollagens (of 300 nm length, 1.5 nm width) are polymerised extracellularly by the formation of cross-links between lysine and hydroxylysine residues, leading to the assembly of a collagen fibril (Figure 1.1). Bundles of these collagen fibrils (of 30-100 nm) are found within the ECM of articular cartilage, these bundles are called collagen fibres and they vary in length from between to 1-20 μm thick in mammals (Ushiki, 2002).

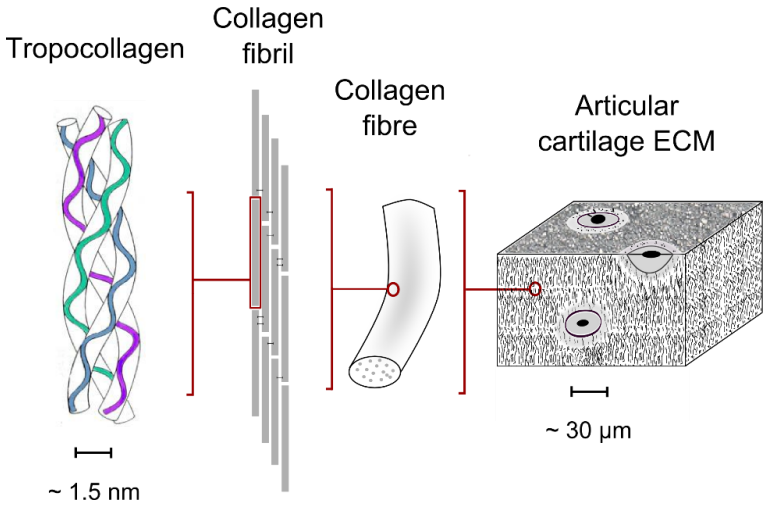

Figure 1.1 Hierarchical structure of a fibrillar collagen such as collagen type II. The spontaneous assembly of the a(II) chains into larger fibrils and fibres in cartilage is shown from left to right.

Most of the collagen in articular cartilage is collagen type II (Eyre, 2002), although collagen types XI, IX and X are also present. The amino acid compositions of collagen type II and III are shown in tables 1.2 and 1.3, for comparison.

Table 1.2 Amino acid composition of human collagen type II. The total number of amino acids is 1487, with a molecular weight 141,785.3 Da (Leinonen, et al., 2004).

Amino acid	% composition	Amino acid	% composition
Glycine	27.3	Threonine	3.0
Proline	18.2	Valine	2.6
Alanine	9.0	Isoleucine	2.3
Arginine	4.8	Asparagine	2.2
Glutamine	4.0	Cysteine	1.3
Glutamic acid	5.3	Phenylalanine	1.7
Lysine	4.5	Methionine	1.1
Aspartame	4.2	Tyrosine	0.7
Leucine	3.8	Tryptophan	0.5
Serine	3.2	Histidine	0.5

Table 1.3 Amino acid composition of human collagen type III. The total number of amino acids is 690, with a molecular weight of 66,157.9 Da (Leinonen, et al., 2004).

Amino acid	% composition	Amino acid	% composition
Glycine	28.2	Glutamic acid	5.0
Proline	19.2	Tyrosine	1.0
Alanine	7.8	Arginine	4.1
Lysine	4.2	Phenylalanine	1.6
Leucine	3.3	Asparagine	3.8
Serine	5.0	Aspartame	2.8
Isoleucine	2.5	Methionine	1.2
Valine	2.5	Histidine	1.0
Threonine	2.1	Tryptophan	0.5
Glutamine	2.9	Cysteine	1.5

Several reports of the Raman spectra of fibrillar collagens can be found in the literature, beginning in the 1970's shortly after the advent of laser Raman techniques (Frushour and Koenig, 1975; Dehring, et al., 2006; Janko, et al., 2010; Zhang, et al., 2011). The Raman spectra of collagens are expected to contain identifiable contributions from the side chains of the constituent amino acids, as well as significant contributions from the peptide bonds that link the amino acids together. Frushour and Koenig (1975) demonstrated that the Raman spectrum of a mixture of the free amino acids (found in collagen) can be used to assign the spectrum of the protein macromolecule. Also, the free amino acids exhibit characteristic vibrational modes of the carboxylate and carboxylic acid groups at difference levels of pH. Vibrational modes that result from amide bonds were not present in the spectra of the constituent amino acids but they appear in the spectrum of the whole protein, as the amide I (1650 cm^{-1}) and amide III (1240 cm^{-1}) bands. Owing to the presence of cross-links of collagen one would expect there to be a degree of contribution from these constituents, however, these have not been reported in work to date (Frushour and Koenig, 1975; Dehring, et al., 2006; Janko, et al., 2010; Zhang, et al., 2011). Essentially the Raman spectrum of collagen reflects the most abundant molecular components within its structure.

More specifically, Raman spectroscopy has been used to study collagen type II extracted from the cornea of mice, although the spectra reported exhibit a low signal-to-noise ratio (Dehring, et al., 2006). There is also a report of a comparative study of Raman spectra obtained from collagen type I and IV (Nguyen, et al., 2012). To our knowledge there are no reports of Raman spectra of collagen type II from human articular cartilage. Also, these collagens are essential collagens of articular cartilage tissue. In chapter 3 we use Raman spectroscopy to study samples of collagen types II and III of human origin for comparison.

1.5.3 Aggrecan

The second most abundant molecular component of articular cartilage by dry weight is aggrecan. Aggrecan belongs to a family of proteins called proteoglycans - a group of protein molecules that are highly glycosylated forming GAGs that are critically important in cartilage biochemistry (Dudhia, 2005). As well as aggrecan, articular cartilage contains other proteoglycans such as decorin, lumican, biglycan and fibromodulin (Hardingham, et al., 1986). However, aggrecan makes up 50-85% of all of the proteoglycans in articular cartilage (Mow, et al., 1992), depending on the origin and age. The amino acid composition of the protein core of this molecule is shown in Table 1.4.

Table 1.4 Amino acid composition of human aggrecan core protein. It contains 2,415 amino acid residues with a molecular weight of 250,193.1 Da (Leinonen, et al., 2004).

Amino acid	% composition	Amino acid	% composition
Serine	12.3	Arginine	3.3
Glycine	12.1	Phenylalanine	2.8
Glutamic acid	11.1	Glutamine	2.5
Proline	9.0	Tyrosine	2.0
Threonine	8.2	Histidine	1.4
Valine	7.7	Cysteine	1.4
Leucine	7.4	Lysine	1.2
Alanine	6.9	Asparagine	1.2
Aspartame	4.5	Tryptophan	1.0
Isoleucine	3.4	Methionine	0.5

Its main feature is an extended linear region that is dedicated to the attachment of GAG chains (Dudhia, 2005). Most of these chains are chondroitin sulphate (CS) (Figure 1.2) although there are significant amounts of keratan sulphate (KS) chains (Figure 1.2); present both here and elsewhere in the protein core (Figure 1.2). In addition, at the N-terminus there are two globular domains (termed G1 and G2), the G1 domain binds non-covalently with hyaluronan (HA), this binding is stabilised by a companion protein termed a proteoglycan

link protein, which contains 345 amino acids (Dudhia, 2005). The protein content of aggrecan is 7%, the CS content is 87 % and that of KS is around 6%, as was determined by chemical analysis of hexosamine, hexuronic acid and amino acid content (Hascall and Sajdera, 1970). Hence it is expected that the Raman spectrum of aggrecan contains contribution from mainly the CS component with some KS, and some protein component too.

The association of multiple aggrecan molecules per HA chain enables aggregation levels that can reach 22.5 million Daltons (Kimura, 1986).

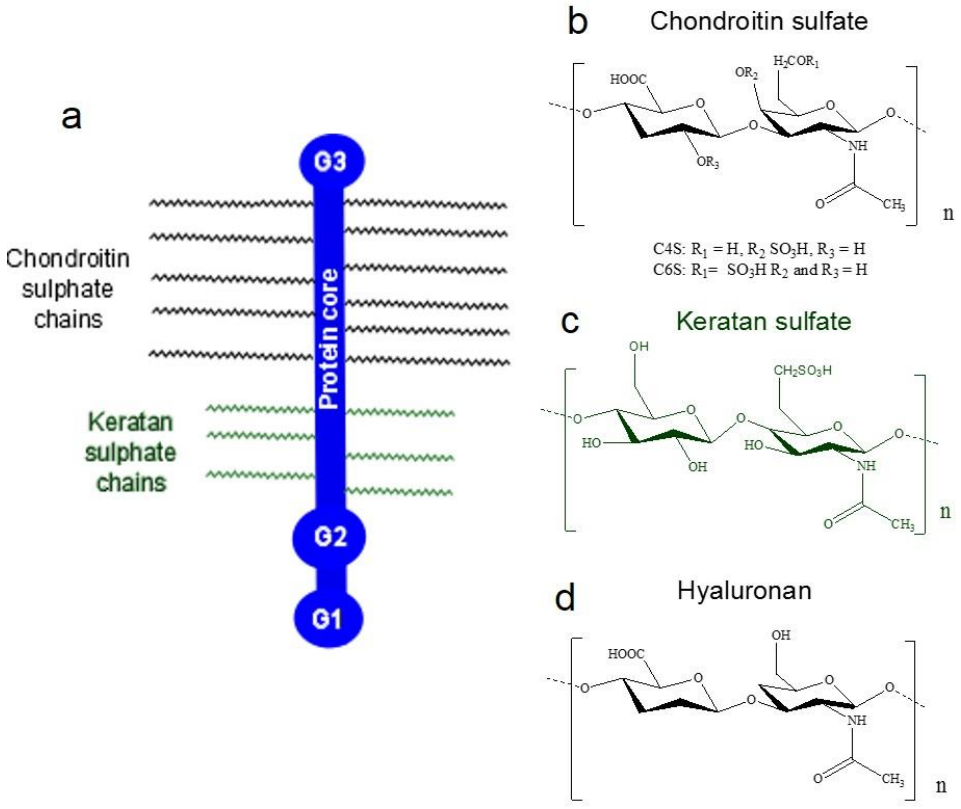

Figure 1.2 Schematic of aggrecan monomer and bound GAGs. ***a)*** *It comprises a protein core, KS and CS chains. Disaccharide repeat units of the GAG's;* ***b),*** *Chondroitin-4-Sulfate (CS4) and Chondroitin-6-sulfate (C6S),* ***c)*** *Keratan sulfate* ***d)*** *Hyaluronan. "n" in each disaccharide represents the repeat unit number.*

KS and CS are polymers of disaccharide repeat units containing either galactosamine

or glucosamine (Jeanloz, 1970). Each aggrecan monomer contains around 110 CS chains in humans with 10 – 20 disaccharides in each chain. Whereas there are about 60 KS chains that are around 5-15 kDa, aggrecan also contains a variable number of O- and N-linked oligosaccharides (Kiani, et al., 2002).

In aggrecan there may be four types of CS; non-sulphated, disulphated, and two mono-sulphated types (chondroitin-4-sulphate (C4S) and chondroitin-6-sulfate (C6S)), C4S and C6S are sulphated at the oxygen attached to the fourth and sixth carbon of galactosamine, respectively (Figure 1.2). The relative amounts of C4S and C6S are subequal in tissue of young humans (<10 years); at up to 20 years the amount of C6S increases and the amount of C4S decreases, these then reach a plateau and the ratio becomes ~80 C6S and ~20 C4S at ages >20 years (Bayliss, et al., 1999).

The Raman spectrum of aggrecan contains a significant contribution from the CS component (Ellis, et al., 2009). Cabassi *et al.* were the first to investigate the structure of CS using Raman spectroscopy (both C6S and C4S were studied using an extraction method reported by Roden *et al.* (1972)) (Cabassi, et al., 1978). They demonstrated that the most significant peak in the Raman spectrum is due to the symmetric stretching vibration of the sulphate S-O bonds of $-OSO_3H$ (at 1065 cm^{-1} for C6S and 1067 cm^{-1} for C4S). Bansil *et al.* published similar results for C4S and C6S, as well as HA (Bansil, et al., 1978). Bansil *et al.* (1978) also noted that the sulphate vibrational peak in C6S was less broad than that for C4S and suggested that this occurred because the sulphate unit is in an axial position, relative to the pyranose ring to which it is bound. This results in greater intramolecular interactions between the sulphate group and the pyranose ring in comparison with C4S which is in an equatorial position and therefore the sulphate groups interacts less with the pyranose ring.

The S-O stretching modes of the $-OSO_3H$ group are distinctive. Figure 1.3 overleaf

depicts the bonding arrangement for these units, including possibilities for the proton switching associated with the O^- charged group.

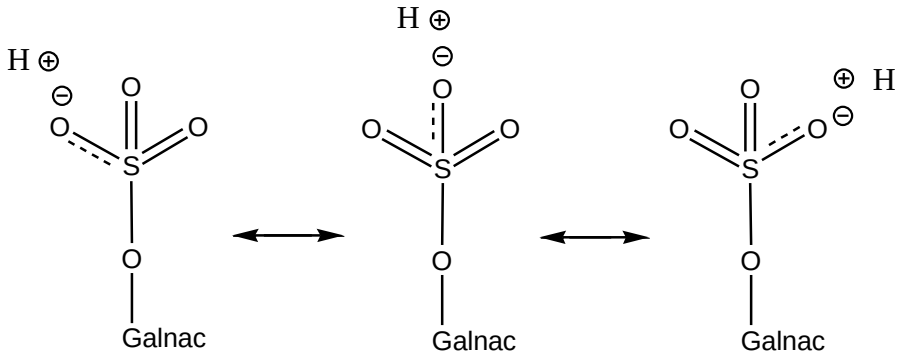

Figure 1.3 The resonance structure of a sulphate group attached to a galactosamine residue (Galnac). The sulphate is bound to the Galnac residue in chondroitin sulphate

For the free sulphate anion (SO_4^{2-}) the ν_1 symmetric S-O stretching mode is typically observed at around 990 cm^{-1} (Klimm and Botcharnikov, 2010). For bound sulphate in carbohydrates, contained within $-OSO_3^-$ or hydrated $-OSO_3H$ groups, the principal ν_s S-O stretching mode is typically observed at between 1060 - 1065 cm^{-1} (Cabassi, et al., 1978; Moger, et al., 2007). Hence the peak in the spectrum is sensitive to the chemical environment of this vibrational mode.

We were primarily interested in the behaviour of this band because of its prominence in the Raman spectrum of CS, the major constituent of aggrecan in articular cartilage (Ellis, et al., 2009). Ellis *et al.* reported a Raman spectroscopic study of aggrecan monomer and aggrecan aggregate molecules (from porcine laryngeal cartilage and chondroitin sulphate), as well as the GAG constituents CS and HA (obtained from various sources). As demonstrated during that study the contribution from the CS component of aggrecan dominates the spectrum. The samples studied by Ellis *et al.* (2009) were obtained from samples of different species and tissue origins, none of which were human.

In this thesis we were interested in investigating the profile of the Raman spectrum of aggrecan extracted from human articular cartilage. Chapter 3 reports the first Raman spectra of a proteoglycan fraction extracted from human articular cartilage, of which the primary component is aggrecan.

1.6 Articular cartilage: depth-wise variation in composition

Healthy articular cartilage is typically between 1–10 mm thick, with a trend for the thickness to decrease with age (Kincaid and Vansickle, 1981). Normal healthy tissue is characterised by a varying morphology and composition along the plane from the synovial joint surface to the subchondral bone. The morphology is typically divided into different zones; 1 to 4; however, they are often referred to as the superficial zone, the middle zone (or transitional zone), the radial zone and the deep zone (Figure 1.3) (Ghadially, 1983; Mow, et al., 1992).

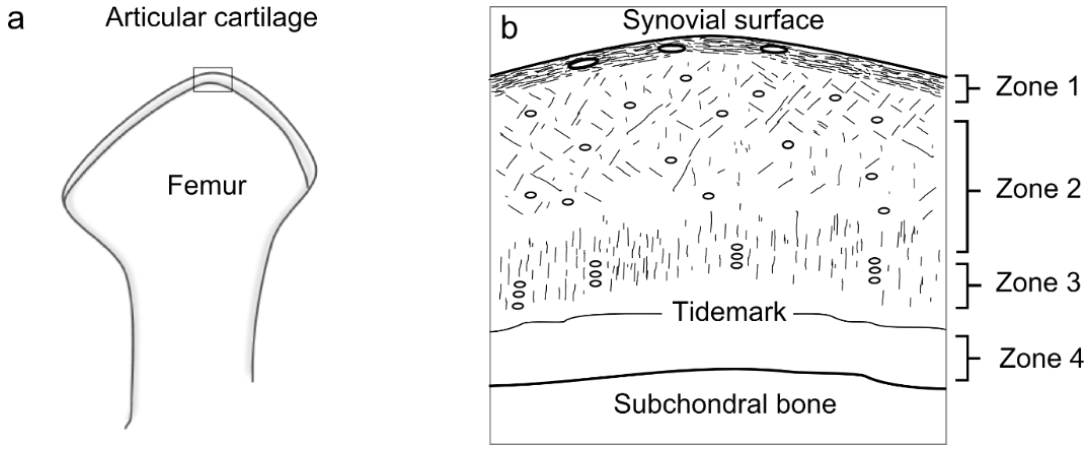

*Figure 1.4 A schematic of zonal organisation of articular cartilage. **a)** articular cartilage at the femoral condyle **b)** cross section of articular cartilage representing the zonal nature of the tissue. The lines indicate collagen fibril orientation in each zone, the spheres indicate the typical shape of the chondrocytes in each zone.*

The tidemark represents the junction of the mature non-calcified articular cartilage and calcified cartilage (Redler, et al., 1975). This is essentially the cartilage-bone interface, that divides the non-calcified cartilage from the calcified cartilage. In the non-calcified tissue, collagen and aggrecan are present in all zones, some local differences exist such that zone 1 contains more collagen and less aggrecan compared to zones 2, 3 and 4, which show increasing amounts of aggrecan in that order (Muir, et al., 1970). This can be demonstrated by histology staining with safranin o and fast green, where collagen appears green and proteoglycan appears red. Safranin o is a cationic dye that binds stoichiometrically to the negatively charged GAGs of aggrecan (Kiraly, et al., 1996; Mononen, et al., 2011).

One of the first studies of collagen and GAG distribution, as a function of tissue depth, was conducted by Muir *et al*. (1970). They performed chemical analyses of serial tissue sections (of 400 μm thickness) harvested parallel to the surface through the full-depth from the synovial surface to the subchondral bone. Hydroxyproline and hexosamine contents were correlated with collagen and GAG content, respectively. The total collagen and GAG contents were found to be 60-80% and 5-20% respectively. The collagen content was around 10% greater in the superficial zone compared to the adjacent deeper layers, whereas, GAG content increased gradually by 5-10% as a function of tissue depth.

More recently, proteomics assays have been applied to study thin tissue sections cut every 10 μm from the surface of the superficial zone to the CBI. These studies revealed a gradual increase in the aggrecan content as a function of tissue depth (Mueller, et al., 2014). Micro-beam fourier transform infra-red (FTIR) spectroscopy and mapping have been applied to investigate the relative collagen and aggrecan contents in articular cartilage (Camacho, et al., 2001). However, IR spectra are dominated by the signal from the aqueous component in the tissue. This makes Raman spectroscopy, where water signals are less dominant, better

suited to the analysis of biological samples such as articular cartilage (Schrader, 2007; Morris, 2010). Fluorescence microscopy has also been applied to study the structural changes in collagen of articular cartilage (Manning, et al., 2013). The focus on that work has been into the effect of degradation of the collagen component of the ECM. The problem with this technique is that it relies on the presence of chromophores, that in articular cartilage are mainly associated with the collagen component, and the fluorescence characteristics are highly dependent on the physicochemical environment (Altekar, 1977).

In chapter 4 micro-beam Raman spectroscopy is applied to studying the distribution of proteolgycan at the micrometre scale within sections of articular cartilage tissue. This demonstrates a means of distinguishing healthy and diseased as well as age related changes.

1.7 High temperature study of collagen and articular cartilage

Chapter 5 describes the use of Raman spectroscopy to investigate structural changes in articular cartilage as a function of temperature. Since Raman spectroscopy enables a detailed examination of molecular structure, it lends itself to the monitoring of structural changes in samples which accompany their exposure to high temperature. This is particularly interesting for characterising structural changes during the denaturation of proteins (Privalov, et al., 1979; Remmele, et al., 1990).

The structure of freeze-dried articular cartilage and collagen samples were studied with Raman and IR spectroscopy, both *in situ* and on samples that had been subjected to temperatures reaching 200°C, then recovered to ambient conditions. *In situ* refers to the analysis of samples during the heating process. The results of those studies reveal that in the same temperature range that unfolding has been proposed previously to take place in dehydrated collagen samples (Miles and Ghelashvili, 1999), our results provide evidence for

the occurrence of protonation in carboxylic acid groups and a decrease in the ability of the samples to retain water. Also, evidence suggested that the freeze-dried samples used in the present study contained H_2O bound within their structure that is released at high temperature. This result supported a previous suggestion that freeze drying might not entirely remove the water component from tissue samples (Nomura, et al., 1977). This interpretation was supported by thermogravimetric analysis and mass spectrometry along with FTIR spectroscopy of the cartilage samples.

Chapter 2 Experimental methods

2.1 Introduction

This research project involves the investigation of articular cartilage and its two main components, collagen and proteoglycan, by micro-beam Raman spectroscopy. Firstly, this chapter describes the preparation of samples used in these studies; hydrated and freeze-dried articular cartilage, full-depth thin tissue sections and collagen and proteoglycan extracts. Secondly, the micro-beam Raman spectrometer that was used to analyse these samples, is described along with the procedure for post-measurement signal processing. Optical parameters, which significantly influence the analysis of samples, as well as other important features of the laser beam are described. Then the experimental procedures for the analysis of samples in ambient conditions, in water, at controlled humidity, at high temperature and for Raman mapping are detailed. Finally, fluorescence is described, as well as the effect of this phenomenon on the Raman spectra obtained during the analysis of articular cartilage samples.

2.2 Sample source and handling

2.2.1 Sample source

Articular cartilage specimens were prepared and collected in advance of experimentation and stored at -80°C. Samples were obtained from femoral condyles of the knee joints of patients undergoing limb amputation due to soft tissue tumours. Joints were free from tumour invasion and the cartilage appeared macroscopically normal. The human tissues were obtained for research purposes with donor consent and with the appropriate Ethics Committee approval from the Stanmore musculoskeletal BioBank, Institute of

Orthopaedics and musculoskeletal research, Royal National Orthopaedic Hospital, Stanmore. The handling, use and disposal of human tissue was in agreement with the appropriate COSHH requirements at the Royal Veterinary College (Research and Welfare Ethics Committee at the Royal Veterinary College, URN 2010 0004H) and UCL.

All samples of articular cartilage samples used in these studies were of the age range 49-58 years, apart from in chapter 4 where samples originating from a mature donor (62 years) and a young donor (9 years) were compared. Whole samples were prepared from tissue of a donor 49 years and articular cartilage used to extract proteoglycan and collagen components was from a 58 year donor.

For whole samples, biopsies were taken from a full depth sample (49 year donor) as follows. A 6 mm biopsy punch was used to prepare full-depth plugs from the synovial surface to subchondral bone direction. Some of these biopsies were placed in microfuge (Eppendorf) tubes and stored at -80°C until use. Such samples were used in the deuterium exchange studies of chapter 3 and hydration studies in chapter 6.

Freeze-dried samples from this source (49 year old donor) were used for reference spectra of articular cartilage (in chapter 3) and for investigation at high temperature and by thermogravimetric analysis (in chapter 5). Biopsy plugs were freeze-dried according to the following procedure. Biopsy plugs were placed in microfuge tubes with perforated Parafilm® as the lid. Freeze-drying was performed at -70°C and a pressure of 1.3×10^{-7} MPA (Vitris Genesis 35XL freeze-dryer) for 24 hours, after which samples were stored in a desiccator under vacuum to reduce rehydration from atmospheric moisture. Freeze-dried cartilage biopsies were between 0.0142 - 0.0425 g before drying and 0.0035 - 0.0085 g after freeze-drying. Samples were freeze-dried to prevent the evaporation of water during the acquisitions time of Raman spectra for hydrated samples. This caused problems by changes

in shape of the sample, resulting in the loss of focus during Raman analysis. The analysis of dehydrated samples also enabled samples to be studied over long time periods.

Also, in chapter 3 a collagen sample from a commercial source was used for experimentation. This was collagen type III from human placenta (Sigma Aldrich, product code C4407, prepared as described by Hill and Harper (1984)). In chapter 5 a sample of gelatin was used, this product was obtained from BDH.

2.2.2 *Preparation of collagen and proteoglycan fractions*

In the initial stages of the research project, our aim was to identify Raman peaks which result from collagen and proteoglycan components of the tissue (chapter 3). Extraction of these components was according to a method described previously (Vogel and Heinegard, 1985).

Briefly, the cartilage tissue (from 58 year donor) was frozen in liquid nitrogen and immediately disintegrated to a fine powder using a ball mill dismembrator, (Mikro-Dismembrator, Sartorius, U.S.A.). The dismembrator was set at a rate of 2,500 oscillations per minute and 2 mins was sufficient to obtain a fine powder. Once pulverised, the powdered cartilage sample was transferred into an extraction buffer (4 M guanidine hydrochloride (GdHCl), and 0.5% ethylene diamine tetra-acetic acid). The ratio of the tissue to buffer solution was 1.45 g to 21.75 ml (1:15), the buffer was adjusted to a pH of 8.0 by addition of Tris buffer.

The sample was rotated in the buffer for 48 h at 4°C to extract soluble proteins. The soluble fraction was separated from the insoluble fraction by centrifugation at 15,000 xg for 20 mins. The supernatant (supernatant means liquid) was recovered to a new sample tube and both the supernatant and insoluble pellet were stored at -20°C until required. A 95%

ethanol solution was added, to the proteoglycan supernatant; at a ratio of 100 µl : 900 µl, supernatant to ethanol solution. The solution was left at -80°C for 2 hours and then the solution was centrifuged and the supernatant removed. The solid precipitates were freeze-dried to finish this precipitation stage and stored under vacuum. The proteoglycan fraction was termed proteoglycan^{f} and the insoluble collagen fraction, collagen^{f}.

Upon initial analysis of the separate fractions of collagen^{f} and proteoglycan^{f}, it was found that there was a Raman signal due to residual GdHCl in the samples. Raman spectra were obtained with a 0.5 N.A. Leica objective (Germany) and at reduced laser power (50%). GdHCl exhibits a strong Raman peak in its spectrum at 1007 cm^{-1}, which overlapped with the phenylalanine peak in samples of collagen^{f} and proteolgycan^{f} (1002-1003 cm^{-1}). Therefore it was important to eliminate GdHCl from the samples. To achieve this a portion of each sample (100 mg of solid collagen^{f} and proteoglycan^{f}) were diluted in a centrifuge tube with 95% ethanol (50 ml), and then centrifuged; the samples were then washed again. This process was repeated seven times in between the acquisition of spectra. Raman spectra of collagen^{f} and proteoglycan^{f} were then obtained following a series of wash steps (wash step 1, wash step 2, wash step 3), each step represents seven washes of the sample (Figure 2.1). A 95 % ethanol solution (50 ml) was used to wash samples.

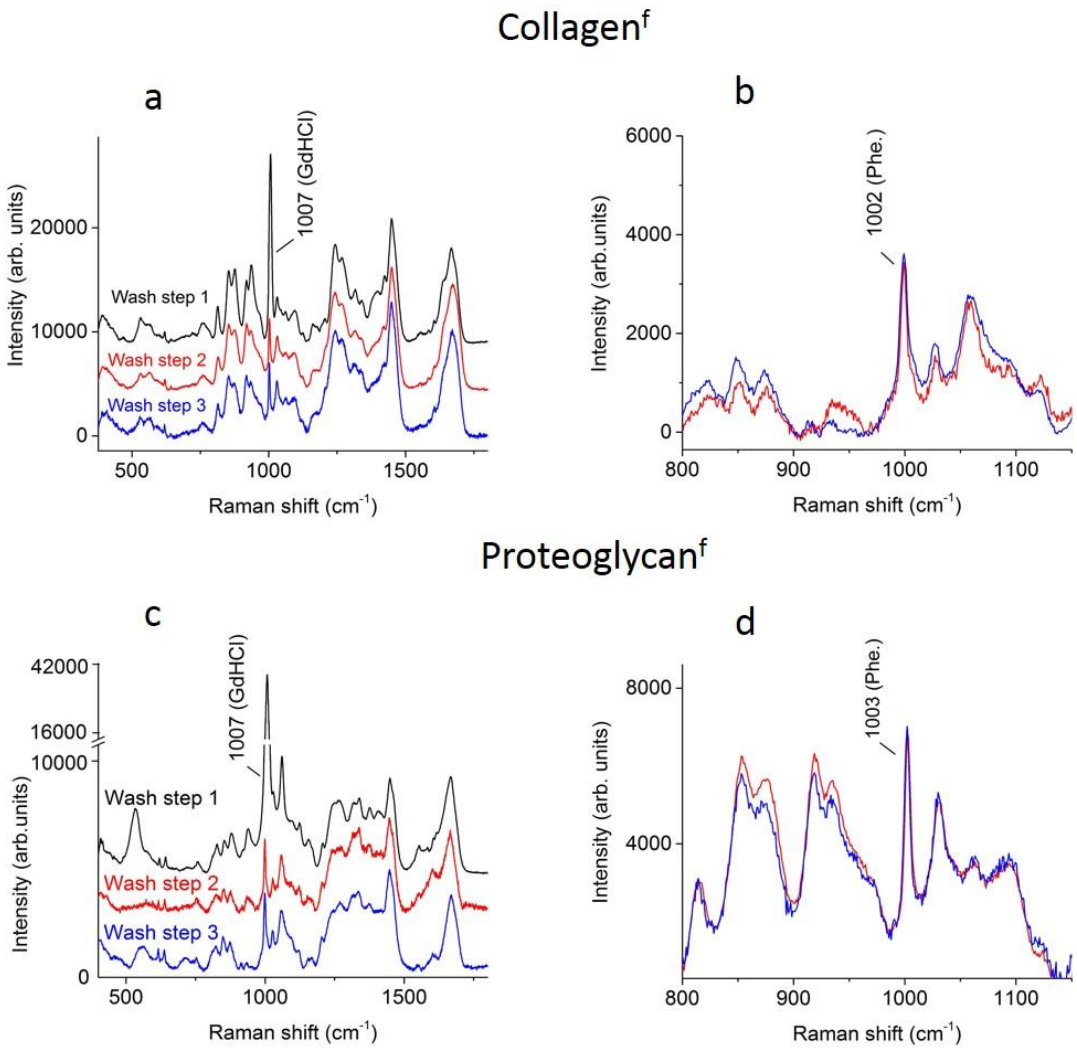

Figure 2.1 Removal of guanidine hydrochloride from collagen and proteoglycan fractions. ***a)*** *Raman spectra of collagen*^{f} *after three wash steps.* ***b)*** *The region of the spectrum around the Phe peak (1003 cm*$^{-1}$*) from the spectra from wash steps 2 and 3, showing that the peak at 1007 cm*$^{-1}$ *was not present.* ***c)*** *Raman spectra of preoteoglycan*^{f} *after each of the three washes,* ***d)*** *region of spectrum at Phe peak (1002 cm*$^{-1}$*), showing only spectra from wash step 2 and 3, again the peak at 1007 cm*$^{-1}$ *was not present.*

The Raman peak at 1007 cm^{-1} (due to GdHCl) is present in both fractions obtained after wash step 1 (one single wash step represents 7 washes carried out). Upon further washing (wash step 2 and 3), the 1007 cm^{-1} peak is no longer evident for samples collagen^{f} and proteoglycan^{f} (Figures 2.1 b and d respectively). The lack of further decrease in the spectral intensity in the region of 1007 cm^{-1} indicated that the GdHCl was eliminated from the samples

by wash step 2. To confirm that there was no contribution from residual GdHCl, the peak centre was determined and it was found to be at 1003 cm^{-1} for the collagen sample and 1002 cm^{-1} for proteolgycan^{f}, the frequency of which was characteristic of phenylalanine and not GdHCl. Hence, the samples of proteoglycan^{f} and collagen^{f} were taken as free from GdHCl, and were characterised further in chapter 3.

2.2.3 Preparation of articular cartilage sections for Raman mapping studies

Sections of articular cartilage tissue of 30 μm thickness were prepared by frozen section histology; the 30 μm sections were easier to obtain during cryosectioning procedures.

A Bright cryostat, (Bright Instruments, Huntingdon, UK (Model 50050 OTS)) was used to prepare sections. Full depth cartilage of 0.5 cm by 1 cm were fixed to a cryostat chuck using water to freeze the tissue onto the chuck. Only the very bottom part of the sample was frozen within the water to leave the rest of the cartilage free of ice to improve the sectioning process. The cryostat was set to a temperature of -30°C. Sections were cut along the longitudinal plane (synovial surface to the cartilage-bone interface) to obtain sections extending the full-depth of the cartilage. Once sections were cut they were transferred to CaF_2 substrate slides (Crystran, Poole UK) and were left to dry overnight at 40°C. Following drying they were found to remain fixed to the CaF_2 substrates. Since the samples self-attached to the surface, and appeared flat, it was deemed that they were sufficiently flat for Raman mapping studies. Tissue sections from the same tissue samples were placed on borosilicate slides and subjected to histological staining procedures, as described in the next section.

For Raman mapping studies it was essential to obtain sections of articular cartilage tissue that were flat when placed on a substrate slide. This was necessary to ensure that the initial focus of the laser beam was maintained whilst the tissue section was translated during

Raman mapping. Furthermore, it was important to utilise a material that would not exhibit an intense signal in the Raman spectrum. Kamemeoto *et al.* (2010) used aluminium foil-coated slides (manually prepared) as the support substrate for tissue sections, which in our preliminary studies were found to produce an uneven surface. In our experiments we used CaF_2 slides (Crystran, Poole UK) which were completely flat and also they are known to exhibit only one single Raman signal at 321.5 cm^{-1}. This peak did not interfere with the region of interest in the Raman spectrum of articular cartilage.

We stored the CaF_2 slides, to which tissue sections were adhered, at ambient temperature in the absence of light. Raman mapping was carried out over long periods of time (without temperature control). Therefore we chose to store tissue sections on the CaF_2 microscope slides at ambient temperature. This was preferred over storage by freezing to avoid the freezing and thawing processes, which would have taken place between storage and analysis stages. That process may have affected the adhesion of the sections to the CaF_2 microscope slides.

2.2.4 Histology staining with safranin O and fast green

Sections were placed on a borosilicate glass slide and the following procedure was carried out meticulously and under strict timing schedules.

After drying out overnight at 40°C, the sections were firstly rehydrated in distilled water by rinsing with water for 15 seconds. Then the sections were stained with fast green dye solution for 5 mins (fast green dye 10 g (Sigma Aldrich, F7258, Lot K37439317) + 1000 ml deionized water). Sections were rinsed with acetic acid solution for 15 seconds. Then they were exposed to a safranin o solution for 5 mins (0.1% Safranin O, 0.1 g + 100 ml deionized water). Then the sections were dehydrated with 70% ethanol (2 mins), 100 % ethanol (2 mins)

and finally again with 100% ethanol (2 mins). The final stage was to clear with histosol and then cover slip mount with DPX mountant. Then the slides were left to dry overnight before imaging was carried out with an Olympus BX60 microscope.

2.3 *Micro-beam Raman spectroscopy*

Raman spectroscopy was performed using a Renishaw InVia Raman spectrometer RM1000 model which was optically coupled to a Leica microscope (Solm, Germany) (Figure 2.2).

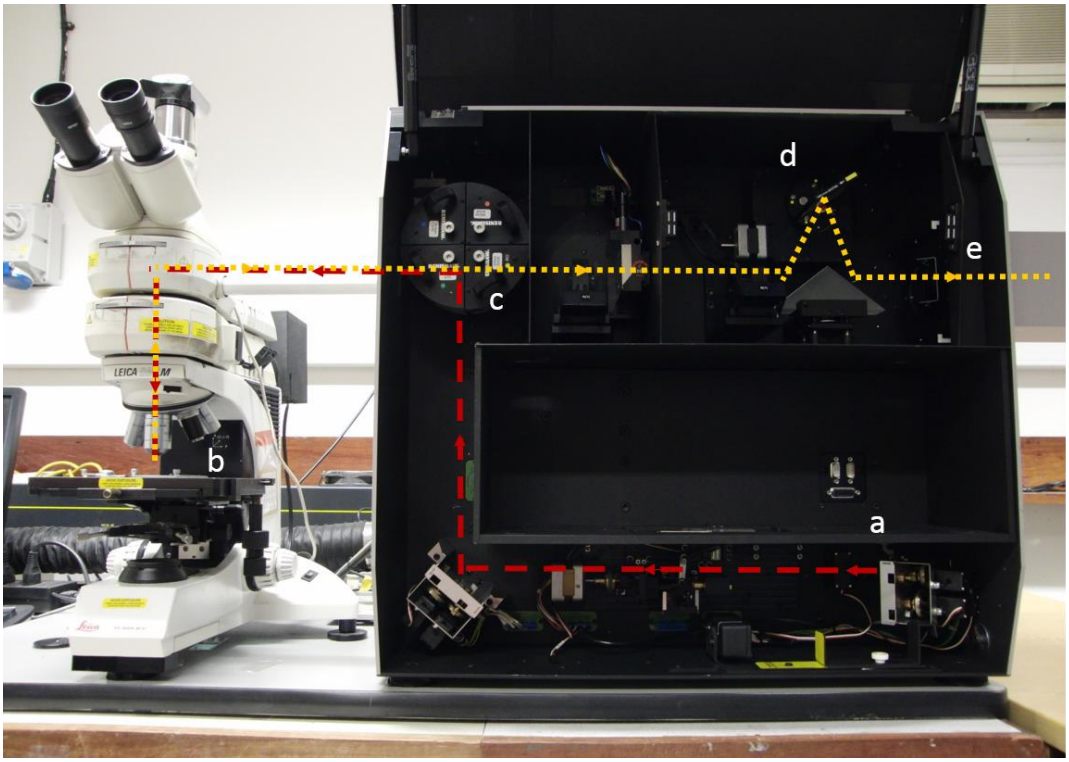

Figure 2.2 InVia Renishaw Raman microscope. The red dashed-line indicates passage of incident laser light; the yellow dotted-line indicates the Raman scattered light. Laser source entry (a). The incident laser enters the spectrometer and is directed from (a) to the objective of the microscope (b). Laser light scattered by the sample passes through the same objective and towards a notch filter (c). This filters any Rayleigh scattered light before the light reaches the spectral analyser (d), and this arranges light beams to be set, as a function of wavelength, onto the detector (e).

Spectra were obtained in the absence of light to avoid extraneous background features. Most experiments were carried out using a 785 nm diode laser (HDNIR Renishaw laser, max power 500 μW), which was air-cooled with an integral plasma filter. In some preliminary experiments a 514.5 nm argon ion laser (Modu-laser, Utah, USA) and a 633 nm helium-neon laser (Renishaw) were also tested. A gelatin-based notch filter was implemented (Kaiser optical systems, USA) which attenuated light at the region of each of the incident laser lines. A holographic diffraction grating was used to separate the light into its component wavelengths (1200 grooves/mm^{-1} for 785 nm and 633 nm lasers and a 2800 grooves/mm^{-1} for use with the 514.5 nm laser). Finally, the detector used was a CCD detector (576 x 384 pixels) cooled to -70°C. The detector converted the light intensity as a function of wavelength to an electrical output, which was recorded by the Wire® software (Renishaw, Gloucestershire).

Samples were visualised *via* the microscope eyepieces or *via* the colour video camera installed in the head of the microscope. The surface of the samples was brought into focus using bright-field microscopy and once this was achieved, the white light was switched off and the laser beam directed into the microscope objective. Raman scattered light was collected *via* the same objective lens, where it was redirected into the spectrometer (180°, backscattering geometry). A 0.5 N.A. and 50x magnification microscope objective (566036 Leica, Germany) was used because it did not exhibit any interfering features in spectra obtained during its use. Only in the Raman mapping study (chapter 4) was a different objective - a 0.75 N.A. microscope objective (556027, Leica, Germany). The 0.75 N.A. objective was the only objective that was both available for use and compatible with the Raman mapping spectrometer.

Before each set of experiments, the Raman system was calibrated to that of a silicon wafer, which has a well-known peak at 520.5 cm^{-1}. The detected wavenumber value for this

sample was calibrated to the known value and the intensity of this peak was monitored for any changes. For each spectrum acquired, the detector was exposed to the Raman scattered light for 30 seconds per pixel of the CCD array detector. This exposure time was chosen because it equated to 4 mins per spectrum and 16 mins per set of 4 accumulations and a set of such data provided a good signal-to-noise ratio. For each spectral acquisition, four subsequent accumulations were obtained, compared for differences and co-added when no differences were observed. For experiments in which a greater signal-to-noise ratio was required, multiple spectral acquisitions were obtained and co-added. Typically, data sets were averaged and grouped according to different variables (sample, conditions, etc.). The total number of accumulations per spectrum shown in this thesis is provided.

2.4 Analysis of Raman signal

Signal may be divided into two parts, one which is caused by the analyte(s) the other by the components of the sample substrate and instrumentation (Hobart H. Willard, 1988). There are signal and response variations in Raman spectra that result from cosmic rays, fluorescence (as a variable background), changes in detector efficiency as a function of spectral range, and intensity variations between spectral acquisitions. This section describes the essential procedures for processing raw data so that signal due to the sample is optimised and any extraneous spectral intensity is reduced. All data manipulation was carried out using the Origin Pro 9.0 graphing software (Origin Lab Corporation U.S.A). Firstly, cosmic rays were removed from data files manually or automatically (by the "zap" function on the WiRE® 2.0 software).

2.4.1 Correction for detector response

It is known that CCD detectors are not equally efficient in output over the full spectral range (Schrader, 2007). This was evaluated to assess intensity differences for the Raman spectral range of interest (100-4000 cm^{-1}). A correction factor was obtained for the detector to be corrected for the difference in detector efficiency over the spectral range. The correction factor was obtained according to the following procedure.

The emission spectrum of a tungsten lamp is known to fit the black body radiation function and the spectrum of a tungsten lamp was recorded by the Raman spectrometer (Figure 2.3a overleaf). These were found to be different because of the difference in sensitivity of the detector. The detector efficiency is lower than expected, at >2000 cm^{-1} and it even reaches a plateau at >3000 cm^{-1}.

Figure 2.3b overleaf shows the intensity difference in the set of peaks due to O-H stretches of H_2O (~3175 cm^{-1}) and O-D stretches of D_2O (~2383 cm^{-1}). The intensity of these peaks should be similar (Walrafen, 1964), but we observe that the O-D stretch peaks appear at much greater intensity because the spectrometer efficiency is higher in the region of the spectrum where they occur.

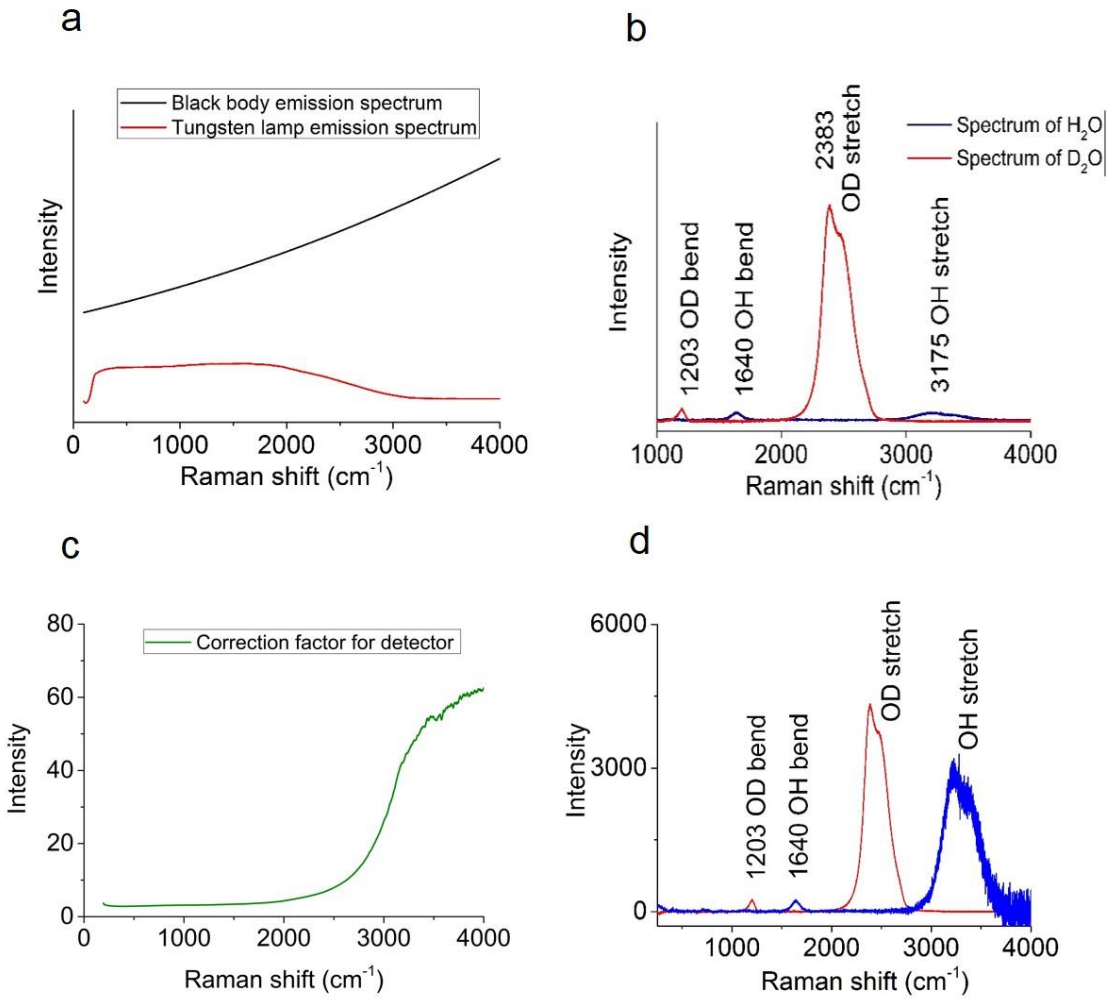

Figure 2.3 Efficiency of Raman CCD detector and correction factor. ***a)*** *Black body emission (red line plot) and the recorded tungsten lamp emission spectrum (black line plot), (both plots would be identical if the detector was perfectly efficient).* ***b)*** *Raman spectra of H_2O (blue line plot) and D_2O (red line plot) recorded with 785 nm laser (spectra were normalised to the O-H and O-D bend peak respectively).* ***c)*** *Correction factor for the compensation of detector inefficiency at long (near-IR) wavelengths.* ***d)*** *Raman spectra after correction factor has been employed showing O-H stretch and O-D stretch.*

The difference between the black body radiation emission spectrum and the recorded spectrum indicates where the detector is less efficient. A plot of this (Figure 2.3c) gives a

correction factor that was used to compensate for varying efficiency of the detector along the full spectral range. Figure 2.3d shows the same spectra of H_2O and D_2O after the application of the correction factor, where it can be seen that the O-H and O-D stretching modes were more comparable. However, the correction factor does not correct the data perfectly, as these would be equal, if that were the case. Separate correction factors were computed for the two different microscope objectives used to correct data reported in this thesis.

2.4.2 Background subtraction procedure

In order to compare only the contribution to the recorded spectra from Raman peaks, a background signal was removed from each spectrum. This signal may be due to a number of factors, including contributions from the material used to support the sample as well as fluorescence from anti-reflective coatings on the microscope objective. In these studies we did not investigate in detail the cause of the background, we focussed on developing techniques of systematically removing it in Raman spectra. For this we approximated the background to the blank spectrum acquired using the same experimental set-up used to obtain spectra in these studies. This was dependent only on the microscope objective that we used because all other optical components of the equipment remained the same.

Most of the Raman spectra were obtained with the 0.5 N.A objective (Leica, Germany), except in the Raman mapping study (chapter 4) where spectra were obtained with a 0.75 N.A. objective (Leica). The background subtraction method for data obtained with these two objectives is described below.

In Figure 2.4 we show the raw spectra obtained for the blank as well as the spectrum of articular cartilage obtained using the 0.5 N.A objective. We note that there are two sharp peaks at 2327 and 1554 cm^{-1}. It is known from previous studies that these peaks are due to the stretching vibrations of molecular N_2 and O_2 respectively (McMillan, et al., 1983). These are observed because of the presence of O_2 and N_2 in the air between the microscope objective and the sample studied.

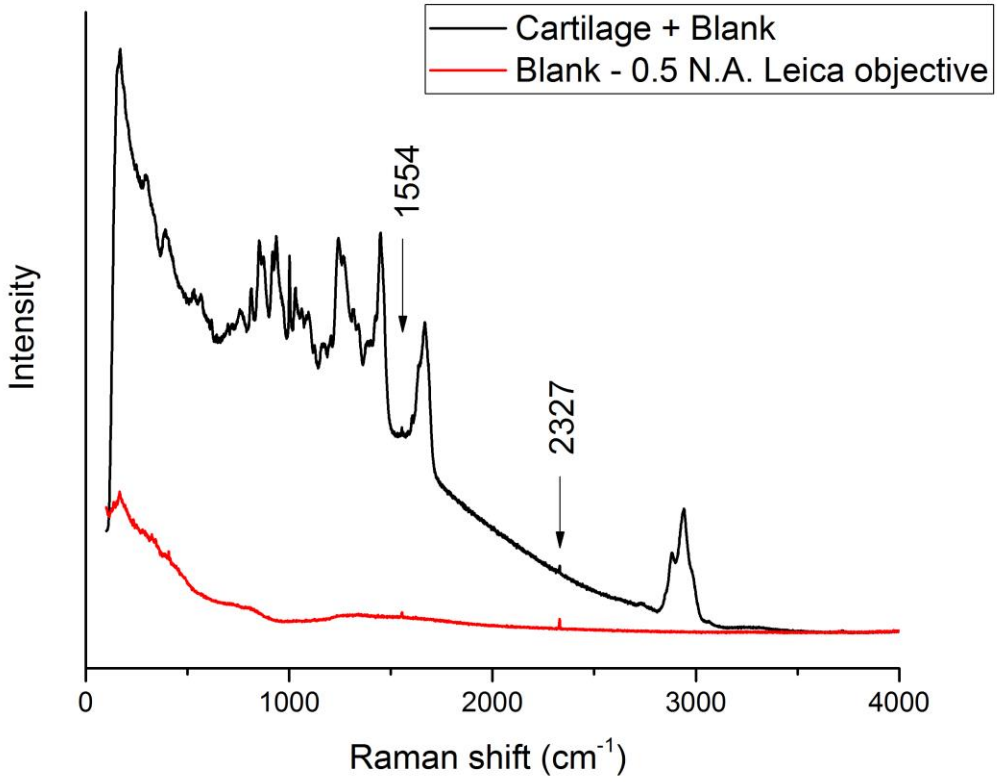

Figure 2.4 Raman spectrum of freeze-dried articular cartilage sample and blank spectrum obtained using 0.5 N.A. Leica objective. Black line plot, spectrum of freeze-dried articular cartilage sample. Red line plot, blank spectrum obtained using 0.5 N.A. Leica objective.

To account for the contribution of the optical set-up of the experiment to the Raman spectra obtained in these experiments, the blank spectrum was scaled-up in intensity, and,

once the baselines of the spectra coincided at 500 cm^{-1} an anchor point baseline was fit broadly to the scaled up blank spectrum and subtracted from the original (Figure 2.5).

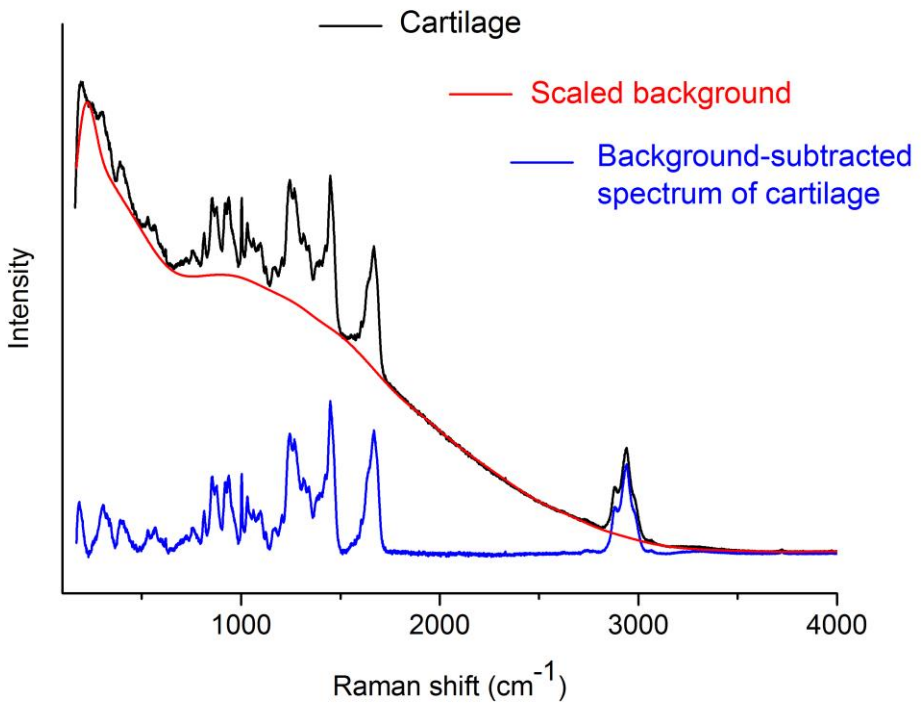

Figure 2.5 Method for background subtraction in Raman spectra of cartilage. Spectrum of cartilage, scaled-up background for subtraction and background subtracted-spectrum of cartilage.

During the course of the research carried out, the focus was to subtract a consistent baseline throughout, this meant that there would be no major variation in the spectra after background-subtraction had been implemented, enabling the comparison of spectra. This background subtraction procedure was employed where the 0.5 N.A objective was used.

Where the 0.75 N.A. objective was used with Raman mapping instrument (in chapter 4), the following background spectrum was characterised and subtracted. The blank spectrum of the 0.75 N.A. microscope objective is shown (Figure 2.6).

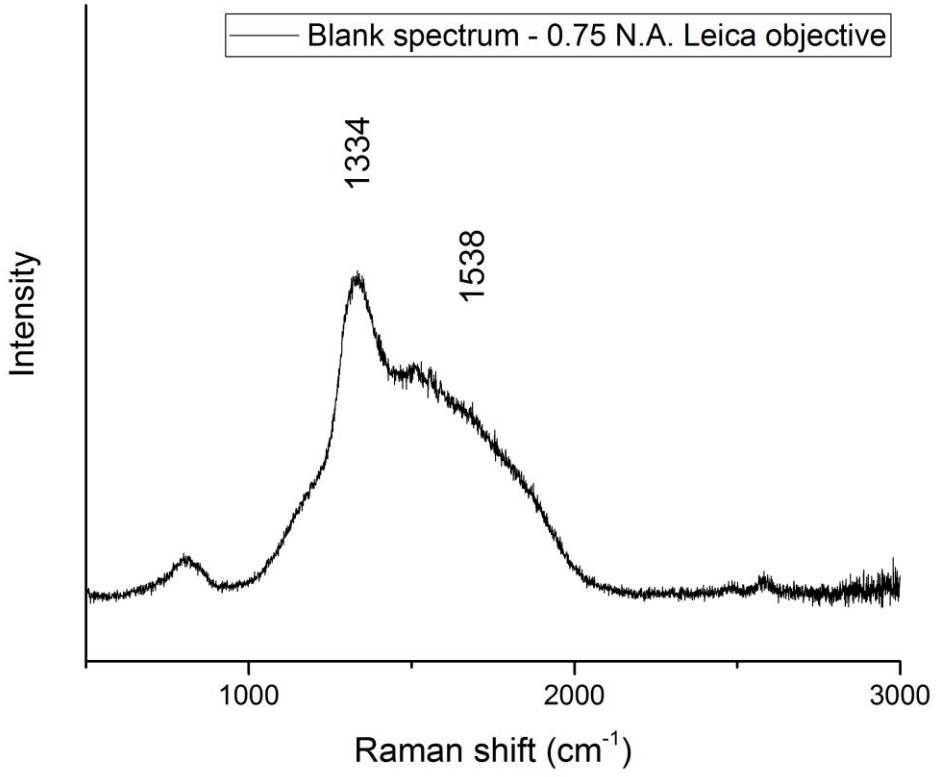

Figure 2.6 Blank Raman spectrum obtained with 0.75 N.A. objective using 785 nm laser, showing region of interest 500-3000 cm^{-1}.

The two broad features at 1334 and 1538 cm^{-1} peaks were not apparent in the blank spectrum of the 0.5 N.A. objective, which was used in the other studies – suggesting the features were inherent to the 0.75 N.A. microscope objective. These bands do not appear to be due to vibrational modes (Raman peaks) as their line widths are broad in comparison with Raman peaks which are known to be characteristically sharp. It is likely that these bands result from fluorescence effects of rare earth ion impurities that might be included in the

coatings of the microscope objective. For example Nd^{3+} ions, which produce a fluorescence signal in the range 1000-2500 cm^{-1} when excited with the 785 nm laser (Chen and Stimets, 2014). It was not possible to obtain information regarding the nature of the lenses, in order to confirm that, as this is usually safeguarded for the commercial interests of the lens manufacturers.

In the Raman mapping work, where the 0.75 N.A objective was used, the blank signal of that microscope objective was taken as the background and used for the background subtraction procedure (Figure 2.7).

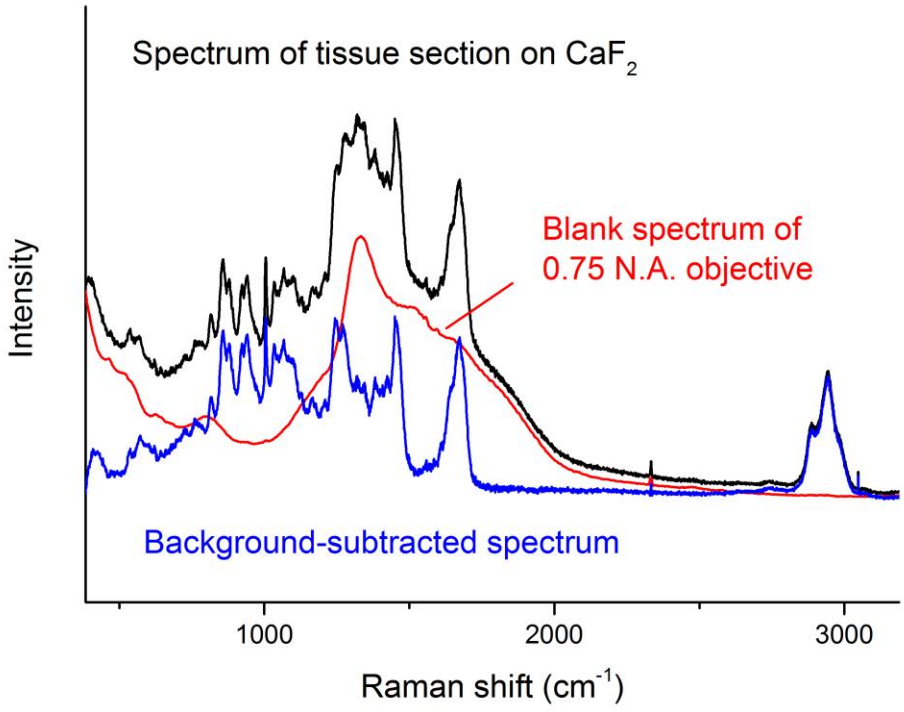

Figure 2.7 Method of background subtraction for spectra obtained with 0.75 N.A objective. Raman spectrum of a section of tissue on a CaF_2 microscope slide using the 0.75 NA Leica objective, background for subtraction and background-subtracted spectrum.

The background spectrum (the blank spectrum) was firstly scaled to the correct level

of intensity as the background of the sample spectrum, and the former was subtracted from the latter. Each background was fit to each spectrum in a way that the resulting spectrum had a similar background as other spectra obtained in that work. To verify this, the background-subtracted Raman spectra were compared for similarity between other spectra of cartilage examined in this thesis. The disadvantage of using such background subtraction procedures was that it meant that quantification of peaks was less reliable._Instead of comparing values for peak areas in Raman spectra, peak intensities were visually inspected for changes in relative intensity.

2.4.3 Peak analysis and data normalisation

Once the procedure of background subtraction was carried out and the correction factor was applied, peak fitting and data normalisation were carried out. Peak fitting was achieved using a Gaussian peak fit to the centre of each peak or multiple peak components. In order to compare spectra and enable consistent comparisons where intensity changes may be relative to the intensity of each spectrum, data were normalised to peaks which were constant in intensity between samples. Normalisation makes each spectrum in a series comparable by virtue of the fact that the intensity of the data in each spectrum is normal to the intensity of one peak in one data set, which was expected to be consistent in the series of spectra. Spectral data was normalised to a peak/peaks of known intensity/contribution to the spectrum. In this study the phenylalanine peak (1003 cm^{-1}) was mainly used for this.

2.5 *Optical parameters and laser beam profile*

The optical parameters of the objectives and laser beam are described in this section. For the objectives, these include the numerical aperture (N.A.) of the objective and depth of focus. These parameters determine the laser beam intensity at the sample and the signal-to-noise ratio of the Raman data.

2.5.1 *Numerical aperture of objectives*

The numerical aperture is given as,

N.A. = $n \sin \theta$

Where θ is a half of the angular aperture (shown in Figure 2.8) and n is the refractive index of the medium within the focal length.

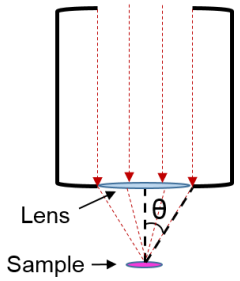

Figure 2.8 Schematic showing half of the angular aperture, θ, of a microscope objective.

The focal length is the distance along the axis from the front of the objective lens to the focal point of the light beam. Essentially the larger the value of θ, the more the numerical aperture tends towards 1 and the shorter the focal length. For example, the objective with the 0.75 N.A. had a focal length of 1.06 mm whereas a 0.5 N.A. objective had a focal length of 3.4

mm. During the acquisition of Raman spectra, the signal which one aimed to measure was the Raman scattered light. This is scattered at random from the point at which the laser beam enters the sample and can be collected more efficiently if the microscope objective can be positioned closer to the sample surface. However, the microscope objective with the longer reach was preferred because it exhibited a lower background signal.

2.5.2 *Depth of focus*

The depth of focus can be described as the distance along the axis of the laser beam for which the sample is in focus. This is a feature of the focal cylinder, which is depicted below in Figure 2.9.

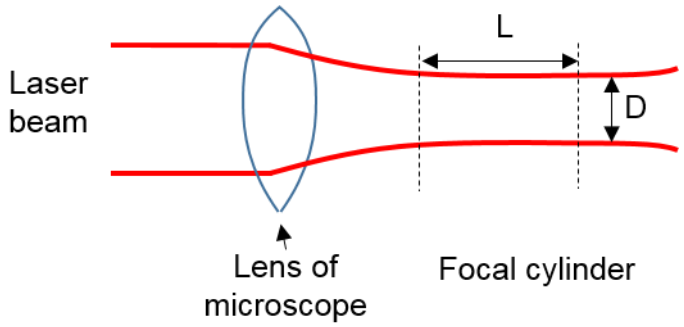

Figure 2.9 Collimated laser light entering a lens and the resulting focal cylinder. D and L represent the diameter and length of the focal cylinder.

The formula for the diameter D, and the length L, of the focal cylinder are given below (Dhamelincourt, 1979). L is effectively the depth of focus.

$$D = \frac{4\lambda f}{\pi d} \qquad L = \frac{16\lambda f^2}{\pi d^2}$$

λ is the laser radiation wavelength, d is the diameter of the unfocused laser beam, f is the focal length of the focusing lens.

For an objective of 0.75 N.A. and a 785 nm laser beam, the focal length is 1.06 mm. For a beam diameter of 0.6 cm, the value for D = 176.5 nm and L = 124.8 nm. The depth of focus is where the laser light is most concentrated, in the z axis. However, laser light is scattered through translucent and transparent samples, and even opaque samples (Schrader, 2007). This means that the analysis of scattered light from a sample comprises light scattered from beyond the depth of focus of the objective.

2.5.3 Power of laser beam power at the sample surface

The 785 nm laser diode was rated at a power output of 500 mW. The flux of the laser beam at the surface of the sample was monitored for the two objectives at 50% and 100% level of laser power (Table 2.1). These were measured by an optical photometer, model AQ2150 (Andor Co Ltd., Japan).

Table 2.1 Laser power of 785 nm laser for each objective used

	0.50 N.A. 50 x mag. objective	0.75 N.A. 50 x mag. objective
50% laser power	13 mw	19 mw
100% laser power	53 mw	70 mw

The exposure of articular cartilage tissue to the laser beam meant that there was a potential risk of thermal damage. Thermal damage was observed in cases where isolated proteoglycan[f], collagen[f] and collagen type III were exposed to 100% laser power, resulting in a high level of fluorescence in the spectra obtained. Also, a brown mark the same size as the laser spot was visible on the surface of the samples. The fractions of collagen[f] and proteoglycan[f] were thin precipitates of around 0.5 mm in thickness and the collagen from commercial sources were fibrous in texture. It is believed that the low volume of sample in

these cases meant that the risk of burning by the laser was greater.

As for samples of whole articular cartilage tissue and tissue sections analysed, none of these effects were observed. Nevertheless, a protocol was performed prior to experiments to confirm that there was no thermal damage to samples during laser beam exposure of a typical spectral acquisition. For this, the number of acquisitions was doubled to that used in the experimental design. Where no changes were observed in the fluorescence background or Raman peak intensities, it was considered that the laser exposure had not caused any damage to the sample during the acquisition of Raman spectra during a given analysis.

2.6 Raman measurements and sample handling

Here the analysis of samples in water and air, under controlled humidity, during Raman mapping and at high temperature are described. The Raman microscope shown in Figure 2.2 was used for this. For Raman mapping experiments a different Raman microscope system, although the model was the same (RM1000).

2.6.1 Studies of hydrated samples and dehydrated samples

During initial experiments, hydrated samples were analysed in air but due to the long acquisition times, ambient conditions and warming by the laser beam, the samples were prone to drying. To prevent this, wet samples were analysed whilst submersed under water: samples were placed in the bottom of a sample holder and deionised water was added to the sample holder (Figure 2.10).

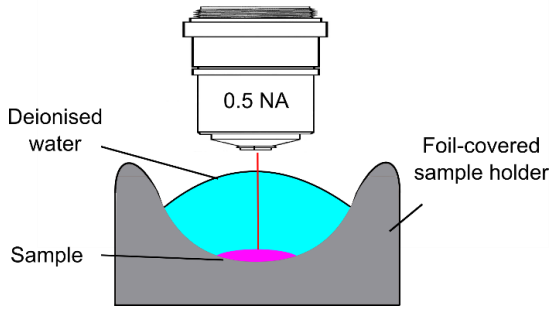

Figure 2.10 Arrangement of hydrated cartilage samples for analysis in water. The sample holder was made from plasticine and moulded into a rounded well, which was covered with a layer of foil. This meant the water did not wick and formed a slightly convex surface.

Focus onto the surface of the sample was made from above the water using a 0.5 N.A. objective (without the lens touching the body of water, which was of 1-2 mm depth). Raman measurements of articular cartilage samples in D_2O liquid were also carried out in this way (chapter 3).

By dehydrating samples before analysis, the potential issues related to water loss during analysis could be avoided. Freeze-dried samples were therefore used in some cases. Raman spectra of freeze-dried samples were carried out under ambient conditions (in an air-conditioned room at 22°C). Solid samples were analysed in a sample holder, which was covered in aluminium. Aluminium was chosen because it lacks Raman bands in its spectrum and has been used in similar studies (Ellis, et al., 2009; Kamemoto, et al., 2010). Freeze-dried biopsy samples were opaque and usually thick enough (1-2 mm) to attenuate the laser beam before reaching the underlying aluminium foil. Thus avoiding any signal due to the aluminium foil below the sample.

2.6.2 *Raman measurements under controlled humidity conditions*

Chapter 6 describes Raman studies of articular cartilage as a function of low and high hydration. A device was fabricated that enabled control of the relative humidity of a sample whilst permitting the acquisition of Raman spectra *via* a quartz window (Figure 2.11 overleaf). A similar set-up was used by Zhang *et al.* (2011) to study collagen samples at varying relative humidity. The sample chamber was air-tight and, because of the permeable sample holder, the sample was in contact with the atmosphere conferred to the sample by the contents of the lower vessel.

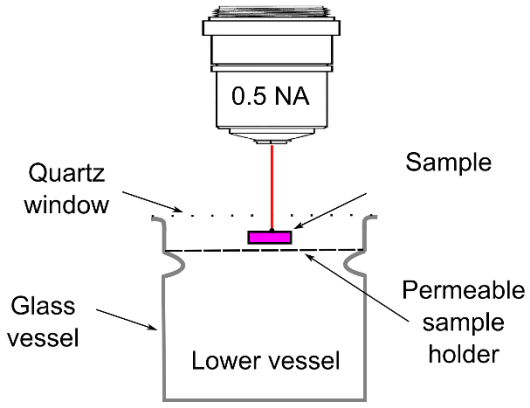

Figure 2.11 A cross section of the humidity cell, showing sample in place during analysis. The lip of the lower vessel which made contact with the window was frosted glass. The window was sealed with a layer of vacuum grease.

2.6.3 *Raman measurements at high temperature*

In chapter 5, Raman measurements were obtained for samples at a range of temperatures between 20-200°C. For these studies, it was necessary to use a specialised heating chamber that enabled both temperature control of a sample, as well as acquisition of Raman spectra from the surface of the same sample. A TS1500 heating stage (Linkam, Surrey,

United Kingdom) was used for this work, with a TS94 thermostat (Linkam). This experimental set-up had previously been used for high temperature Raman spectroscopy of collagen and DNA samples (Dong, et al., 2004), and is shown in Figure 2.12 overleaf. The heating stage contains a platinum heating filament, which was linked to a thermostat. This system enabled control of the temperature of the sample chamber while Raman measurements could be obtained *via* the transparent (quartz) stage lid of the heating stage.

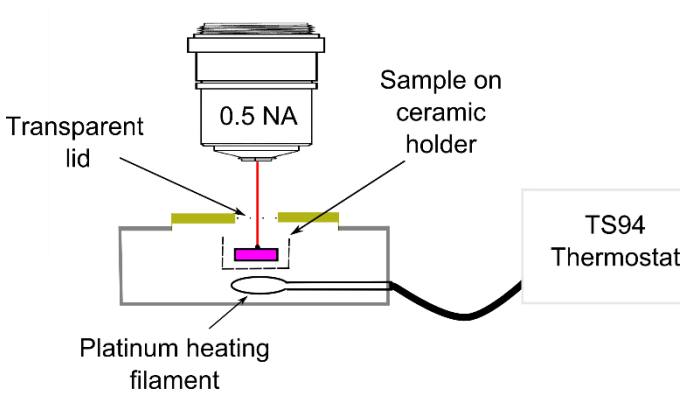

Figure 2.12 A cross section of the set-up for high temperature Raman analysis. The grey box represents the TS1500 heating stage, a sample is shown in place.

Surrounding the quartz window, on the exterior of the heating stage lid and below the microscope objective, was a chamber with an inlet and outlet for water. During experimentation at high temperature, water was circulated through this chamber of the sample lid to prevent heat from reaching the objective lens of the microscope. This was essential since contained within the microscope objectives are numerous lenses, which are known to be bound by temperature sensitive adhesives.

2.6.4 Micro-beam Raman mapping

For Raman mapping studies (chapter 4) an InVia Renishaw system (RM 1000) was used with a sample chamber housing that contained a computer-controlled sample stage (Figure

2.13 overleaf). The stage was an H101a Prior scientific Proscan™ II (United States). It was controlled automatically by the Wire® system software, or manually by a joystick. This enabled the automated analysis of the sample systematically at different points on its surface by translation of the stage in x or y directions.

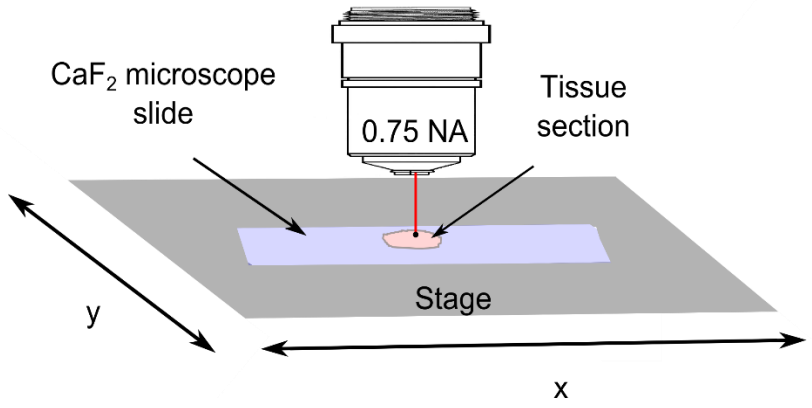

Figure 2.13 Schematic showing the experimental set-up for Raman mapping. The sample was manoeuvred by the automated stage in x and y directions, tissue sections were supported on CaF_2 microscope slide placed on the stage.

Microscope slides made from CaF_2 were used to support samples because it exhibits a Raman peak at 321 cm^{-1}. This peak is due to the single Raman active lattice mode of fluorite-structured CaF_2. In these experiments, the spectral region of interest was around 700 - 2000 cm^{-1}, therefore the peak at 321 cm^{-1} was of no obstruction in this work. There were different mapping functions for scanning. Line scans were performed along the depth of the tissue instead of grid scans because grid scans require intensive data analysis processes to produce Raman maps (Camacho, et al., 2001).

2.6.5 *Fluorescence in Raman spectra of articular cartilage samples*

One common issue encountered during Raman spectroscopic studies of biological samples is that of fluorescence interference (Tu, 1982). Fluorescence is commonly produced when using ultraviolet light to excite molecules in a sample and record an emission spectrum of the emitting photons, however molecules can also be excited by visible light of the 400-900 nm range that is used in Raman spectroscopy. Fluorescence involves spontaneous emission of a photon when a molecule transforms from an excited state into a ground state (Figure 2.14).

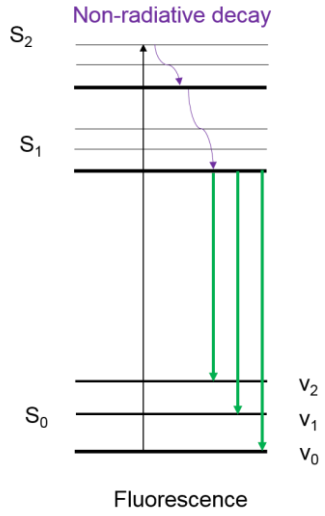

Figure 2.14 A schematic of the fluorescence excitation and emission process. The vertical black arrow indicates photon excitation and the green arrows indicate photon emission. S_0 is ground state energy, S_1 is excited state, S_2 is second excited state. v_0, v_1 and v_2 represent vibrational states of a molecule undergoing fluorescence emission.

Molecular orbitals implicated in such molecules are typically n – π* or π – π*. Since the gap between π-π* is lowest of all molecular orbital energy differences, molecules with a greater degree of π bonding exhibit greater levels of fluorescence. So, in proteins for example, polypeptides consisting of amino acids with aromatic side chains such as Tyrosine (Tyr),

Tryptophan (Trp) and Phenylalanine (Phe) exhibit the greatest degree of fluorescence (Wagnieres, et al., 1998).

In these studies a fluorescence signal was observed in the Raman spectra of articular cartilage. A fluorescence contribution can be seen as the broad feature underlying Raman spectra of freeze-dried articular cartilage obtained with exciting lines 514.5 nm, 633 nm and 785 nm (Figure 2.15).

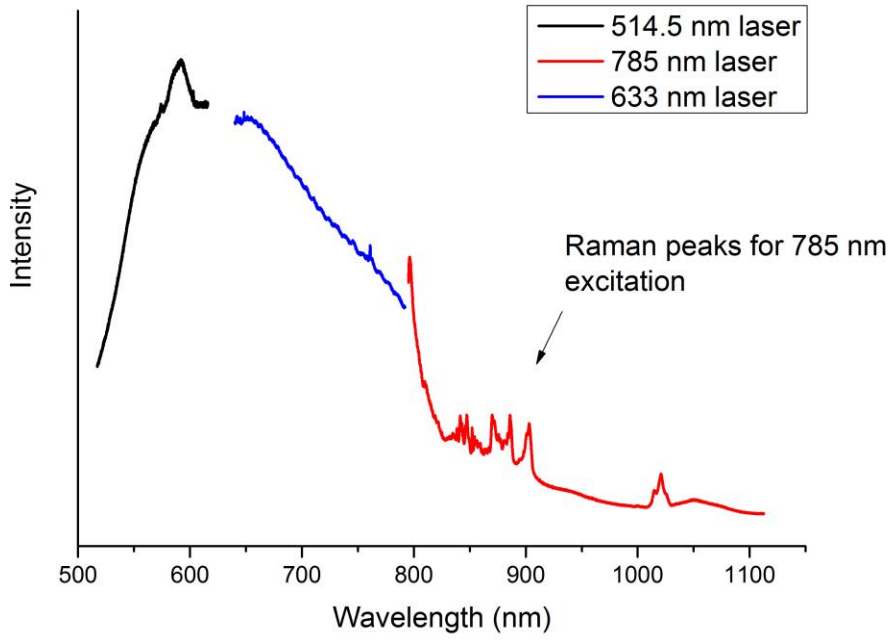

Figure 2.15 A series of Raman spectra obtained with lasers 514.5, 633 nm and 785 nm. Raman bands were only apparent in the spectrum acquired with 785 nm laser. The fluorescence signal is broad, covering the range of wavelengths from 500 nm and appears to tail off at around 900 nm, with a maximum at around 630 nm. By comparison, the Raman peaks are sharp (covering 1-20 nms).

It is important to note that the Raman spectra obtained with the 785 nm laser exhibit Raman peaks, however, spectra acquired with lasers 514.5 and 633 nm do not. That is because where lasers of 514.5 nm and 633 nm were used, the fluorescence signal overwhelmed the

Raman signal. Since no Raman signal was observable in the spectra obtained with these lasers it is certain that the fluorescence is enhanced in that part of the spectrum because of the greater intensity of the exciting lines.

A part of the underlying background of the Raman spectrum of articular cartilage obtained with the 785 nm laser is due to fluorescence because Raman spectra obtained at the same site exhibit photobleaching. Figure 2.16 shows a series of spectra obtained at the same site of a freeze-dried sample of articular cartilage. The acquisition time for each spectrum was four minutes so the total time for obtaining this series of spectra was 16 minutes.

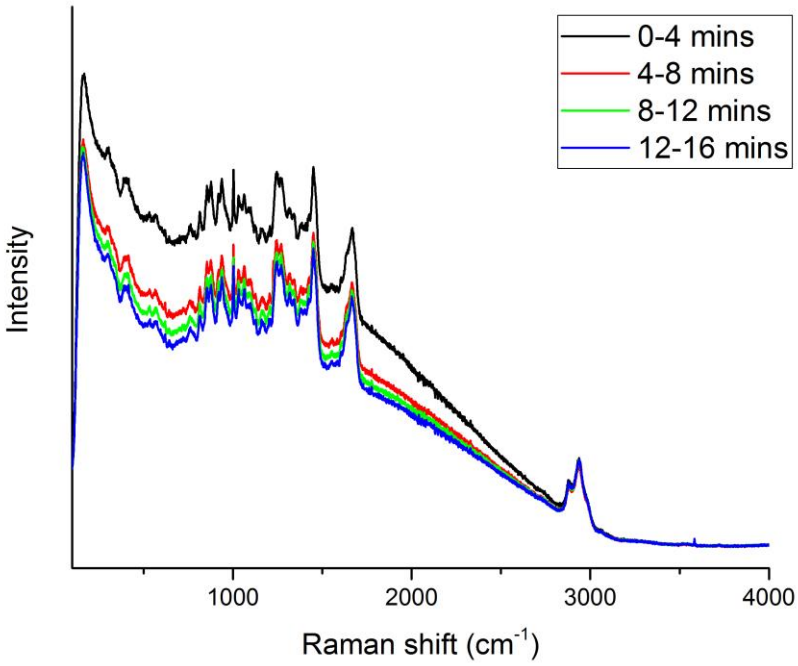

Figure 2.16 Photobleaching in Raman spectra of freeze-dried articular cartilage. Raman spectra obtained sequentially at the same site, the decrease in the underlying background is indicative of the photobleaching effect.

Photobleaching occurs in this case as the laser beam excites molecules in the sample

causing a decrease in the population of molecules that are able to be excited to the excited state, which therefore means that the molecules exhibit a lower level of fluorescence. Hence the reduction in the background intensity as a function of time.

In order to avoid fluorescence excitation, time-gated fluorescence spectroscopy could be used (Matousek, et al., 1999). For this research project the use of a 785 nm excitation source sufficed to reduce significant fluorescence. The disadvantage with the use of the 785 nm laser was (as described in Section 2.5.2), the low efficiency of the CCD detector in the >3000 cm^{-1} range of spectra recorded relative to the incident light.

In articular cartilage the main source of fluorescence is collagen (Manning, et al., 2013). A typical collagen polypeptide contains 7 Tryptophan, 10 Tyrosine and 25 Phenylalanine residues (Wagnieres, et al., 1998). Their fluorescence maxima appear at 348, 303 and 282 nm respectively. There are also cross-links and AGE cross-links, which are believed to contribute to the fluorescence characteristics of collagen, which fluoresce at 460 nm (Verzijl, et al., 2002; Manning, et al., 2013). In the series of spectra shown in Figure 2.15, it can be seen that the maximum of the fluorescence background is around 600 nm for articular cartilage. This differs from the maximum of the fluorescence signal of amino acid residues in collagen and AGE cross-links. It is difficult to ascertain the origin of this background from the studies we carried out, some attribute it to light scattering effects (Bonnier, et al., 2012). The focus of our research was on the relative changes in the Raman peaks observed above the fluorescence background.

Chapter 3 Characterisation of the macromolecular components of articular cartilage

3.1 Introduction

The work described in this chapter was aimed at assigning features of the Raman spectrum of articular cartilage tissue. Firstly, we extracted the soluble and insoluble components of articular cartilage. The soluble component was taken as proteoglycan (which is mostly aggrecan) and the insoluble component taken as collagen (mostly collagen type II). Here we refer to these two fractions of the extracted tissue component as proteoglycan^{f} and collagen^{f} where the "f" denotes fraction. The Raman spectra of collagen^{f} (collagen type II) was compared with collagen type III for differences. The hypotheses being that the Raman spectra of collagen II and proteoglycan would enable better identification of the peaks in the spectrum of cartilage that are due to these components. Also, to investigate whether or not collagen types II and III of human origin have similar Raman spectra. In the final part of this study, articular cartilage was studied by Raman spectroscopy following isotopic substitution by deuterium/ hydrogen exchange. The aim of that part of the study was to identify spectral changes which were consistent with assignments to peaks in the Raman spectrum of articular cartilage.

3.1.1 Raman spectroscopy of proteoglycan and collagen

The Raman spectrum of human articular cartilage tissue has been shown to contain contributions from its primary constituents, proteoglycans and collagen (Esmonde-White, et al., 2011). In that work, peaks in the spectrum of articular cartilage were assigned by referring to the spectra of the collagen and proteoglycan components reported in previous work (Frushour and Koenig, 1975; Ellis, et al., 2009). To our knowledge, there have been no studies

by Raman spectroscopy on collagen and proteoglycan extracted from human articular cartilage itself. The separation of these major components from whole tissue provides a means of characterising the spectra of these constituents, which facilitates assignment of peaks in the spectrum of articular cartilage tissue to these two components.

The Raman spectrum of aggrecan, the major proteoglycan of articular cartilage, has previously been reported for samples extracted from porcine laryngeal cartilage (Ellis, et al., 2009) and more recently from bovine articular cartilage (Gamsjaeger, et al., 2014). The Raman spectrum of collagen was obtained from a sample of bovine Achilles tendon (collagen type I) (Frushour and Koenig, 1975). In this study, we set out to characterise the collagen and proteoglycan components extracted from human articular cartilage.

Proteoglycans have previously been extracted from tissues including articular cartilage by using GdHCl. This substance solubilises the proteoglycan component of the tissue (Hascall and Sajdera, 1970), meaning the collagen component, which is insoluble in this buffer can be separated by centrifugation. It was assumed that the Raman spectrum of the soluble fraction would reflect mainly aggrecan, since it is the major proteoglycan component of the tissue (Roughley, 2006). There would be minor amounts of the small proteoglycans decorin, lumican, biglycan and fibromodulin (Hardingham, et al., 1986), but the signal was not expected be great from these minor constituents. Likewise, the insoluble fraction was expected to represent mainly the Raman spectrum of collagen type II, as articular cartilage contains mostly collagen type II with minor amounts of other collagen types that include, collagens type IV, IX, X and type XI collagen (Eyre, 2002).

Following that work we compare the spectrum of collagen^{f}, which is expected to be representative of the most abundant component of that fraction, collagen type II; with that of collagen type III of human origin.

3.1.2 Hydrogen-deuterium exchange study to assign Raman peaks resulting from exchangeable protons in articular cartilage

Vibrational spectroscopy combined with H/D isotopic substitution permits clear identification of those modes involving significant hydrogen motions. In this study, the aim was to reveal which parts of the Raman spectrum of cartilage results from contribution of exchangeable hydrogen species. By obtaining spectra of samples in water and after deuterium change it was possible to edit the spectrum and reveal the peaks that contain contributions from NH and OH groups in cartilage. Exposing samples to H_2O *vs* D_2O fluids can aid in identification of hydrogenated species that are readily exchangeable. Both effects were implemented here to study the components of cartilage tissue immersed in D_2O *vs* H_2O.

Previously, Raman spectroscopy has been used to study D_2O-exchanged samples of collagen (Frushour and Koenig, 1975; Zhang, et al., 2011) and various proteins (Williams, et al., 1984) but to our knowledge this has not been reported for samples of human articular cartilage. For comparison with articular cartilage in D_2O, the Raman spectrum of articular cartilage in H_2O is shown.

Following D/H exchange the frequency of O-H(D) stretching and O-H(D) bending vibrations are reduced by a factor of approximately 1.4 due to the change in reduced mass involving substitution of the heavier atom (Tu, 1982; Havel, 1995). Similarly, studies on proteins have shown that amide III mode shifts from 1240 to 990 cm^{-1} (Miyazawa, et al., 1958). The reason for this is that the vibrational mode includes 40% C-N stretch, 20 % C-C stretch and 30 % N-H in-plane bending (Miyazawa, et al., 1958), therefore the shift is due to the exchange of the N-H, causing the component of this band that is due to the in-plane bending mode, to be shifted to lower wavenumber.

3.2 Experimental methods

Firstly, we show the Raman spectra of freeze-dried samples of human articular cartilage, collagen^{f} and proteoglycan^{f}. The fractions were prepared from tissue of a donor of 58 years of age (chapter 2). The fractions were initially found to contain GdHCl, which was eliminated by washing the samples according to the procedure described in chapter 2. The sample of freeze-dried cartilage was from a 49 year donor.

The final fractions of collagen^{f} and proteoglycan^{f} were freeze-dried and analysed with reduced laser power (50%) because they were susceptible to thermal damage at 100% laser power. Spectral acquisitions (of four accumulations) were obtained with the 0.5 N.A. objective at four different sites at the surface of these samples and the data were pooled to afford a single spectrum. No variation in the spectra were observed in the series of spectra obtained.

The Raman spectrum of collagen^{f} is compared with collagen type III from human placenta (both spectra obtained with four acquisitions). Finally, for the H/D exchange studies untreated biopsy plugs (from tissue of 49 year donor) were taken from storage at -80°C and were treated by exposure to D_2O (GOSS Scientific, Batch 07-10D) and H_2O (distilled on site) for one month, and at 4°C to enable isotopic exchange and saturation of water of the samples respectively. Samples were analysed in water and deuterium oxide as described in chapter 2.

3.3 Results

3.3.1 Raman spectra of collagen^f and proteoglycan^f

The Raman spectra of collagen^f and proteoglycan^f samples are shown below. The spectra were not normalised in this case. The Raman spectra contain numerous peaks which often overlap and for certain peaks there may be more than one single assignment.

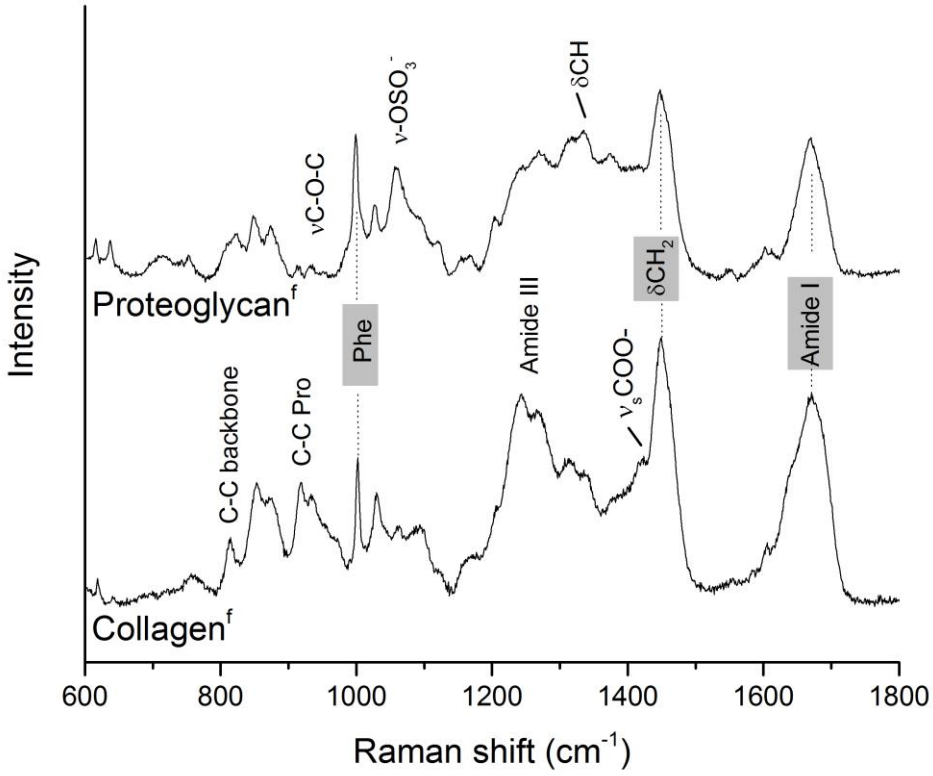

Figure 3.1 Raman spectra of proteoglycan^f and collagen^f. The bands highlighted in grey overlap in and result from the same vibrational modes in the two fractions.

The main peaks which overlap and result from the same vibrational mode in the separate samples are due to the amide I vibrational mode (1665 cm^{-1}), CH_2 bending mode (1450 cm^{-1}), Phe peak (1003 cm^{-1}).

The spectrum of proteoglycan^{f} shows characteristic peaks of the major component of this fraction, aggrecan. These peaks are; Amide I (1665 cm^{-1}), Amide II / δC-H (at 1377 cm^{-1}) (Tu, 1982; Ellis, et al., 2009), δC-H (at 1339 cm^{-1}), -OSO_3^- (1063 cm^{-1}) (Ellis, et al., 2009), C-O-C stretch (at 940 cm^{-1}) (Ellis, et al., 2009). Bansil *et al. (1978)* assign the peak at 1377 cm^{-1} to CH_3 deformation, this is supported by others for assignments to other oligosaccharides (Kacurakova and Mathlouthi, 1996). Finally, the peak at 1063 cm^{-1} is due to the vibrational mode of sulphate that is present on the GAGs of aggrecan (Bansil, et al., 1978). The FWHM of this peak was found to be 16.4 cm^{-1} and it had a centre at 1063.2 cm^{-1}.

The Raman spectrum of the collagen^{f} fraction contains characteristic features such as that due to $\nu_s COO^-$ at 1420 cm^{-1}, amide I at 1242 cm^{-1}, C-C of proline ring at 919 cm^{-1} and C-C of polypeptide backbone at 813 cm^{-1} (Frushour and Koenig, 1975). It is important to note that both proteoglycan and collagen^{f} fractions contain amide band contributions (mainly I and III). The amide peaks are more intense in the spectrum of collagen because of the greater protein content in comparison with that of proteoglycan.

Comparing the results with those for the Raman spectra of aggrecan and collagen in the literature (which these samples represent in their Raman signal), we find the following differences. Ellis *et al.* (2009) reported the spectrum of aggrecan although there was no phenylalanine peak present. Our spectrum of proteoglycan^{f} contains a peak for phenylalanine at 1002 cm^{-1} (Phe peak). The reason for the difference could either be due to differences in the species examined or to differences in the preparation method, as Ellis *et al.*(2009) purified aggrecan extracts by CsCl density gradient centrifugation. We would expect a peak due to phenylalanine because the protein component of aggrecan contains phenylalanine. The Raman spectrum of proteoglycan from bovine articular cartilage (commercial source) (Gamsjaeger, et al., 2014), also showed a similar spectrum to

proteoglycan^{f}, although the peak at ~1003 cm^{-1} (Phe) was stronger in intensity in their study (Bovine aggrecan core protein contains 3.4% phenylalanine (Leinonen, et al., 2004)). We note that in human samples a peak due to Phe is expected but it is not expected to be greater than that for collagen, which was the case for the result of Gamsjaeger *et al*. (2014). The reason for this is that the Phe content in the protein core of aggrecan is 2.7 %, however, the protein content is only 7 % of the aggrecan sample. In human collagen type II Phe content is 1.7 %, meaning the contribution of the Phe peak to a spectrum of proteoglycan should not be greater in intensity than the Phe peak of collagen. Furthermore, if the Phe peak was much greater in intensity in the aggrecan sample that peak would be greater when spectra were acquired at positions in the spectrum of articular cartilage where the sulphate peak is greater, and this is not found to be the case (chapter 4).

The collagen^{f} sample spectrum was very similar to Raman spectra obtained of collagen type I elsewhere (Frushour and Koenig, 1975; Dong, et al., 2004). Assignments to the collagen^{f} and proteoglycan^{f} components are made in tables 3.1 and 3.2.

Table 3.1 Assignments to bands in Raman spectrum of collagen[f]

Band frequency	Assignments to collagen type I (Frushour and Koenig, 1975)	Assignments to specific amino acid residues (De Gelder, et al., 2007)	Other assignments
617	Phe		
642	-	Pro	
760	-		δ (COO^-) (Williams, et al., 1984)
813	C-C of polypeptide backbone		
854	C-C of Pro ring	Ala	
876	C-C of Hyp ring	C-C Gly	
919	C-C of Pro ring	Ala + Pro	
936	C-C residue of protein backbone		$N\text{-}H_3^+$ (Collado and Ramírez, 1999)
960	-		
982		Arg	
1003	Phe		
1034		Phe	
1043	Pro		
1063			C-N stretch (Anigbogu, et al., 1995)
1068	Pro		
1085	ν(CN)		C-C gauche (Anigbogu, et al., 1995)
1098	C-N		
1125	-		C-C trans (Anigbogu, et al., 1995)
1160	-		γw (CH_2) Hyl (Carcamo, et al., 2012)
1214	Hyp, Tyr		
1242	Amide III		
1250	Amide III		
1315	γt (CH_3, CH_2)	Ala	
1344	-		γw (CH_2) Glycine (Carcamo, et al., 2012)
1380	γw (CH_3, CH_2)		Amide II (Tu, 1982)
1412	$\nu_s(COO^-)$		
1450	δ(CH_2, CH_3) (protein)		
1583	Pro, Hyp		
1604	Phe, Tyr		
1639			δ O-H bend
1664	Amide I		
2879	ν_s CH_3		
2936	ν_s CH_2 ν_{as} CH_3		
2983	ν_{as} CH_2		

Table 3.2 Assignments to bands in Raman spectrum of proteoglycan[f]

Band Frequency	Aggrecan assignments (Bansil, et al., 1978; Ellis, et al., 2009)	Other assignments (Barrett and Peticolas, 1979)
618	C-S stretch of C4S	
643	C-S stretch of C4S	
757		Glucuronic acid
832	ν_s CH_2-OS	
852	δ C1-H for α-anomers	
878	δ C1-H for β-anomers	
917		C-C Glucuronic acid
939	C-O-C	
997	ν_{as} CH_2-OS	
1002		Phe
1034	δ C-OH	
1063	ν_s OSO_3^- of C4S, δ C-OH (HA)	
1080	δ C-OH	
1102	δ C-OH	
1123	δ C-OH	
1159	-	C-O, C-C
1209	-	
1249	ν_{as} OSO_3^- of C4S	Amide III protein core
1270	-	Amide III protein core
1338	δ_s CH	
1378	δ_s CH_3	
1408	ν_s COOH	
1450	δ_s CH_2	
1615		- COOH (Cabassi, et al., 1978)
1667		Amide I protein core
2883	ν_s CH_3	
2934	ν_s CH_2 ν_{as} CH_3	
2980	ν_{as} CH_2	

Figure 3.2 shows the Raman spectrum of freeze-dried articular cartilage compared with those of the fractions of collagen^{f} and proteoglycan^{f}. The Raman spectrum of freeze-dried articular cartilage was similar to that previously reported (Esmonde-White, et al., 2011). The Raman spectra of the main constituents of the tissue can be seen to represent the spectrum of articular cartilage when co-added.

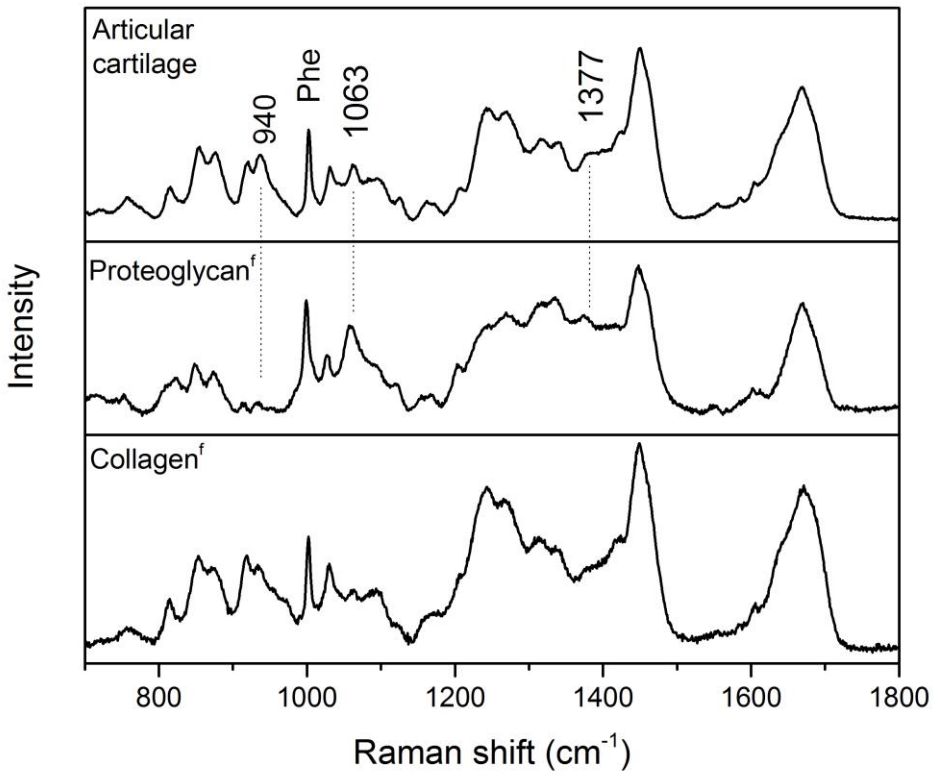

Figure 3.2 Raman spectra of collagen^{f}, proteoglycan^{f}, and articular cartilage. Raman markers for proteoglycan^{f} component highlighted.

Highlighted are the peaks which are best suited for Raman markers of proteoglycan^{f} in the spectrum of articular cartilage. These are at 1063 cm^{-1} (-O-SO_3H), 940 cm^{-1} (C-O-C linkage), and 1377 cm^{-1} (δCH_3). We were interested in determining the most suitable peaks in the spectrum of proteolgycan^{f} for use as markers for proteoglycan (aggrecan) content in articular

cartilage tissue. For this, peaks in the spectrum of proteoglycan should not overlap with a band(s) in the spectrum of collagen. Most importantly, the band should be relatively intense, to enable peak fitting and to extend the limit of detection and the dynamic range (the range of intensity levels which enable quantification of an analyte) (Hobart H. Willard, 1988).

Of the peaks selected in the spectrum above, the peak at 1377 cm^{-1} is the least strong in intensity but in a recent study by Gamsjaeger *et al.* (2014), it was suggested that this peak is more suitable than the peak at 1063 cm^{-1} for use as a marker of aggrecan in articular cartilage. The reason suggested was that there is no overlapping peak at 1377 cm^{-1} in collagen, whereas the peak at 1063 cm^{-1} of aggrecan overlaps with a peak in the collagen spectrum. However, we find that in the Raman spectrum of collagen[f], and that reported by Frushour *et al.* (1975) there is also a band at 1377 cm^{-1}. Despite the fact that the band is weak in intensity compared to the peak at 1377 cm^{-1} in proteoglycan[f], its presence makes the use of other Raman peaks more suitable, especially the peak at 1063 cm^{-1}. The peak at 940 cm^{-1} is due to the glycosidic bond between disaccharide units of KS, CS and HA (Ellis, et al., 2009). The peak at 940 cm^{-1} of the collagen component is also present in this region of the spectrum, and it is also sensitive to hydration (Zhang, et al., 2011), making this region of the spectrum variable regardless of the aggrecan content and therefore less suited for use as a Raman marker for aggrecan.

Finally, the peak at 1063 cm^{-1} has been used previously as a marker for aggrecan content (Draper, 2009). We note that it overlaps with a band at 1063 cm^{-1} in the collagen[f] spectrum in the same region, which is also apparent in spectra of collagen obtained previously (Frushour and Koenig, 1975). However, the peak at this position in the spectrum of collagen is weak relative to the intensity of the peak at 1063 cm^{-1} for proteolgycan[f]. Thus the significant intensity in the peak at 1063 cm^{-1} would provide a greater range of intensity to detect varying amounts of proteoglycan in the ECM of articular cartilage.

3.3.2 *Comparison of collagen^f with collagen type III*

The fingerprint region of the Raman spectra of collagen^f (which represented collagen type II) and collagen type III from human placenta are compared (Figure 3.3).

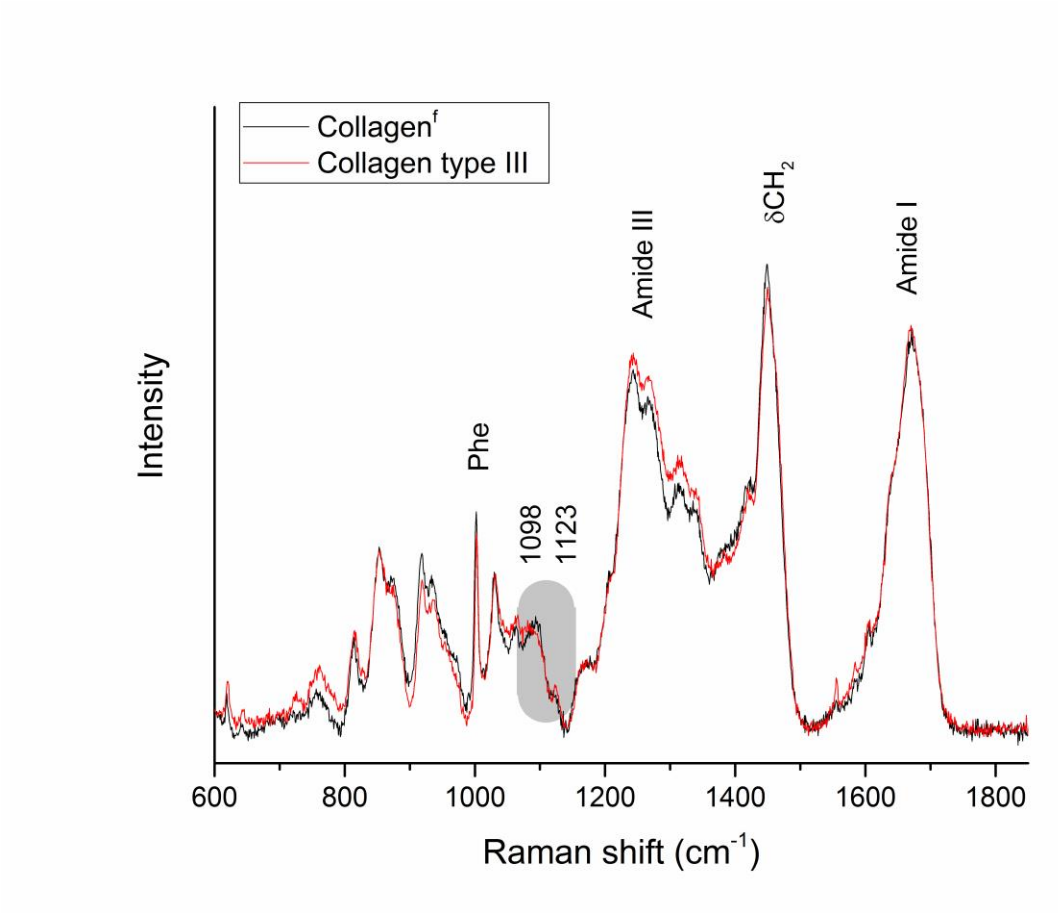

Figure 3.3 Raman spectra of collagen^f and collagen type III from human placenta. Spectra were normalised to the peak at 1003 cm^{-1} (Phe). The shaded areas show peaks that differ.

The profile of the spectra are broadly similar, for example the amide I and III bands, as well as the band at 1450 cm^{-1} (δC-H) and the peak at 1003 cm^{-1} (Phe). The main differences in these spectra are highlighted in grey and are shown in greater detail in the Figure 3.4 overleaf.

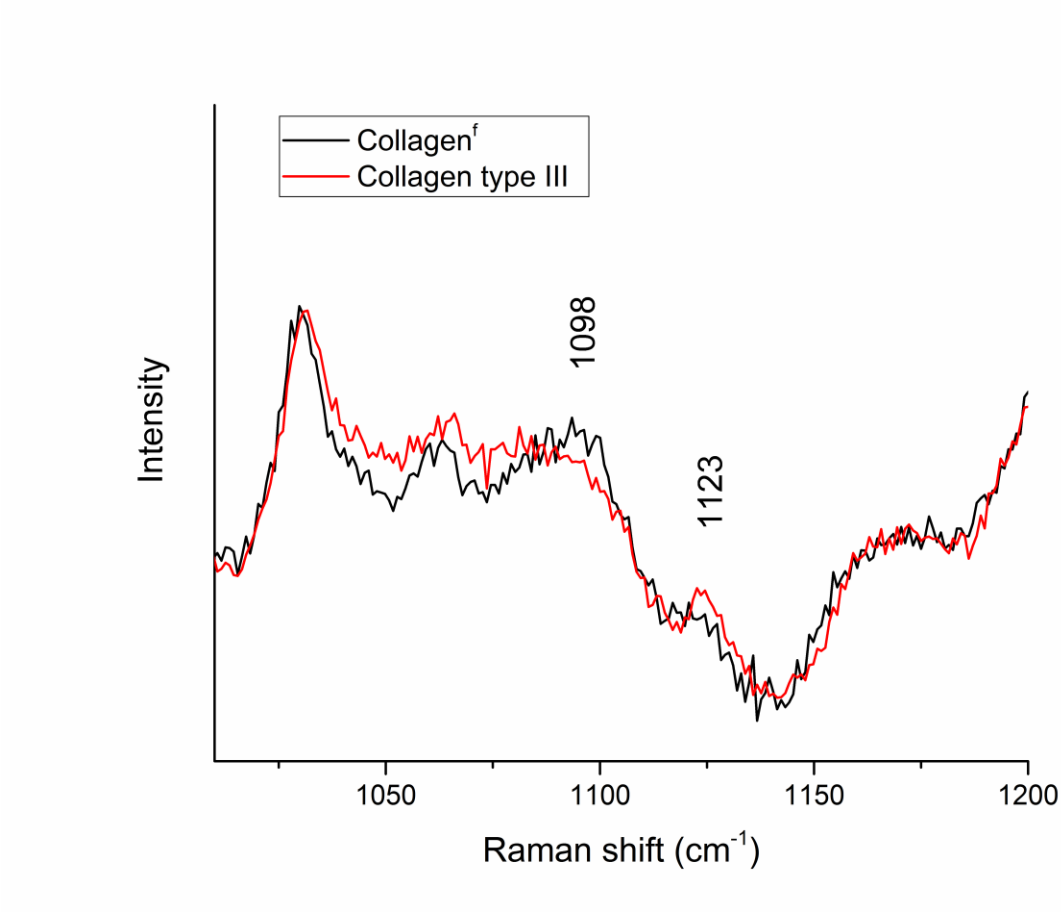

Figure 3.4 Raman spectra of collagen samples showing peaks at 1098 and 1123 cm^{-1}.

The peak intensity at 1098 cm^{-1} has a lower intensity in the spectrum of collagen type III compared to collagen[f], this peak has been assigned to C-N stretching by Frushour and Koenig (1975). Further reading of the literature revealed that there is a prominent peak in this part of the spectrum of glutamic acid (De Gelder, et al., 2007), and glutamic acid is the only amino acid residue that exhibits an intense band at 1098 cm^{-1}. The mode has been attributed to the CH_2 wag of this molecule (Shurvell and Bergin, 1989). Collagen type III contains 5.0% glutamic acid, whereas collagen type II contains 5.3%. This means that the difference in peak intensity must be due to another factor. Finally, the peak at 1123 cm^{-1} has greater intensity in the Raman spectrum of collagen type III. This peak has been assigned to NH_3^+ (due to lysine)

in type I collagen by Frushour and Koenig (1975). We note that there is a significant difference in the peak intensity but the difference in amount of lysine in collagen type III is 4.2 % and 4.5 % for type II collagen, therefore we could not attribute the significant increase in intensity to a slight increase in lysine content only. Elsewhere this peak has been attributed to C-C stretching vibrations in the trans conformation (Anigbogu, et al., 1995). It is difficult to assign this band to a known structural difference in type III collagen. Further investigations would be necessary to confirm these differences before further consideration of the cause of these differences.

3.3.3 Comparison of articular cartilage in D_2O and H_2O

In organic and biological molecules, it is well known that C-H bonds do not exchange under normal conditions, whereas the exchange of protons with deuterium occurs readily at N, O and S sites. Therefore in this study, changes in the Raman peaks are due to the exchange of protons at these sites. The comparison of Raman spectra obtained from cartilage in H_2O and in D_2O reveals the peaks that are due to exchangeable species by the shift in their position on the spectrum.

The Raman spectra reported in this section were normalised to the peak at 814 cm^{-1}, as it was not affected by the isotopic substitution and it remained distinct from overlapping bands in both samples. In contrast, the Phe peak that was used as an intensity calibrant throughout most of the studies exhibited an overlapping peak in D_2O at 990 cm^{-1} (due to N-D bend (Miyazawa, et al., 1958)), that made peak-fitting less reliable than in other studies. The Raman spectra for articular cartilage in H_2O and D_2O are shown in Figure 3.4, the data shown represent an average of 20 spectra per sample. The C-H stretching modes at 2850-2950 cm^{-1} remained unaffected by the isotopic substitution, as expected for these non-

exchangeable species.

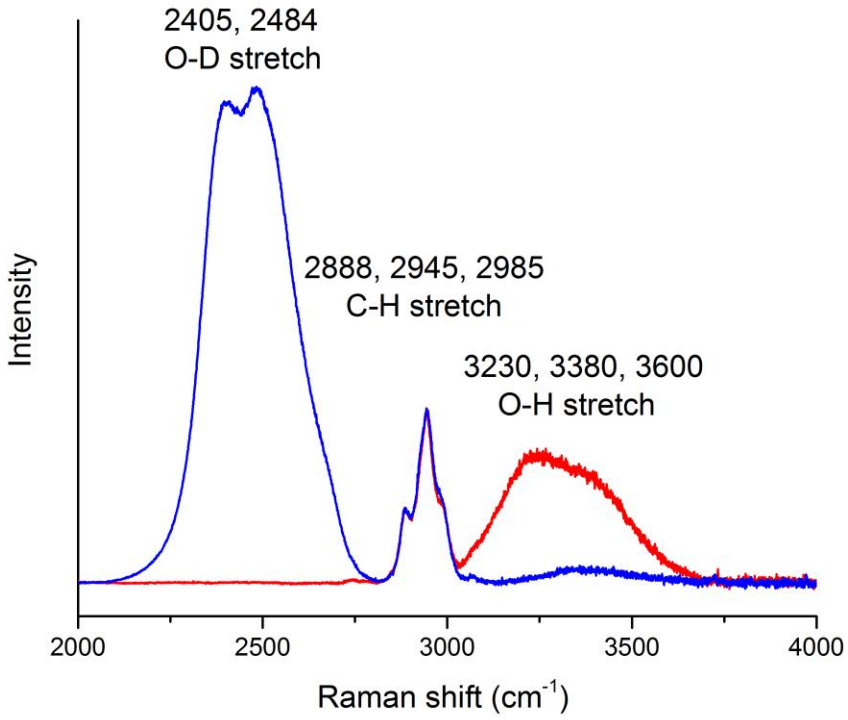

Figure 3.5 Raman spectra (region 2000-4000 cm^{-1}) of articular cartilage in D_2O and H_2O. The CH stretch peaks are similar but the OD stretch peak is greater in the deuterated sample (blue plot), compared to OH stretch being greater in the hydrated sample (red plot).

The Raman peaks for the O-H stretching vibrations in the 3200-3600 cm^{-1} region appear to be considerably lower in intensity than the O-D stretching features in the 2400-2600 cm^{-1} range. This result was initially surprising as the intensity of these peaks should be similar (Walrafen, 1964), however, this difference in intensity results from the detector sensitivity in this extreme range of the spectrum, that lies well beyond its normal operating limits. In Figure 3.6 overleaf the Raman spectra of articular cartilage in H_2O and D_2O are shown.

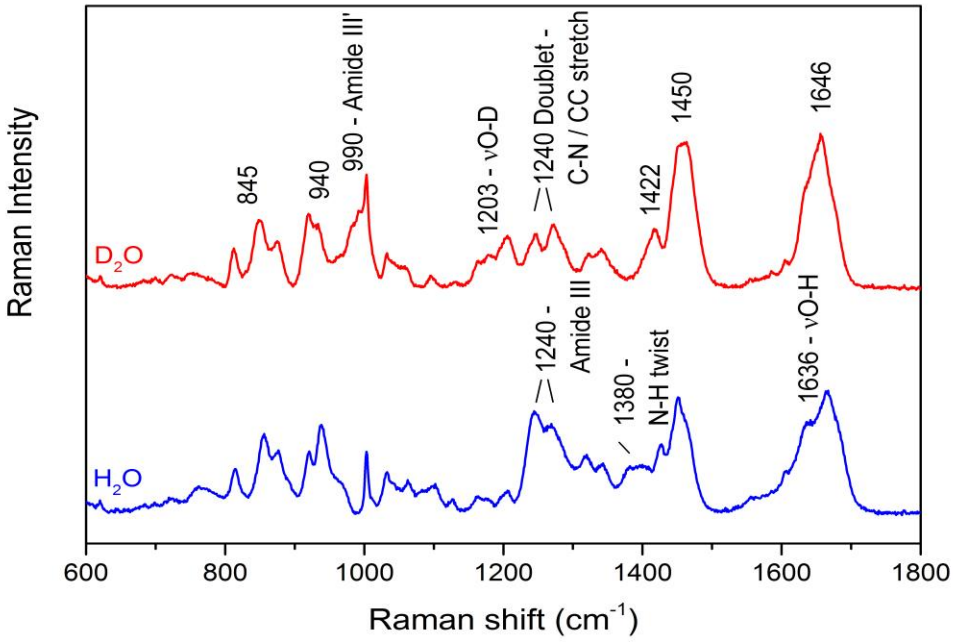

Figure 3.6 Raman spectra of articular cartilage in H_2O (blue line plot) and D_2O (red line plot).

Raman spectra of articular cartilage after exposure to D_2O compared to H_2O, exhibited the following changes; the Amide I band (1646 cm^{-1}) is less broad and the high frequency component shifts, there is an increase in intensity of the band at 1450 cm^{-1}, the peak at 1380 cm^{-1} shifts and reveals a broad and slightly downshifted peak at 1412 cm^{-1}, the amide III at 1240 cm^{-1} shifts, the appearance of a peak at 1203 cm^{-1} (this is due to O-D bending of D_2O), the Amide III' band appears at 990 cm^{-1}, the peak at 940 cm^{-1} is shifted, as well as the increase in intensity of the band at 845 cm^{-1}.

The amide I band is predominantly due to C=O stretching but contains a 20% contribution from the N-H bend (Miyazawa, et al., 1958). The decrease in width of this peak and shift at the high frequency part can be explained by the following factors. A shift in the component of this band due to the N-H bending modes, a lack of the contribution at the

shoulder of this band at 1633 cm^{-1}, (due to the O-H bending mode of water) and it is expected that there will be a shift to lower wavenumber of the C=O bonds which will be subjected to a lower degree of hydrogen bonding in the deuterated sample (compared to the hydrated sample). The trough in the difference spectrum is due to the decrease in the O-H bending contribution. The shift in the high frequency component at the high frequency part of this band must be due to the shift in the N-H bend and / or the lower hydrogen bonding with C=O of water in the dehydrated sample.

The band at 1446 cm^{-1} exhibits an increase in intensity, as was apparent in the spectra of deuterated collagen reported by Zhang *et al.* (2011), and this is probably due to the N-D in plane bend shifted from higher in the spectrum. The decrease in frequency of the peak at 1419 cm^{-1} can be observed in the sample in D_2O, owing to a shift in the neighbouring band at 1380 cm^{-1}. This revealed the width of $\nu_s COO^-$ (at 1419 cm^{-1}) of collagen and its assignment is supported by the fact that it shifts to lower frequency upon exposure to D_2O. The result of a shift at 1380 cm^{-1} was surprising as this peak has been attributed to C-H bending of collagen (Frushour and Koenig, 1975). This region of the spectrum has also been attributed to N-H twisting mode (Riauba, et al., 2006) or amide II (Tu, 1982). Since the peak at 1380 cm^{-1} shifts upon deuteration, it is more likely that this peak is due to the N-H twisting mode or amide II than the C-H bending mode as suggested by Frushour *et al.* (Frushour and Koenig, 1975).

The amide III band is a doublet and the lower frequency component of this band (1240 cm^{-1}) shifts whereas a significant component of the high frequency component of this band remains after deuteration. The band is known to result from 40% C-N stretch, 30% N-H in plane bending, 20% C-C stretch (Miyazawa, et al., 1958). It seems therefore that the lower frequency component of this amide III band is due mainly to the N-H component, which has been shifted to 990 cm^{-1} (Tu, 1982). There remains two peaks in the amide III doublet region,

these are likely to be due to the C-N and C-C stretching modes.

There was also a decrease in the intensity of the peak at 940 cm^{-1}. This was attributed to C-C vibrations by Frushour *et al*. (1975), C-C vibrational mode adjacent to the peptide bond carbonyl (Zhang, et al., 2011). Others attribute this peak to C-C of a helical polypeptides in a study on lysine (Carrier and Pézolet, 1984). It could also be due to carboxylate of amino acid residues (Edsall, 1937), or NH_3 rocking, which have also been associated with this region of the spectrum (Riauba, et al., 2006). It was not possible to define the vibrational mode that it is due to, despite the understanding that it shifts upon deuteration. This peak assignment is important because this peak is also dependant on hydration in collagen of articular cartilage (chapter 6). Further studies are required to investigate the assignment to this peak.

In Figure 3.7, the spectra of the sample in D_2O and H_2O are overlaid showing only the region 1020-1140 cm^{-1}, where the sulphate peak is found.

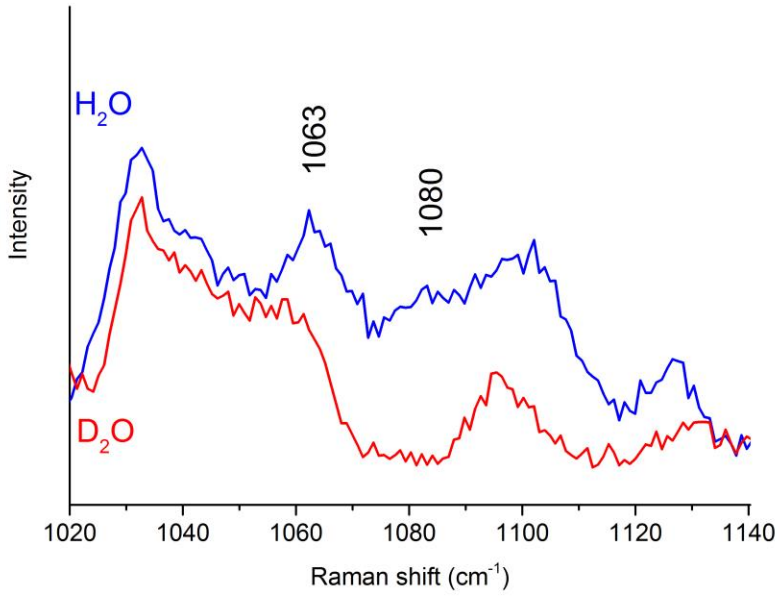

Figure 3.7 Raman spectra of cartilage in H_2O and D_2O, showing the peaks at 1063 and 1080 cm^{-1}.

A decrease in the peak at 1080 cm^{-1} is apparent in the spectrum above after deuterium exchange. A similar change in the spectrum is observed for deuterated collagen in this region (Zhang, et al., 2011). In terms of assignments to this peak in the spectrum of collagen, there are some differences in the literature; C-C stretch (Frushour and Koenig, 1975), or C-OH stretch vibrations which are known to occur in this region of the spectrum (Daimay Lin-Vien, 1991). This peak is more likely to be due to C-OH stretch rather than C-C stretch, since it is shifted upon deuteration. We note that in the spectrum of deuterated collagen reported by Zhang *et al.* (2011) the same changes in this part of the spectrum was observed. We also note that in the spectrum of the sample in H_2O we observe the weak peak at 1063 cm^{-1} that was

also present in the spectrum of collagen[f] and it exhibits a similar intensity. It appears therefore that these spectra were obtained at a part of the articular cartilage tissue that was mostly collagen. Assignments to the peak at 1063 cm^{-1} of the collagen component include vC-N (Anigbogu, et al., 1995) and C-C stretch (Frushour and Koenig, 1975). The fact that this peak is shifted indicates that could be due to a C-N stretch coupled to an adjacent exchangeable N-H for example, however we cannot confirm an assignment to this peak with this data alone. This is an important peak because it overlaps with that of the sulphate stretching mode in proteoglycan.

3.4 Discussion

In summary, we were able to obtain Raman spectra of the soluble and insoluble components of articular cartilage, proteoglycan[f] and collagen[f]. These spectra compared well with previously reported spectra of aggrecan and collagen type II, the major components of these fractions. As for the analysis of collagen type III, we found spectral features which differ to those of collagen[f] (collagen type II). In the third set of studies, the results show that it is possible to investigate the reliability of certain peak assignments using the technique of deuterium exchange. The method was particularly successful at revealing changes in components of the amide bands.

Assignments to peaks in the Raman spectra of collagen[f] and proteoglycan[f] are provided for these components in tables 3.1 and 3.2 respectively. The main difference observed in the spectrum of proteoglycan[f] is that it exhibits a Phe peak which is of lower intensity compared to that in the spectrum of aggrecan from bovine articular cartilage reported by Gamsjaeger *et al.* (2014). The result we obtained was expected as the phenylalanine content is less in human aggrecan core protein and the peak is similar in intensity to that for collagen because of the

relative amounts of Phe in collagen of the tissue. This peak is present in both constituents therefore it serves as a useful internal standard when comparing relative amounts of collagen to proteoglycan in articular cartilage, where these components are both present. Also, the peak is a sharp peak with no overlapping bands which is why it was used in work previously reported by Dudhia *et al.* (2010) and Draper *et al.* (2009).

The Raman spectra of collagen[f] and proteoglycan[f] were compared with the spectrum of articular cartilage (Figure 3.3), where it was seen that the contribution of those two components account for the signal in the spectrum of articular cartilage. This enabled direct comparison of the Raman peaks of the two components with those in the tissue. This also enabled us to evaluate the most suitable peaks for Raman markers of proteoglycan in the spectrum of articular cartilage. We found that the peaks at 940 cm^{-1} (COC stretch), 1063 cm^{-1} ($-OSO_3^-$) and 1377 cm^{-1} (δCH_3) were the most promising peaks for this, with the 1063 cm^{-1} being the best suited.

In Section 3.3.2 the Raman spectra of collagen[f] (type II collagen) was compared with collagen type III from human placenta. The spectrum of collagen type III obtained from human placenta exhibited differences in two peaks. The lower intensity of the peak at 1098 cm^{-1} and a greater intensity in the peak at 1123 cm^{-1}. We were able to assign the peak at 1098 cm^{-1} to glutamic acid (due to CH_2 wag (Shurvell and Bergin, 1989)). The peak at 1123 cm^{-1} has been attributed to C-C or C-N or Lysine. It was difficult to associate this with a difference in structure because the amino acid content of those amino acids was similar. Further investigations would be necessary to confirm that the changes were real and from there further considerations for the cause of these differences would be warranted. The Raman spectra of these collagens were similar, however, reflecting the similarity in their amino acid content.

In Section 3.3.3 the Raman spectra of articular cartilage in D_2O and H_2O were compared. It was first of all noted that the O-H stretch signal was much lower in intensity than the signal for O-D. This appears to be a result of an inaccuracy in the correction factor.

Much of the changes in the features in the fingerprint region of the spectrum of the articular cartilage sample in deuterium were due to the effect of proton exchange. The most significant changes were due to the amide vibrational modes. This enabled the characterisation of subcomponents of these bands, for example, the shift in the high frequency component of the amide I and a shift in the low frequency component of the amide III band. We were able to elucidate the high frequency component in the amide I band to a N-H component or decrease in the hydrogen bonding. We also noted that there are two components of the bands in the amide III band, the one which is at lower wavenumber is due mostly to N-H bend, since there is a shift in the peak in this region. Whereas the other peak remains even after deuterium exchange. We note that these changes were also observed in the amide bonds of the collagen sample reported by Zhang *et al*. (2011).

Furthermore, the experiment enabled the validation / alternative assignment of certain peaks that were previously attributed in the literature. For example, the shift in the peak at 1380 cm^{-1}, indicated that it is more likely to be due N-H twisting (Riauba, et al., 2006), than a previous assignment to C-H bending (Frushour and Koenig, 1975). The decrease in intensity of the peak at 1380 cm^{-1} revealed that the band at 1419 cm^{-1} appears to be a broad band. This was not obvious previously, and it may indicate that there is a series of $\nu_s COO^-$ stretching vibrations, due to the presence of carboxylic acid groups of the amino acids of collagen being in different environments (aspartic acid and glutamic acid).

Finally, the profile of the spectrum in the region 1020-1140 cm^{-1} was investigated in detail because this region of the spectrum contains many discrete vibrational modes in the

region of the sulphate peak (at 1063 cm^{-1}). The peak intensity at 1063 cm^{-1} was low, reflecting a minimal amount of sulphate content, and the peak appears to be present in the spectrum of collagen and it is shifted upon deuteration (Zhang, et al., 2011). We can attribute that band as being a result of C-N stretching that may be coupled with and N-H vibrational mode. We note that the peak at 940 cm^{-1}, which is shifted has previously been assigned to C-C of proline, we provide some alternative assignments but further work would be necessary to confirm the assignment to that peak. Finally, the peak at 1080 cm^{-1} was found to be shifted. This peak has been assigned to C-C stretch and CO-H stretch. The shift in intensity upon deuteration indicates that the most likely assignment to this band is due to CO-H stretch.

4.1 Introduction

In this chapter, micro-Raman mapping spectroscopy was used to investigate the varying distribution of proteoglycan content as a function of depth in samples of articular cartilage. This was carried out for two samples of different age groups, a younger specimen (9 years old) and a more mature specimen (62 years old). The hypothesis to be tested was to what degree there are detectable changes in the sulphate content as a function of depth in the two specimens.

We observed an increase in width of the peak at 1063 cm^{-1} for spectra obtained in the young specimen relative to the width of the same peak in spectra obtained from the mature specimen, which may be related to age-related differences in biochemistry of these samples. We also observe a greater proteoglycan content in the articular cartilage section of the young specimen. Samples from both specimens exhibit variability in the markers for proteoglycan at different depths, indicating the localization of the proteoglycan component in cartilage tissue.

4.1.1 Varying composition of articular cartilage tissue with the depth

It was indicated in the introduction to this thesis that the major compositional change in articular cartilage is due to the variation in aggrecan content as a function of depth. The general understanding is that that the superficial zone contains the least aggrecan content, then the mid zone and transitional zones and finally the deep zone contains yet more aggrecan (Muir, et al., 1970; Mueller, et al., 2014). It has been reported by Muir *et al.* (1970) that there can be as much as a 5-10% increase in GAG content as a function of depth from the

superficial to the deep zone (the GAG content was attributed to aggrecan content). It is also known that tissue from young specimens contain greater quantities of aggrecan than tissue of mature individuals (Bayliss, et al., 1999; Wells, et al., 2003).

We used tissue sections of articular cartilage to obtain spectra along the depth from the cartilage surface to the cartilage-bone interface (CSU to CBI). Raman markers for proteoglycan[f], evaluated in chapter 3 were used to demonstrate changes in proteoglycan content relative to collagen. Histology was also performed on these samples to stain for proteoglycan.

4.2 Method

4.2.1 Cryostat sectioning of articular cartilage tissue sections

Tissue sections of 30 μm were obtained from full-depth cartilage samples of two specimens (an 9 year donor and a 62 year donor). Sections of 30 μm were used in this work because they were found to self-attach to the CaF_2 microscope slides whereas thinner sections (which are typically used for histology) did not. The overall thickness of the non-calcified cartilage pieces was approximately 10000 μm and 5000 μm for the young and mature specimens, respectively (excluding subchondral bone). Sections were cut from the tissue blocks (as described in chapter 2) perpendicular to the plane of the synovial surface i.e. longitudinal sections relative to the long axis of the femur. Care was taken to ensure that the orientation of the sections was recorded, CSU to CBI. The tissue sections sliced from the sample of the mature specimen did not show visual evidence of bone, however, this did not present a problem as we traced the orientation of the sample with respect to the synovial and bone surfaces.

Alternate tissue sections were collected on microscope slides of CaF_2 and normal glass

microscope slides, for Raman analysis and histology respectively. This meant that the histology sections could be compared with the adjacently cut sections for Raman mapping. Histology was carried out as described in chapter 2 and sections of the two specimens were treated with the same staining procedure.

Composite micrographs of the sections scanned in the Raman mapping study and adjacent stained sections are shown in Figure 4.1

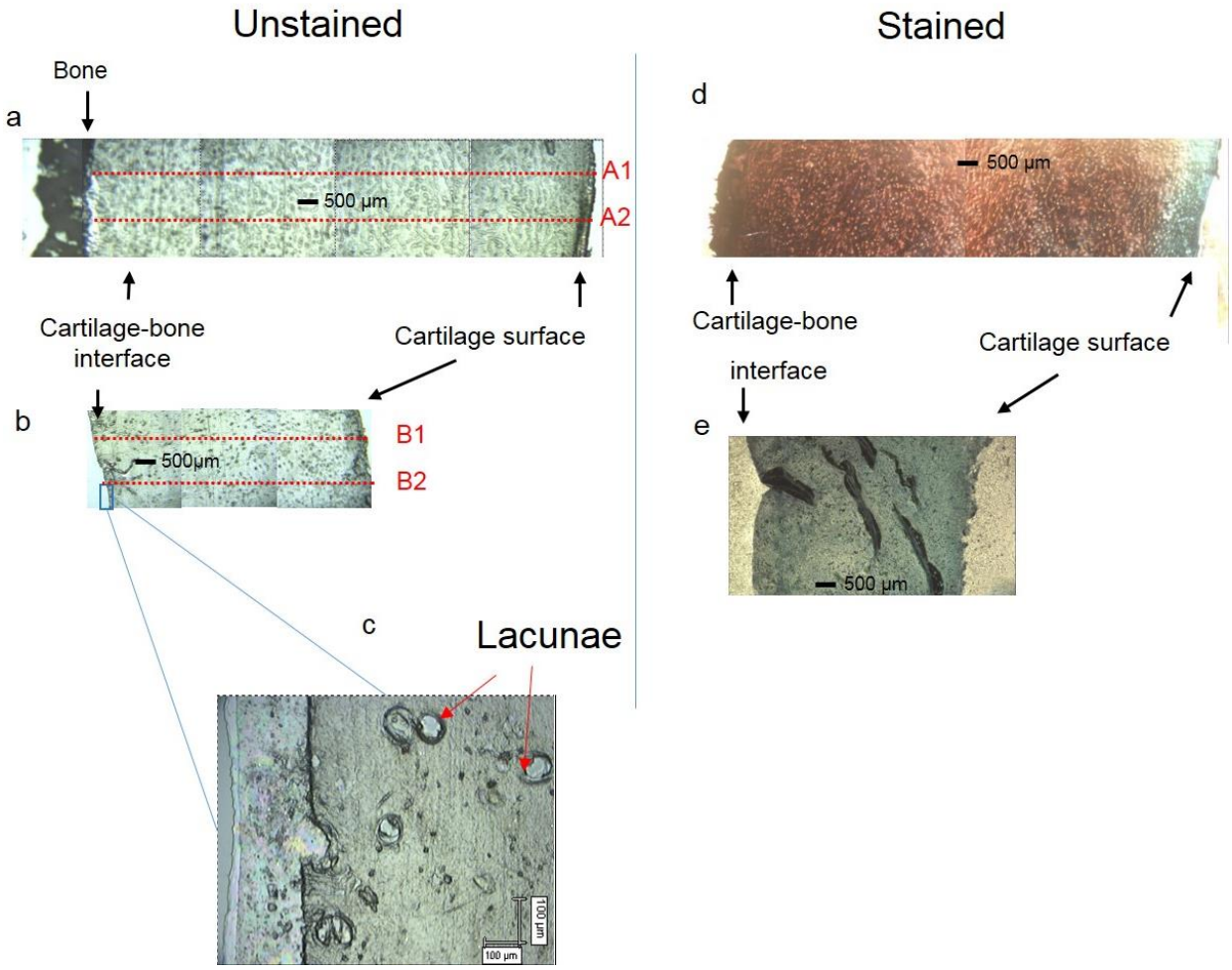

Figure 4.1 Micrographs of unstained and stained sections of articular cartilage (all 30 µm thick), from a young (9 years) and a mature specimen (62 years). Micrographs obtained with a 10x magnification objective, of tissue sections that were not stained from, ***a****) the young specimen and* ***b****) the mature specimen, showing the cartilage-bone interface to the left and cartilage surface to the right. The positions where Raman line scans were carried out on the unstained sections are shown.* ***c)*** *micrograph showing lacunae in tissue sections (20x). Stained tissue sections with safranin o and fast green for* ***d)*** *young specimen and* ***e)*** *mature specimen (4x microscope objective).*

The tissue sections shown in Figure 4.1 a and b were obtained serial to those shown in micrographs of Figure 4.1 d and e.

In terms of the histology staining, the section from the young donor (Figure 4.1 d) stained red, showing an obvious superficial zone (which stained green). The section obtained

from the mature specimen (Figure 4.1 e) appeared to be stained green without any obvious red staining. The micrograph of the mature tissue section shows that the detailed structure was not discernible because the DPX glue formed bubbles, also the tissue folded over itself, this was a recurring problem with the tissue of the mature specimen. We concluded that the young specimen showed a full-depth section from synovial surface to CBI, however in the case of the sections cut from the mature specimen we did not observe the same features.

The tissue sections from the mature specimen showed evidence of thinning. Thinning is known to be a factor in ageing and would explain the much lower thickness of the section from the mature specimen (Hall, 2005). It is not known whether it occurs at the synovial surface, middle or CBI. This meant that we could not reliably compare equivalent depths in the samples analysed (of the different specimens), or attribute the CSU and CBI to such regions *per se* in the sections of the mature specimen. Herein we refer to the surface of each tissue specimen as the CSU for clarity. The unstained tissue sections were analysed as described in the next section.

4.2.2 Raman mapping set-up and data analysis

An InVia Raman microscope (RM1000, Renishaw, Gloucester) coupled to a translatable sample stage was used for Raman mapping experiments (as described in chapter 2). Spectral acquisition was carried out at 50 points in sequence along the axis of the tissue sections (CSU to CBI). The distance between the edge of the tissue section at the CSU and the edge of the tissue before the subchondral bone (at CBI) was measured and divided by 50 to give the step size – distance between the positions at which spectra were obtained. We chose to obtain the same number of spectra along the depth for both sections (one for each specimen). Owing to the difference in depth of the cartilage tissue sections of young and mature specimens, the

step size was approximately every 200 μm and 100 μm along the tissue sections respectively. Two line scans were performed per tissue section and each line scan took approximately 12 hours to complete.

The positions along the tissue samples where these scans took place are shown in Figure 4.1 above at positions 1000 μm along the axis parallel to the cartilage surface. Since the cartilage surface of the tissue sections was not completely flat, the lengths of each line scan varies. Table 4.1 below summarises the line scans performed, including; total length of scan (from first scan at CSU to the last scan at the CBI), step size and points along the series where spectra were missing.

Table 4.1 Line scan properties for samples scanned

Sample	Line scan	Length (μm)	Step size (μm)	Spectra absent
Young specimen	Scan A1	9972	195.53	27
	Scan A2	10063	201.26	7, 18, 29 and 39
Mature specimen	Scan B1	5017.6	102.4	8, 19, 40 and 43
	Scan B2	5944	118.88	6, 23, and 35

At certain positions along the depth of the tissue Raman spectra were absent in the data obtained, this was a result of the acquisition of spectra where the lacunae in the tissue sections were present. These lacunae are shown in Figure 4.1 d, and appear as voids where the space for the chondrocyte cells were present and is made up of mostly collagen type VI (Poole, et al., 1988). The cells appear to no longer be present as a result of the sectioning process.

In the raw data obtained, we also observed varying contribution from the 0.75 N.A. objective, which affords bands in the spectrum at 1334 and 1538 cm^{-1} (see chapter 2). The contribution was subtracted by the method described in Figure 2.7. As a result of this, and

also a difference in the peak width of the 1063 cm^{-1} peak in the spectra obtained from the different specimens, a peak fitting study was less viable. To avoid the potential misrepresentation of peak intensity data by comparing values for peak areas in Raman spectra, peak intensities were visually inspected for changes in relative intensity. Therefore we aimed to semi-quantitatively indicate differences in the proteoglycan content, by changes in the relative intensity of the markers for proteoglycan in the spectra we obtained along the depth of the tissue section. The data was normalised to the peak at 1003 cm^{-1} (Phe). This peak is best suited to normalisation because it is sharp, absent of overlapping peaks, and it is similar in both samples of collagen and proteoglycan, as revealed in chapter 3.

4.3 Results

4.3.1 Raman spectra of tissue sections as a function of depth

Spectra obtained along the depth of the tissue, from the CSU, at 50% depth and at the CBI (obtained at points 1, 25 and 50 steps along the tissue depth), are shown for the young and the mature specimen (Figure 4.2 overleaf).

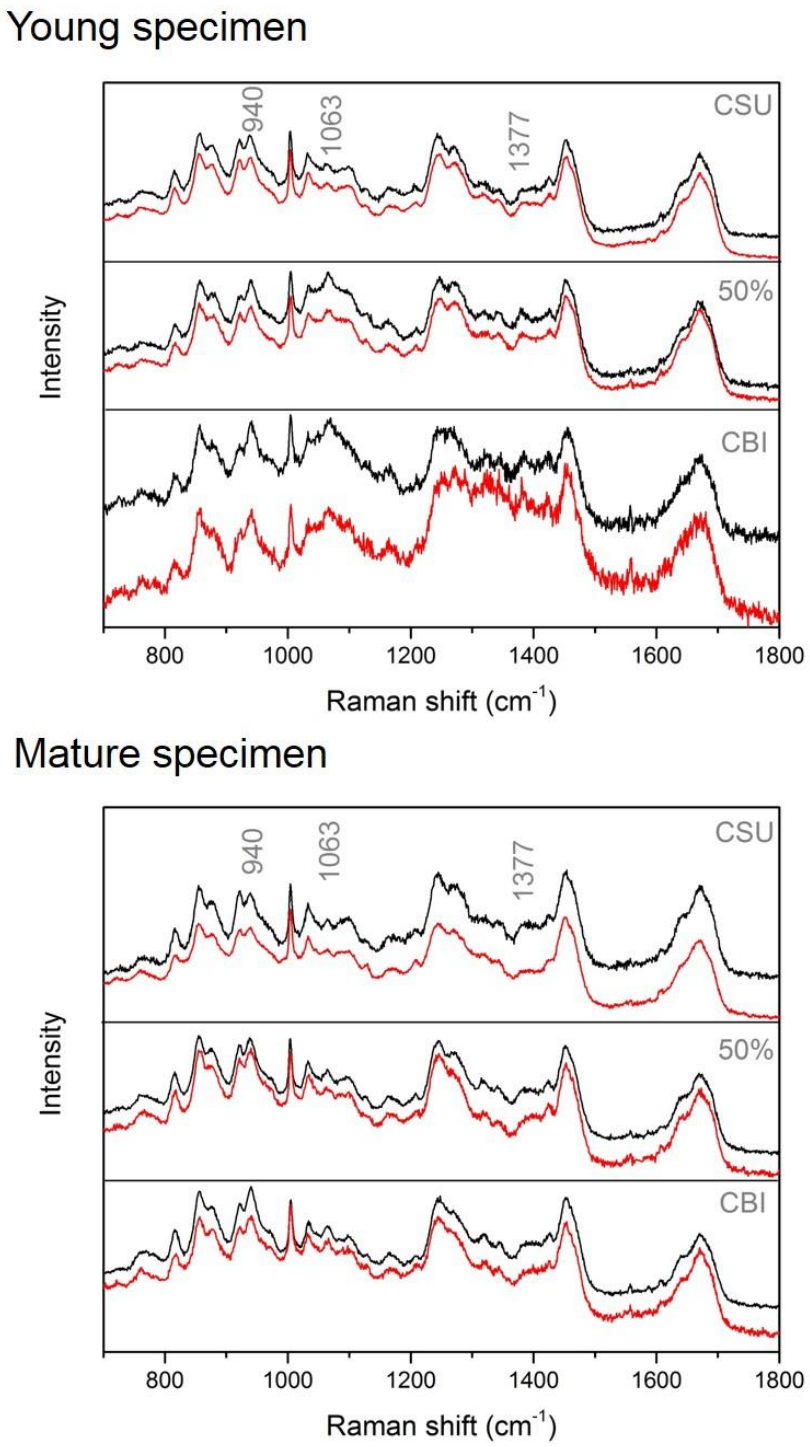

Figure 4.2 Normalised Raman spectra at three points along the full depth of tissue sections of young (9 years) and mature specimens (62 years). Red line plot and black line plots indicate spectra of line scans 1 and 2 along the surface of the respective samples of the two specimens (A1 versus *A2 and B1* versus *B2). Spectra shown are those obtained at the cartilage surface, 50 % depth and cartilage-bone interface.*

The results for the duplicated line scans from both specimens at these depths were comparable, with slight changes in signal-to-noise ratio along the depth. This indicated that the results were consistent and relate to the changes in tissue composition. The sample from the young specimen showed an uneven surface at the CBI, where the subchondral bone was still attached to the tissue. This explains the low signal-to-noise ratio in that depth of the tissue section.

For the young specimen, spectra obtained at position 1 exhibited little evidence of contribution to the spectrum from the proteoglycan component of the tissue. This was expected since the region close to the CSU is known to have the highest collagen content in the tissue (Muir, et al., 1970). At 50% depth into the tissue, the most significant changes were in the increase in intensity of the peaks at 940 cm^{-1}, 1063 cm^{-1} and 1377 cm^{-1}. As for the spectra obtained at the CBI there was a lower signal-to-noise ratio, but we could discern that there was no further increase in the peaks due to proteoglycan by comparing the peak at 1063 cm^{-1} with that of the spectrum obtained at 50% depth. This is demonstrated in Figure 4.3 overleaf and is infact not representative of what we observe for the other spectra obtained at this depth. The markers for proteoglycan were unusually high at the position 25, and in the neighbouring scans, a lower intensity of these peaks was observed and a gradual increase in the markers of proteoglycan was observed between the 50 % depth and the CBI.

As for the mature specimen, there was also a low proteoglycan content at the cartilage surface, with a very discrete increase in the 1063 cm^{-1} peak at 50 % depth. At the CBI there was a further increase in the 1063 cm^{-1} peak to the same degree. It was possible to observe a concomitant increase in the 940 cm^{-1} peak commensurate with the increase in the 1063 cm^{-1} peak but this was not possible for the peak at 1377 cm^{-1}.

The main finding was that the peak at 1063 cm^{-1} was much greater in intensity in the

young specimen along the depth beyond the cartilage surface of these samples. Furthermore, that peak at 1063 cm^{-1} in the spectra of the young specimen showed an increase in width associated with the increase in intensity (Figure 4.3a).

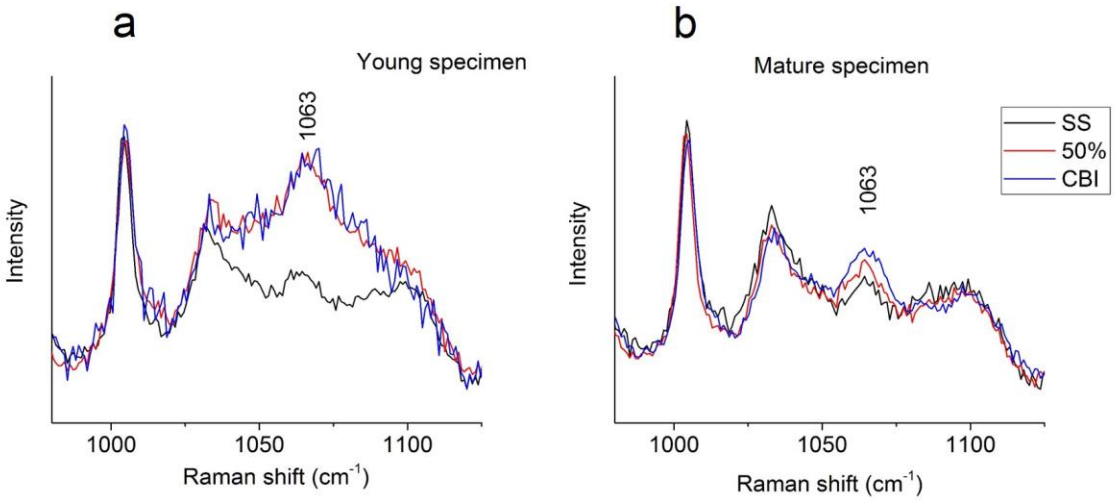

Figure 4.3 Intensity of the peak at 1063 cm^{-1} at three points along full the depth for the young (9 years) and mature specimen (62 years). ***a****) young specimen and* ***b****) mature specimen, at cartilage surface, 50 % depth and cartilage-bone interface.*

By comparison, the gradual increase in the 1063 cm^{-1} peak in articular cartilage from the mature specimen does not appear to show such broadening (Figure 4.3b). From this data alone it was not possible to determine whether this was due to the much greater intensity in the peak at 1063 cm^{-1} in the spectra of the young specimen compared to the mature specimen peak, or because of a real increase in width. We discuss this further in the next section.

4.3.2 *Variability in proteoglycan content along the depth*

Upon further examination of the spectra obtained along the full depth of the tissue sections, we noted that there was a degree of variability in the peak intensities that resulted from the proteoglycan component of the tissue. Despite this variability in the peak intensity

for the tissue of the young specimen we found that at the extremities of the tissue section, at the CSU and the CBI, the intensities of the proteoglycan markers were distinctly low and high with respect to the rest of depth of the sample. To demonstrate this, spectra of line scans A1 obtained along the full depth and in these regions are shown in Figure 4.4. We show the peaks at 940 cm^{-1} and 1063 cm^{-1}, their intensities change concomitantly with changes in the proteoglycan content (both being markers for proteoglycan).

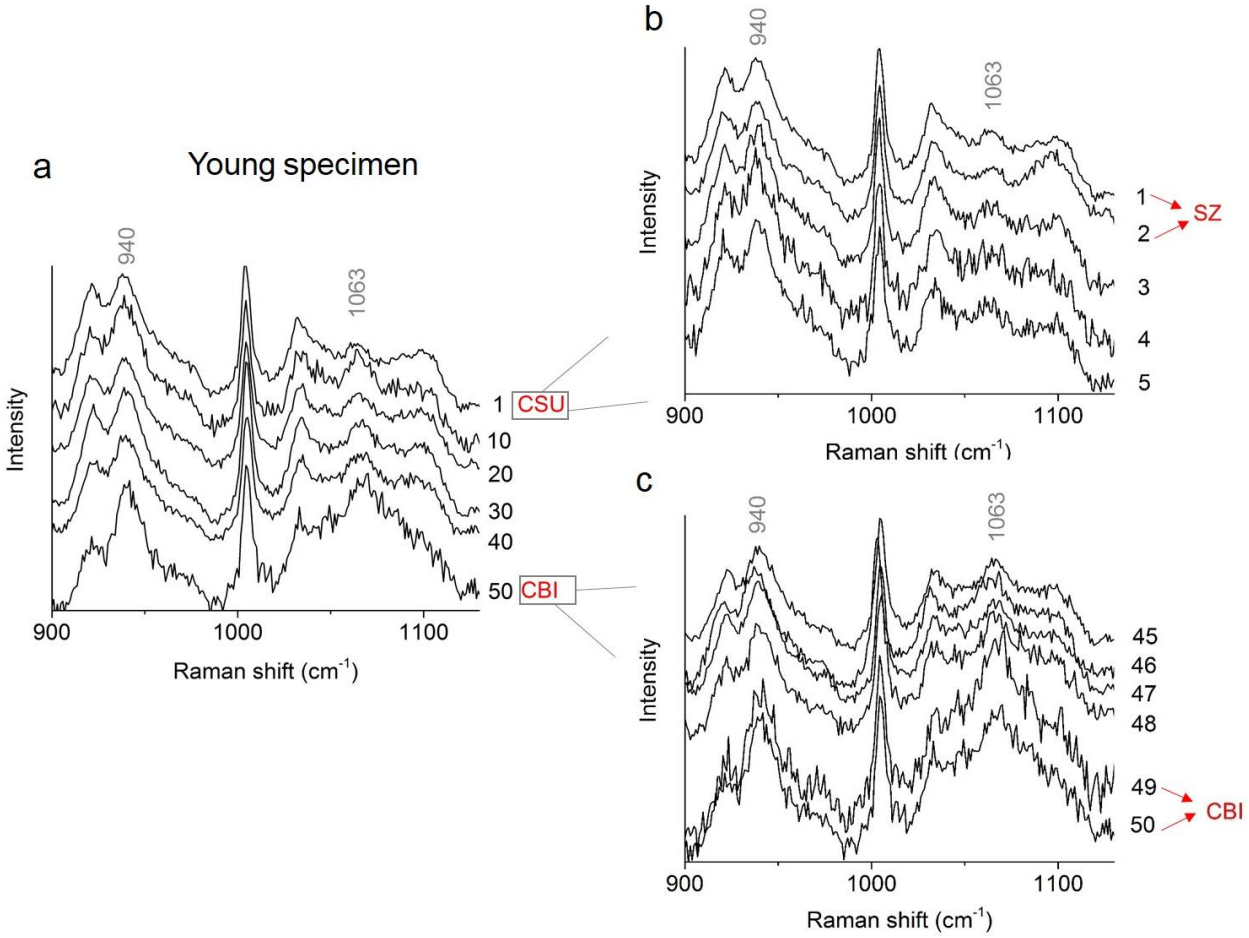

Figure 4.4 Variability in the proteoglycan markers in Raman spectra obtained for the young specimen along the depth, at cartilage surface and cartilage-bone interface. ***a****) Along the full depth at positions 1, 10, 20, 30, 40 and 50.* ***b****) In the vicinity of CSU, at positions 1, 2, 3, 4 and 5.* ***c****) In the vicinity of CBI, at positions 45, 46, 47, 48, 49 and 50.*

Figure 4.4a shows the increase in intensity of the peaks at 940 and 1063 cm^{-1} as a function of depth, but also at position 10 compared to position 20 those peaks are greater in intensity, indicating that as there are positions where the proteoglycan is in greater amounts despite being at a position closer to the cartilage surface. We note that the spectra obtained at similar positions along the depth in the second scan (line scan 2) did not show commensurate changes in the intensities for these peaks, i.e. the intensity of the peaks for proteoglycan were not equal at position 10 for line scans A1 and A2. It is unlikely that this variability is due to positions where the lacunae occur, this is because that would have led to a lower intensity in the signal from the cartilage, and by normalising we correct for this. We discuss the possible causes of variability in the markers for proteoglycan in the next section.

Figure 4.4 b shows that spectra at positions 1 and 2 (0 to 391.06 μm into the depth) exhibit a distinctly lower intensity in the peaks at 940 and 1063 cm^{-1}, compared to those obtained at 3 – 5 . In the series of spectra obtained at the CBI (Figure 4.4c), the 940 and 1063 cm^{-1} peaks are greater in intensity for spectra obtained at positions 49 and 50 compared to positions 48, 47, 46 and 45. This highlights that in the region of the CBI, up to 391.06 μm away from the bone there is a much greater proteoglycan content in the tissue.

In summary, the results showed a variability along the depth, however we could not confirm that these were due to variability in the layers because the variations in intensity as a function of depth did not correspond in the separate line scans. On the other hand, we observed distinct regions at the CSU and CBI where the proteoglycan-related markers were consistently low and high respectively for both line scans. Furthermore, the results for spectra obtained in series; 1 + 2 and 49 + 50 were consistent at adjacent positions in the duplicated line scans, indicating that the changes were due to a change in composition associated with these depths of the tissue.

In Figure 4.5, we show the Raman spectra obtained during line scan B1 at points along the full depth, at the CSU and the CBI for the mature specimen (62 years).

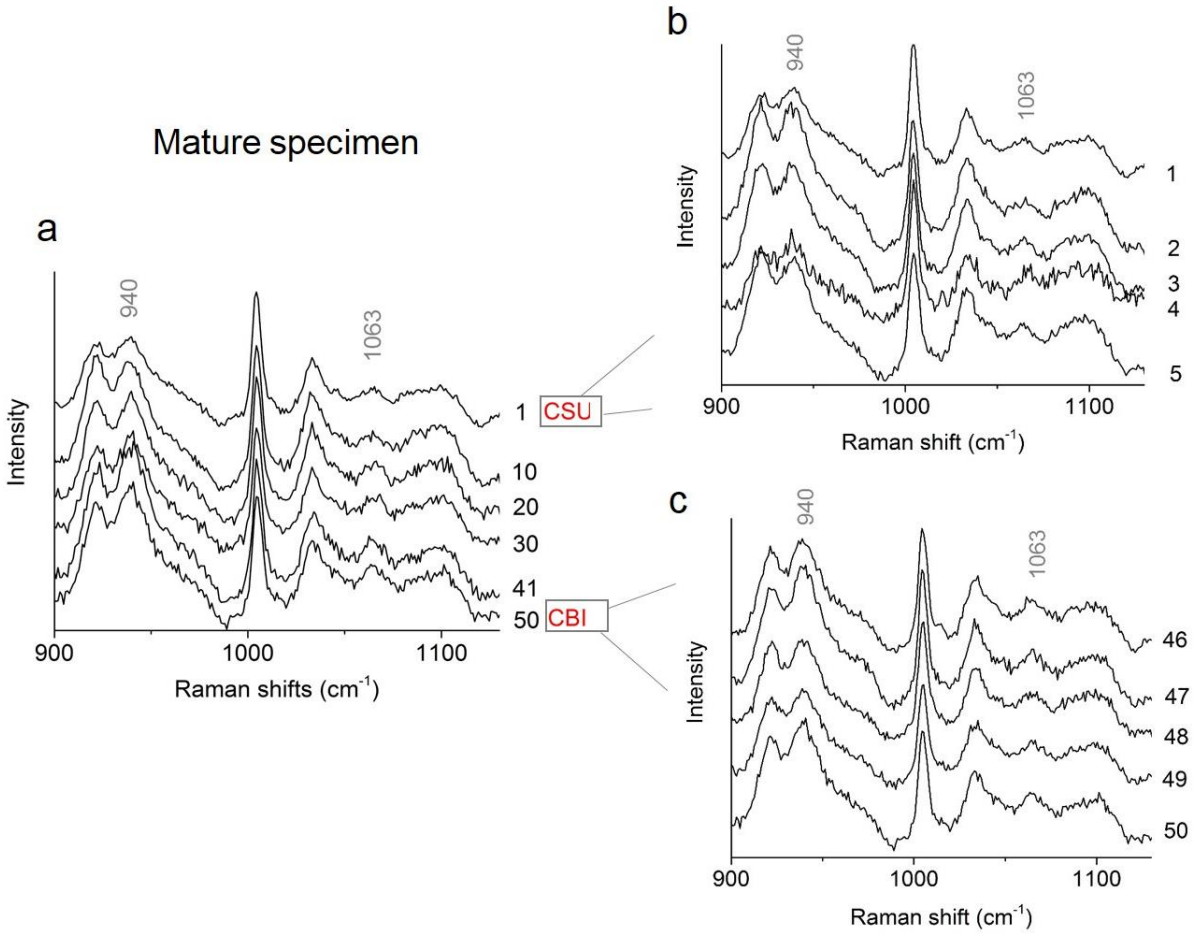

Figure 4.5 Variability in the markers of proteoglycan in Raman spectra obtained for the mature specimen along the depth, at cartilage surface and cartilage-bone interface. ***a****) At positions 1, 10, 20, 30, 41 and 50.* ***b****) In the vicinity of the cartilage surface, at positions 1, 2, 3, 4 and 5.* ***c****) In the vicinity of the CBI, at positions 46, 47, 48, 49 and 50.*

Along the full depth (Figure 4.5a), there is a gradual increase in the peaks at 940 and 1063 cm^{-1}, pointing towards an increase in proteoglycan content as a function of depth. Figure 4.5c shows some variability along the depth, where the peak at 1063 cm^{-1} is greater at position 46 than the peak at 47 and 48. We could not observe commensurate changes in spectra obtained at equivalent positions of line scan B2.

Figure 4.5b shows the spectra obtained in the region of the CSU; in that series (spectra 1-5), there was no obvious region of low intensity in the peaks at 940 and 1063 cm^{-1}, as we had observed for the spectra obtained at similar depths for the young specimen. A similar result was obtained for the CBI region, a lack of obvious increase in intensity of the proteoglycan markers in this region. Even at ~400 μm away from the CBI, at position 46 we did not observe a difference (and for the layers not shown, 45, 44).

In summary, we observed also variability in the intensity of the proteoglycan markers. However, in comparison with the data obtained for the young specimen, where there appeared to be depths of tissue of ~400 μm from the CSU and CBI with characteristically low and high proteoglycan contents, we did not observe such regions in the tissue for the mature specimen. The likely causes of this are discussed below.

4.4 Discussion

In this study, an increase in intensity in the peaks due to proteoglycan was taken as an increase in proteoglycan content. These were the peaks at 1063 cm^{-1} (due to the symmetric stretch of the sulphate group), at 940 cm^{-1} (due to C-O-C stretch of glycosidic bonds) and at 1377 cm^{-1} (due to CH_3 bending). The peak due to the sulphate stretching mode exhibited the greatest increase in intensity in these studies, we also found it was also useful to show the changes in the peak at 940 cm^{-1}, which changed concomitantly, and appears in the same region of the spectrum. Peak intensity was not plotted as a function of depth as the variability in the background contribution meant that such values would not be comparable (see Section 2.4.2).

In agreement with the biochemical studies (Muir, et al., 1970; Mueller, et al., 2014), we

observed evidence for an increasing amount of proteoglycan content as a function of depth in the articular cartilage samples studied (in both age groups). We also found that there was a significant degree of variability in the peak intensity at different positions; at points closer to the CSU their intensity was sometimes greater than in spectra obtained at points closer to the CBI. This pointed towards localised regions of higher proteoglycan content. This was observed in spectra obtained at different positions along the depth but changes were not commensurate in spectra obtained in the duplicate line scans. This however may have been due to the fact that, the depths were different for the separate line scans for each specimen (see line scan length in table 4.1). An alternative explanation, is that there are indeed localised variations in specific cartilage components which are highlighted by the sensitivity and molecular scale resolution of Raman spectroscopy. We note that localised regions of greater proteoglycan content have been observed recently in a study using IR spectroscopy beyond the superficial zone (Khanarian, et al., 2014). Also more localised concentrations of components can occur e.g. the collagen type VI rich periphery of chondrocytes (Poole, et al., 1987). Therefore, while the overall molecular composition may be highly similar at each zone of cartilage, there may exist previously undefined localised variations within each zone. More detailed scans with more lines is now required to resolve this intriguing finding.

The depth of the articular cartilage tissue of the younger specimen (9 years) was twice as thick as the mature specimen (62 years), along the longitudinal axis. Therefore, what we analysed as 50 points along the depth in the mature specimen may not have contained a CSU or CBI. Thus the two specimens were not compared as a function of depth in this study, we discuss this aspect for the two specimens separately.

In the young specimen, spectra obtained at up to 391.06 μm depth exhibited a distinct profile (similar to the profile of the spectrum of collagen[f] reported in chapter 3) compared to

adjacent depths, indicating that this depth was characteristically low in sulphate content and high in collagen. We surmise that this was the superficial zone. In spectra obtained beyond > 391.06 μm we observed a greater intensity in the 1063 cm^{-1} peak in the younger specimen Beyond the spectra obtained at positions 1 and 2, there was a gradual increase in intensity. At the CBI (at 391.06 μm), we observed that there was a region of distinctly high sulphate content and the same results observed in the duplicates line scan for this specimen. This suggests that at the CBI proteoglycan content was much greater. From this we can conclude that for the young specimen we were able to detect regions of characteristically low and high sulphate content in the superficial zone and CBI respectively

As for the mature specimen there was no evidence for regions of low and high proteoglycan content in the region of the CSU and CBI. Even at ~400 μm from those depths and deeper, where the young specimen exhibited characteristic changes, we were not able to observe distinct regions of the tissue using the Raman markers for proteoglycan. Whether this was because of the absence of a synovial surface and / or CBI in the sections cut from this specimen, or whether it is because of the lower proteoglycan content for which it was more difficult to detect changes is not yet known. During age-related thinning of cartilage there is debate on whether the thinning occurs due to a loss of the superficial zone or advance of the calcified zone or indeed loss from the middle zones of cartilage. Therefore, further studies may be useful and enable investigations into this.

A surprising result was that the 1063 cm^{-1} appeared to be much broader for the young specimen compared to the mature specimen. The studies performed in this thesis and previous studies have involved tissue specimens from mature individuals, this was the first investigation of the Raman spectrum of articular cartilage tissue from a young specimen (9 years). Comparing the width of that peak in the young specimen with the width of the same

peak in the samples of the mature specimen in this chapter and those of Figure 3.2 and Figure 6.4 (of 49 year old donor), it appears that the peak width in spectra of the young specimen is related to age. It could relate to the relative amounts of C4S and C6S in articular cartilage tissue of these different age groups. As stated in the introduction chapter, the ratio of C4S : C6S is sub-equal in the younger specimen but in mature specimens there is more C6S and less C4S. Also, we know that the C4S exhibits a broad vibrational mode at 1063 cm^{-1} whereas the C6S exhibits a sharper peak at 1063 cm^{-1} (Bansil, et al., 1978). The greater amount of C4S in the younger specimen would therefore explain why there is a broad contribution in the spectra where the 1063 cm^{-1} peak increases in intensity in the spectra of the young specimen. Further studies on different samples would be necessary to confirm this supposition.

Taking the intensity difference in the sulphate peak at the CBI, where the sulphate peak was most intense in samples from both ages; and both samples were at a similar depth, we observe that the peak was at least four times greater in the young specimen compared to the mature specimen (Figure 4.3). The result confirms a greater degree of proteoglycan in the articular cartilage tissue of the young compared to the mature specimen (Wells, et al., 2003).

Despite this limitation in the study due to the background contribution, it was still possible to make semi-quantitative investigations into the changes in the proteoglycan content along the depth of these samples of articular cartilage tissue. For the first time, we have demonstrated that with Raman mapping spectroscopy it is possible to detect localized changes in the proteoglycan content in different regions along the depth of the tissue. Also, with Raman mapping we can detect the regions of the superficial zone and cartilage-bone interface in tissue of a young specimen. This was not possible for the mature specimen analysed, further investigations are necessary to reveal the differences that we observe in the composition of the mature specimen compared to the young specimen.

The limitation of these results were that we used samples from only two individuals and they were of different age ranges (young and mature). We were able to demonstrate changes in sulphate content of healthy cartilage as increasing as a function of depth, confirming our hypothesis. In order to develop quantitative data for comparison with peak areas, a more reliable means of estimating the background to be subtraction from spectra would need to be developed. Further studies of different samples from the same age groups would be necessary to confirm the differences of the two ages that we observed.

Chapter 5 High temperature studies of articular cartilage and collagen

5.1 Introduction

This chapter describes investigations into structural changes of freeze-dried articular cartilage and freeze-dried collagen[f] at high temperature. We were interested in demonstrating the nature of structural changes in articular cartilage and collagen in the temperature range of denaturation. It has not previously been studied by Raman spectroscopy, and we were able to demonstrate the process of peptide bond dissociation in dehydrated articular cartilage.

Previous studies proposed that endothermic signatures at 60-70°C in differential scanning calorimetry (DSC) scans of hydrated collagen samples (type I) were due to unfolding of the polypeptide triple-helix, resulting in denaturation (Miles, *et al.*, 1995; Miles and Ghelashvili, 1999). For freeze-dried collagen samples recent evidence suggests that there is an irreversible change in structure upon heating above the temperature at which the endothermic peak occurs, at 150-200°C (Miles and Ghelashvili, 1999). In this study, we found that within that temperature range samples of freeze-dried articular cartilage and collagen undergo ionisation carboxylic acid groups and exhibit a lower tendency to reabsorb water. Thermogravimetric analysis (TGA) and mass spectrometry (MS) revealed the presence of remaining bound H_2O within the freeze-dried samples of articular cartilage.

5.1.1 Introduction to denaturation in articular cartilage and collagen

Denaturation of protein and polypeptide materials was first defined in 1970s as any process that alters or destroys the secondary or tertiary structures characteristic of a protein, resulting in loss of functionality (Kauzmann, 1959). Denaturation does not involve changes

in the primary structure of protein molecules.

Most studies of denaturation have used differential scanning calorimetry (DSC) to characterise the denaturation event (Privalov and Dragan, 2007). This technique measures and compares, quantitatively, the amount of thermal energy required to increase the temperature of a sample, compared to that of a reference sample, by a given amount. The difference between the two reveals the exo- or endothermic signatures related to conformational or phase changes within a sample, or reaction process. DSC studies or measurements by the related technique of differential thermal analysis (DTA) are usually carried out to investigate denaturation of proteins, which is observed as an endothermic event in the DSC thermogram.

Since the early studies on collagen denaturation in the 1970s, it has been assumed that the endothermic peak in the DSC thermogram of collagen samples is due to unfolding of the collagen triple-helix while the primary structure remains intact (Privalov and Tiktopul.Ei, 1970; Finch and Ledward, 1972). In subsequent work - this interpretation has been retained and the process of unfolding of this macromolecule continues to be associated with the endothermic peaks observed at 60-70°C for hydrated collagen (Miles, *et al.*, 1995). The characterisation of the triple-helix unfolding of hydrated collagen samples has been carried out using circular dichroism (CD) (Hayashi, *et al.*, 1979) or optical rotation (Burjanadze and Bezhitadze, 1992).

In the last twenty years, there has been interest in the denaturation of partially dehydrated collagen samples (Miles and Ghelashvili, 1999; Trebacz and Wojtowicz, 2005). Such samples may be described as partially dehydrated because they are known to retain some water despite rigorous dehydrating procedures such as freeze-drying (Nomura, et al., 1977). Miles and Ghelashvili (1999) have shown that as levels of hydration are reduced in

collagen samples (of rat tail tendon), the endothermic peak appears at increasingly higher temperatures (Figure 5.1 overleaf).

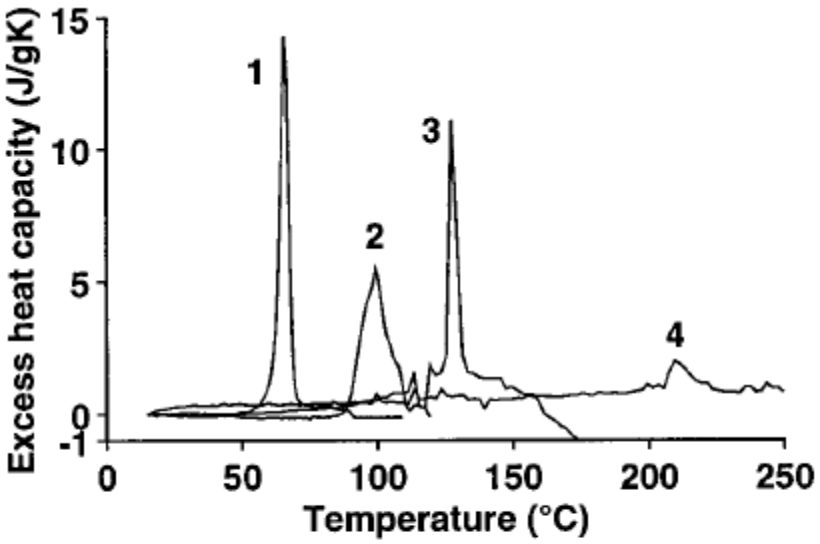

Figure 5.1 DSC thermograms of collagen at different levels of hydration. Peaks indicate endotherms in this plot). All scans were carried out at a rate of 10°C/min. (1) In excess water (98.2% volume water /volume collagen), (2) in 48.5 % v. water /v. collagen, (3) 14.3% v. water /v. collagen and (4) 0.9% v. water / v. collagen (samples were exposed to the water vapour of different salt solutions which afforded different levels of water content). Reproduced from Miles and Ghelashvili (1999).

Curve 1 shows a DSC thermogram for collagen type I hydrated in excess water showing the typical peak in the 60-70°C range. Whereas curves 2, 3 and 4 represent samples which are progressively less hydrated, and the associated endothermic features of these samples appeared at higher temperatures reaching, 100, 150 and 210°C respectively (Miles and Ghelashvili, 1999). The increase in temperature at which the peak was observed for less hydrated samples and has been attributed to a higher temperature being required for unfolding (Garrett and Flory, 1956; Privalov, et al., 1979). Miles and Ghelashvili (1999) developed a theory to explain this. It states that the presence of water in hydrated collagen fibrils provides a medium that enables conformational freedom of the fibrils within collagen

fibres. Whereas less hydrated collagen samples do not contain such a medium, meaning a higher temperature is required to enable unfolding in collagen samples of lower levels of hydration.

Miles and Ghelashivili (Miles and Ghelashvili, 1999) also demonstrated that freeze-dried rat tail collagen (i.e. of low hydration), heated beyond the temperature at which the endothermic peak appears in its DSC thermogram, undergoes an irreversible structural change. This was indicated by the absence of the characteristic endothermic peak if the sample was cooled, rehydrated and the DSC scan was repeated (Figure 5.2, curve 4).

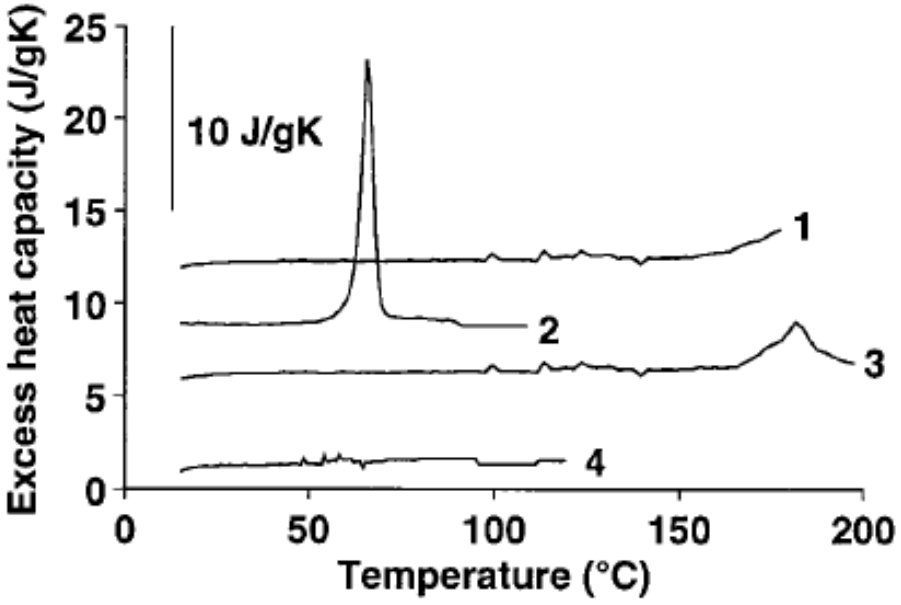

Figure 5.2 DSC evidence for irreversibility in collagen denaturation studies. 1) Freeze-dried collagen sample scanned to the onset of the denaturation endotherm. 2) When the sample heated in scan 1 was rapidly cooled, the sample was rehydrated and this DSC curve was observed upon its heating. 3) Collagen fibre scanned to the end of the denaturation endotherm. 4) The sample heated in scan 3 was rehydrated and rescanned with no evidence of the endotherm for native collagen. Reproduced from Miles and Ghelashvili (1999).

The cause of this structural change has been suggested to be due to irreversibility in the

unfolding of the triple-helix (Miles and Ghelashvili, 1999), although no further structural studies have been carried out to investigate the nature of this irreversible change in structure.

In the studies described in this chapter, experiments were carried out on freeze-dried articular cartilage and a sample of collagen[f] (extracted from human cartilage and described in chapter 3). This collagen sample is predominantly collagen type II. Collagen samples investigated by DSC are usually type I because it is the most abundant protein in mammals and it is relatively easy to prepare (Privalov, et al., 1979; Miles and Ghelashvili, 1999; Miles, et al., 2005). Collagen type I is a fibrillary collagen, the amino acid sequence is similar for fibrillar collagens and collagen type II has been shown to exhibit similar thermal and denaturation characteristics as collagen type I (Miles and Bailey, 2001).

Initially, the aim of these studies was to characterise structural changes in freeze-dried articular cartilage and collagen at high temperature (20-200°C). Following this, a TGA/ MS study was carried out on freeze-dried articular cartilage, IR spectroscopy was used to characterise further freeze-dried cartilage after heating to 190°C, Raman spectroscopy was used to characterise gelatin, and a final study where freeze-dried articular cartilage samples were heat-treated and rehydrated before analysis (quench recovery study).

5.2 *Experimental methods*

An initial series of experiments was carried out using hydrated articular cartilage samples. However, the fluorescence background became so intense, that by 90°C no Raman signal was observable. Following this, it was deemed more practical to work with articular cartilage and collagen samples of low hydration which exhibited fluorescence at higher temperatures. Samples of freeze-dried articular cartilage (age of donor 49 years) and collagen^{f} (age of donor 58 years) were used in the reported studies, the method of freeze-drying was described in chapter 2.

For the acquisition of spectra whilst samples were heated, the heating rate of the Linkam stage was set at 10°C per minute. Temperature points were reached as a continuous process of heating the sample, allowing for equilibration (2 minutes) and then spectral acquisition (16 minutes) in a step-scan fashion. Raman spectra were obtained every 10°C for the freeze-dried articular cartilage sample and collagen^{f} samples, and the same sample was analysed throughout both of these experiments. Raman spectra were obtained within the range 20-190°C of the articular cartilage sample (at the synovial surface) and collagen^{f}.

Figure 5.3 below shows the heating ramps as a function of time for the samples analysed by *in situ* heating and spectroscopy (black line plot), it also shows the typical heating program for denaturation studies by DSC (Miles and Ghelashvili, 1999; Miles, et al., 2005).

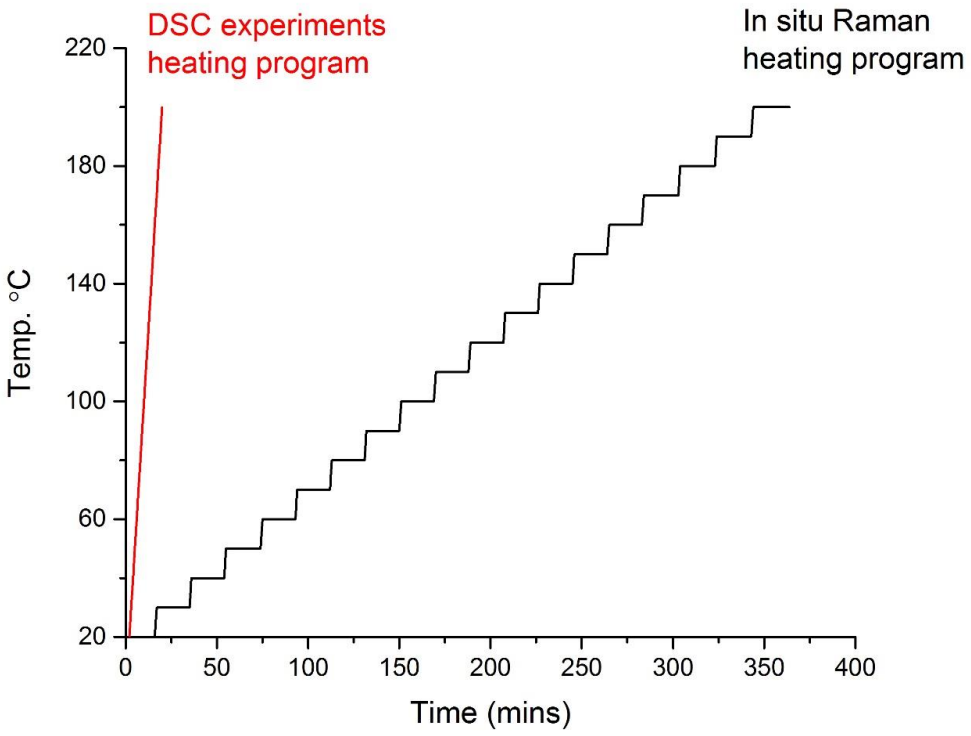

Figure 5.3 A plot of the heating ramps for the different types of thermal analysis. DSC analysis at 10°C per minute represents an example of an iso-heating ramp (red line plot). Raman analysis of collagen and articular cartilage (black line plot), representing a step-scan heating ramp, including the time for heating and spectral acquisition.

The time-period of heating was much greater for the Raman studies compared to the DSC studies. In order to permit comparison of our Raman data with that of the DSC studies described in the literature (red plot of Figure 5.3), a quench recovery experiment was carried out. For that study, separate samples of freeze-dried articular cartilage were heated at a rate of 10°C per minute to temperature points 20, 80, 150 and 200°C, and another sample was heated at 200°C for 30 minutes. These were then submerged in water and left at 4°C for 12 hours overnight, and analysed by Raman spectroscopy the following day. The heat-treated samples were analysed in water as described in chapter 2.

For IR spectroscopic analysis of samples a Bruker ATR-FTIR instrument was used. The spectral range was 400–4000 cm^{-1}. The resolution was 2 cm^{-1} and the number of acquisitions was 1000 per acquisition. IR spectra were obtained of a freeze-dried sample of articular cartilage before and after heating to 190°C.

TGA experiments were carried out using a Netzsch STA449C thermal analyser, Germany, attached to a quadrapole mass spectrometer Netzsch QMS 403C for analysis of evolved gases. These studies were performed by Mr. Nicholas Spencer, an undergraduate research student working in the McMillan/ Dudhia group. The sample weighed 5.4 mg before analysis and was heated at a rate of 10°C/min within the range 20-400°C.

5.3 *Results*

5.3.1 *Fluorescence contribution to high temperature spectra*

The background signal was observed to increase significantly when articular cartilage was heated to temperatures 120-180°C (Figure 5.4).

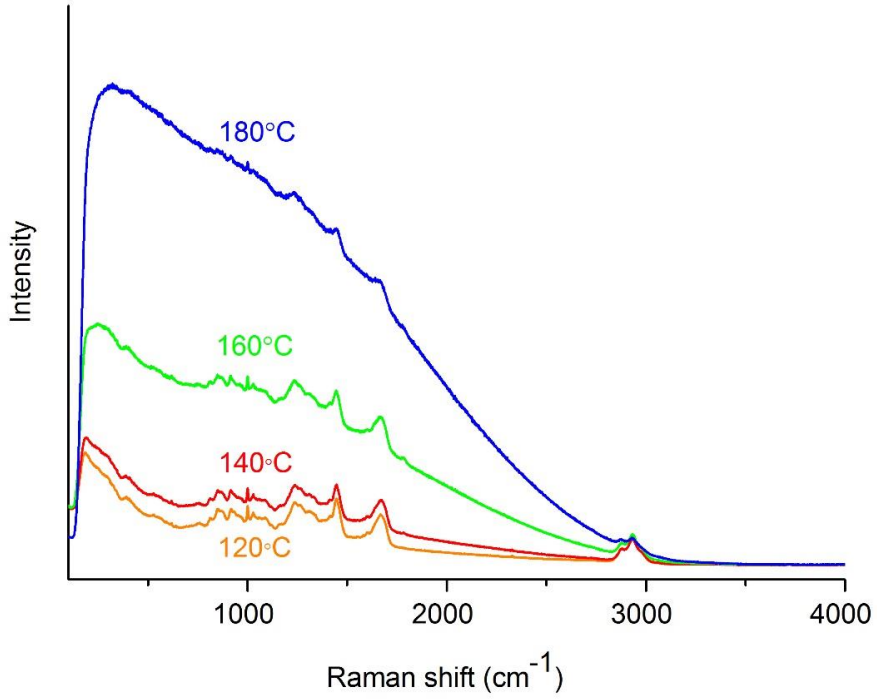

Figure 5.4 Raman spectra of freeze-dried articular cartilage at temperatures between 120-180°C, demonstrating a rise in the background of the spectra with temperature.

The background was approximately three-fold greater in the spectrum obtained at 180°C compared to those obtained at 120-140°C. At 190°C the fluorescence background totally masked the Raman signal (130,000 counts, data not shown). The photobleaching effect was negligible for these spectra, which is probably due to the dramatic increase in fluorescence. At 190°C the fluorescence intensity was too great to obtain a Raman spectrum. We also noted for collagen heated above 120°C the fluorescence background increased in the

same way. The fluorescence contribution in the Raman spectra is described in the discussion of this chapter.

Figure 5.5 shows spectra obtained between 20-100°C at 20°C intervals. The contribution of the background to the spectrum was found to decrease as a function of increasing temperature in these spectra.

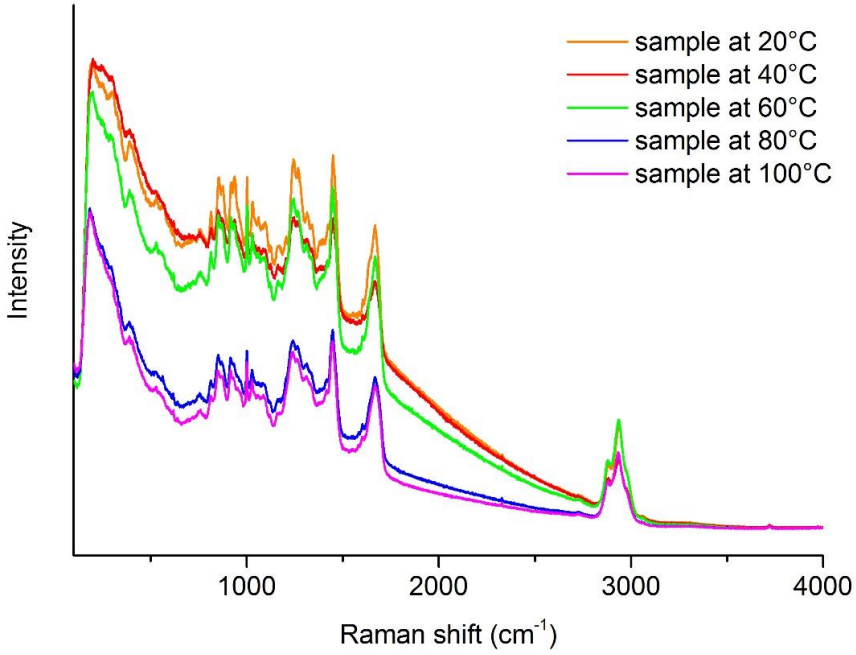

Figure 5.5 Raman spectra of freeze-dried articular cartilage obtained at temperatures between 20-100°C.

What appears to be a decrease in background as a function of temperature is actually the effect of photobleaching as Raman spectra were obtained at the same site during the course of these spectral acquisitions. This was demonstrated previously for a sample scanned multiple times at the same site and at room temperature (chapter 2).

5.3.2 *Raman spectra of articular cartilage and collagen during heating*

Background fluorescence subtraction was conducted (method described in chapter 2) to provide consistent Raman data despite the variation of fluorescence contribution. Figure 5.6 shows the background-subtracted Raman spectra of freeze-dried articular cartilage and collagen[f] (20-180°C). The data were signal-averaged and normalised to the intensity of the ring-breathing mode of phenylalanine at 1003 cm^{-1}. The intensity of this peak remained constant in the spectra obtained throughout these high temperature experiments.

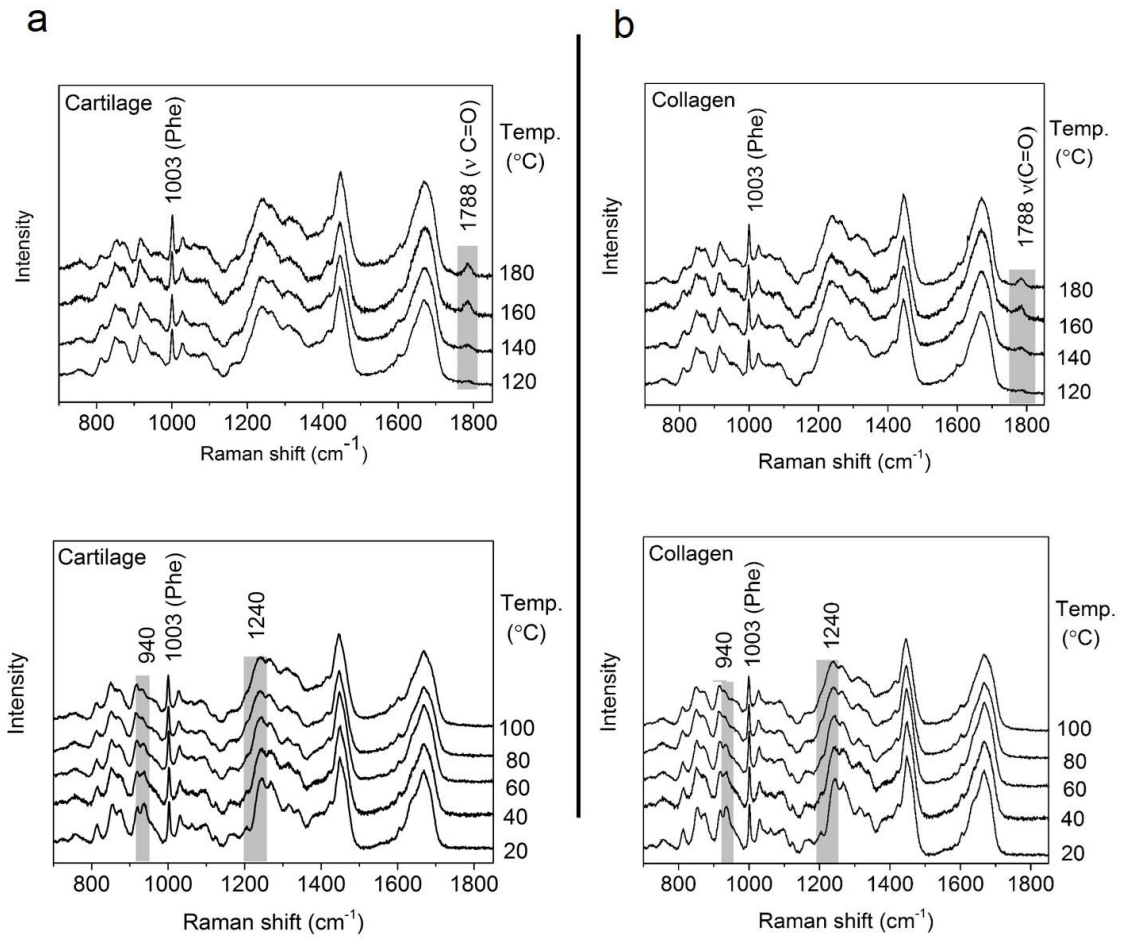

Figure 5.6 Background-subtracted Raman spectra of freeze-dried articular cartilage and collagen at 20-180°C. ***a)*** *spectra of cartilage and* ***b)*** *spectra of collagen. The boxes in grey highlight spectral changes which occur as a function of increasing temperature.*

The spectra of articular cartilage and collagen obtained in the temperature range 20-100°C show a gradual decrease in the peak intensity at 940 cm^{-1} (assignments for which were discussed in chapter 3) and a shift to lower wavenumber in the band at 1240 cm^{-1}. These changes were also reported to occur in the Raman spectra obtained from a collagen sample as a function of decreasing hydration (Zhang, *et al.*, 2011). This suggested that in this temperature range water loss from the collagen component took place.

In the temperature range ≥120°C, the most obvious change in the spectra of articular cartilage and collagen was the appearance of the peak at 1788 cm^{-1}. The fact that spectra of both samples exhibited this change indicated that the structural change was due to the collagen component of articular cartilage. The peak at 1788 cm^{-1} appears in the region of the spectrum where free carbonyl stretching modes are typically observed. According to Tu *et al.* (1982), the carbonyl group frequencies in Raman spectroscopy can be characterised according to their frequency as follows; 1500-1610 cm^{-1} for carboxylate, 1640-1670 cm^{-1} for peptides, 1750-1780 cm^{-1} for carboxylic acid, 1690-1800 cm^{-1} for ketone, 1720-1760 cm^{-1} for esters and 1760-1820 cm^{-1} for acid anhydride. This peak occurs at very high frequency for a carbonyl stretching mode, indicating a carboxylic acid, ketone or ester.

We note that during a study of free amino acids in the ratio that they occur in collagen, within a solution of low pH, a peak and at 1788 cm^{-1} was apparent (Frushour and Koenig, 1975). This peak was attributed to unionised carboxylic acid in that work. The peak for carboxylic acid is typically of higher frequency compared to the carbonyl stretching mode of a carbonyl group within a peptide bond (which appears at 1650 cm^{-1}) because of the mesomeric effect (Daimay Lin-Vien, 1991). It has been reported that a peak at around 1750 cm^{-1} occurs in the spectra for carboxylic acids in the unionised form, whereas the ionisation causes the peak at around 1750 cm^{-1} to disappear and a peak to appear at 1410 cm^{-1} (Edsall,

1937).

The peak in the spectrum at 1788 cm^{-1} for the cartilage and collagen samples must appear because the process of heating results in the formation of unionised carboxylic acid. This peak is at relatively high frequency for a carboxylic acid, but it is in the range suggested by Tu *et al.* (1982) and the peak is present in the Raman spectra of free amino acids reported by Frushour *et al.* (1975) in the same region of the spectrum. The higher than usual frequency for this group may be explained by the fact that the functional group is likely to be in a monomeric form, this results in a higher frequency for carboxylic acid modes (Olbert-Majkut, et al., 2011). It was unclear whether the process of COOH formation involved peptide bond hydrolysis or whether the side chains of the amino acids in collagen were transforming from the ionised to the unionised form. We discuss this in the final section of this chapter.

In the low temperature range 20-100°C, we observed evidence for water loss. This inferred that the starting sample of freeze-dried articular cartilage contained water, in the region of the Raman spectrum exhibited no changes where the O-H stretching mode of water occurs (Figure 5.7). This was due to the low detector efficiency in this region of the spectrum (see chapter 2).

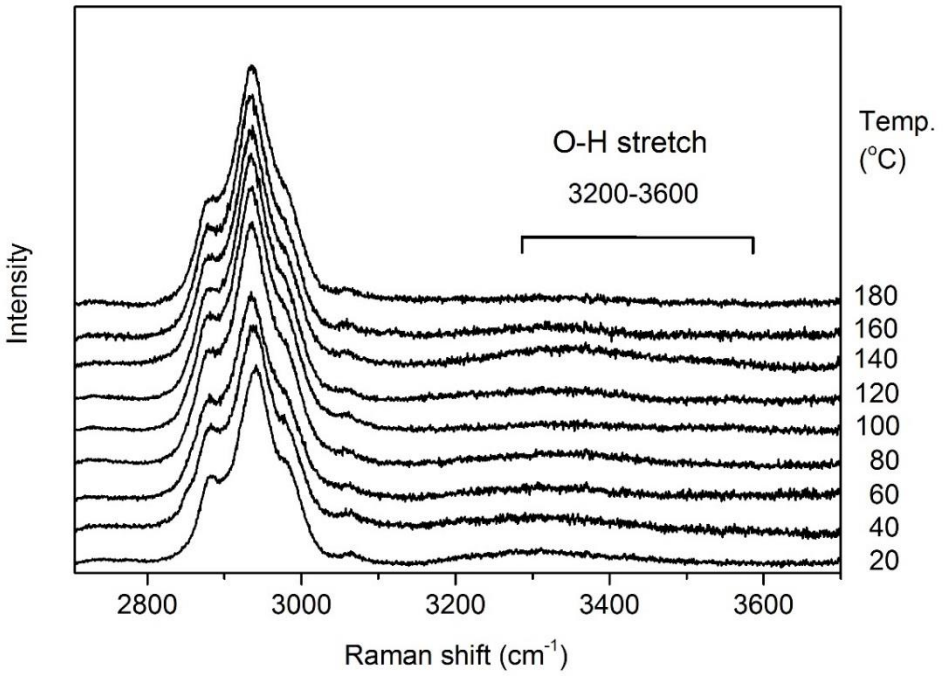

Figure 5.7 Raman spectra of freeze-dried articular cartilage between 20-180°C, shown at 20°C intervals (2900-3700 cm^{-1}). The O-H stretching mode is expected to occur at 3200-3600 cm^{-1}.

To investigate further the loss of water from freeze-dried cartilage we used TGA, as described in the following section.

5.3.3 TGA/MS analysis of freeze-dried articular cartilage

TGA measures mass loss as a function of temperature and MS was used to detect water, CO_2 and H_2O gas evolution during the heating process. CO_2 gas was monitored to reveal the process of decomposition and H_2O gas was monitored to reveal water loss. Figure 5.8 shows the mass loss detected by TGA, and the evolution of CO_2 and H_2O gases from the sample by detection of CO_2^+ and H_2O^+ by the MS, at the outlet of the heating chamber. The electric ion current (E.I.C) is an indication of the relative amounts of these positively charged gases reaching the detector of the MS.

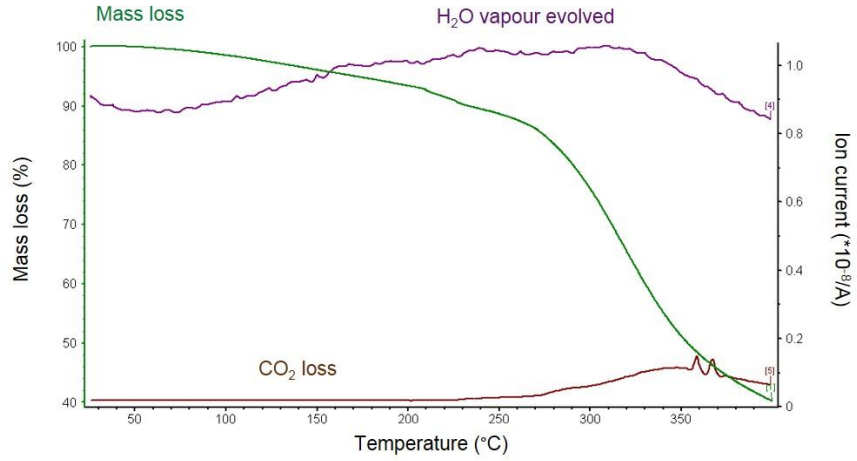

Figure 5.8 TGA and mass spectrometry data of articular cartilage heated from 20-400°C. The green curve represents loss in mass of freeze-dried articular cartilage as a percentage of the original weight. The purple and brown curves represent the electric ion current (E.I.C.) of H_2O^+, and CO_2^+, respectively (Data obtained by N. Spencer in collaboration with JD and PFM).

In the temperature range 20 - 150°C we observe an upwards gradient in the water E.I.C. that coincides with a gradual decrease in mass. This indicated a gradual decrease in water content of freeze-dried articular cartilage and it correlates with the Raman spectroscopic evidence that pointed towards a gradual decrease in water content in the same temperature range. Above 250°C there was a significant decrease in mass and a concomitant increase in the CO_2 evolved from the sample, this is due to degradation of the sample, which releases CO_2 gas in the process (Qian, et al., 1993).

It was not possible to determine whether the water present in the sample was reabsorbed upon exposure to air (this may have occurred between the process of freeze-drying and the time for acquisition of Raman spectra, whether it was retained throughout the freeze-drying process, or, whether both of these events contributed. An attempt was made to investigate this by IR microscopy, which is more sensitive to hydrous component of samples than Raman spectroscopy. We tried to entrap a freeze-dried sample into a vial

containing argon gas and obtain spectra of the sample from the exterior. However, the glass vial, in which the freeze-dried sample was placed, exhibited a strong IR spectrum, impeding the acquisition of IR spectra from the sample of cartilage within.

5.3.4 IR study of freeze-dried articular cartilage after heating to 190°C

To investigate the structural change in cartilage, we analysed a sample of freeze-dried articular cartilage before and after heat treatment to 190°C by IR spectroscopy (Figure 5.9). The band at 1626 cm^{-1} is due to the amide I mode (predominantly C=O stretch (Miyazawa, et al., 1958)) of the amide bond in the peptide components of articular cartilage. Since this band was not affected by temperature it was used here as an internal standard to normalise the data.

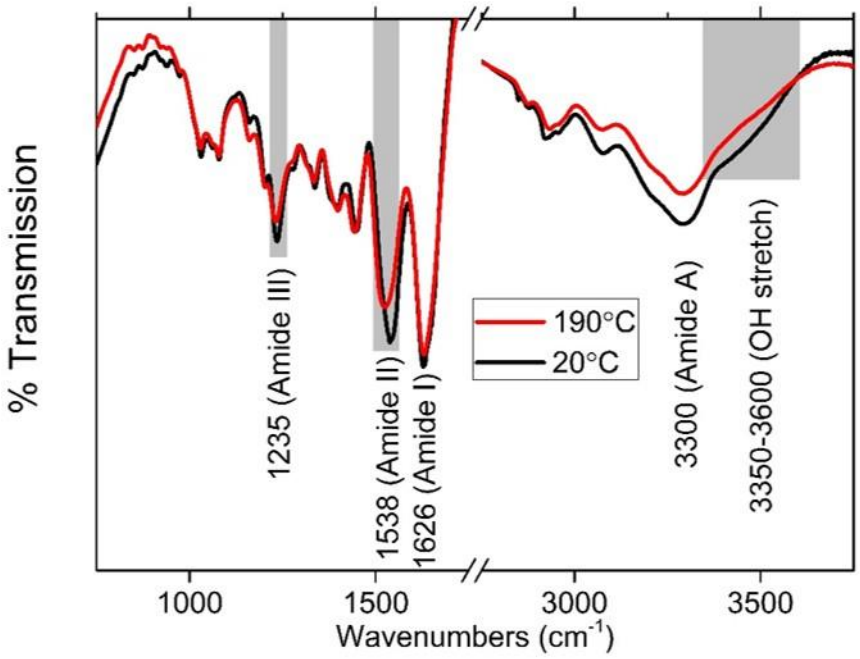

Figure 5.9 ATR-FTIR spectra of freeze-dried articular cartilage at 20°C (black line plot) and after heating to 190°C (red line plot). Bands that changed significantly are shaded in grey.

We observed a decrease in the intensity of band due to the O-H stretching mode of water in the spectrum of the sample after heating compared with before heating. The band is at 3350-3600 cm^{-1} and is mostly due to the ν_1 and ν_3 stretching mode of water (Venyaminov and Prendergast, 1997). Figure 5.10 shows the difference spectrum of before and after heating in this part of the spectrum.

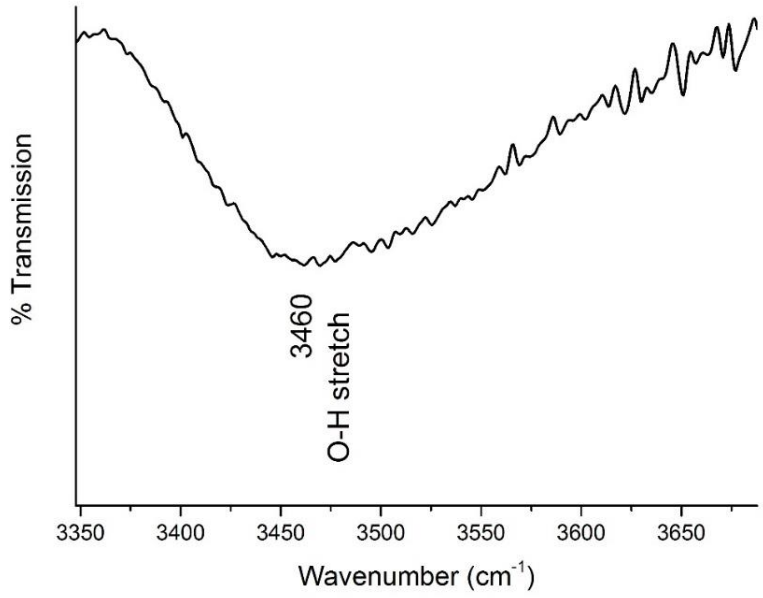

Figure 5.10 A difference IR spectrum of the freeze-dried articular cartilage before and after heating to 190°C, showing O-H stretching mode. The band at 3460 cm^{-1} is due to ν_1 stretching mode of water (Venyaminov and Prendergast, 1997).

The trough indicates that the water content of the sample was less after heating, and this consolidated evidence for water being present in the freeze-dried articular cartilage starting sample. Apart from the change in the peak due to O-H stretch, the most significant differences between the IR spectrum of the sample before and after heating are the decrease

in intensity of the band at 1235 cm^{-1} and the decrease in intensity and the shift to lower wavenumber of the band at 1538 cm^{-1}.

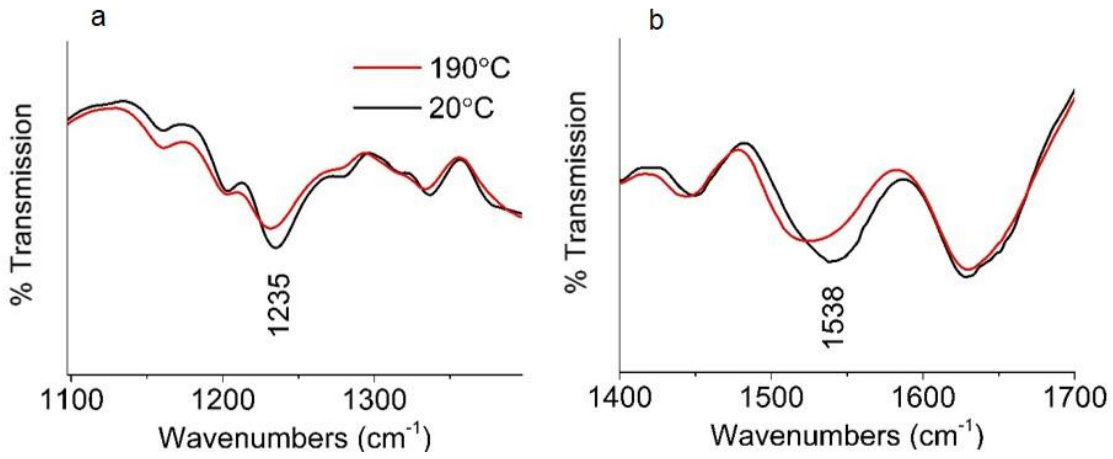

Figure 5.11 ATR-FTIR spectra at 1235 cm^{-1} and 1538 cm^{-1} for freeze-dried articular cartilage before and after heating to 190°C. ***a)*** *Peak centring at 1235 cm^{-1} and* ***b)*** *peak centring at 1538 cm^{-1}.*

Figure 5.11a shows the band at 1235 cm^{-1} (amide III), which results from a vibrational mode involving 40% C-N stretch, 20 % C-C stretch and 30 % N-H in-plane bending (Miyazawa, et al., 1958). Figure 5.11b shows the band at 1538 cm^{-1} (amide II mode), which is due to 40% C-N stretch and 60% N-H in-plane bending (Miyazawa, et al., 1958). In an IR study of bone heated to 200°C, Lozano *et al.* (2003) observed a decrease in these vibrational modes (amide II and III) and they attributed this to peptide bond dissociation of the collagen component of bone. However, we note that in a separate study on dentin, the organic matrix, which consists of collagen, has been shown to exhibit the same peak at 1235 cm^{-1} and its reduction in intensity was reversible upon denaturation to 100°C and rehydration (Bachmann, et al., 2005). This is the temperature range for water loss, which means that the decrease in intensity and the regaining of intensity upon rehydration may be due to dehydration and rehydration of the sample. We observe a similar result for the peak at 1538 cm^{-1} in an IR study of collagen where the peak decreases upon heating of collagen to only

100°C, although in that study renaturation was not tested (Pielesz, 2014). Therefore the decrease in intensity of these two peaks may be due to the process of water loss rather than peptide bond hydrolysis, as proposed by Lozano *et al.* (Lozano, et al., 2003).

Hence the results in the IR study enabled us to confirm changes in water content, however it was not possible to confirm whether the decrease in the peaks at 1235 and 1538 cm^{-1} for heat-treated cartilage to 190°C were due to hydrolysis.

5.3.5 Gelatin at room temperature

Following the indications of the results from the IR and Raman studies, we were unsure whether the peak at 1788 cm^{-1} was apparent as a result of peptide bond hydrolysis. Therefore we investigated the Raman spectrum of gelatin. Gelatin is known to be the fragmented and denatured form of collagen due to peptide bond hydrolysis (Hattrem, et al., 2015). The fingerprint region of a Raman spectrum of gelatin in the solid form (commercial source, BDH), is shown with the spectrum of collagen[f] for comparison (Figure 5.12 overleaf).

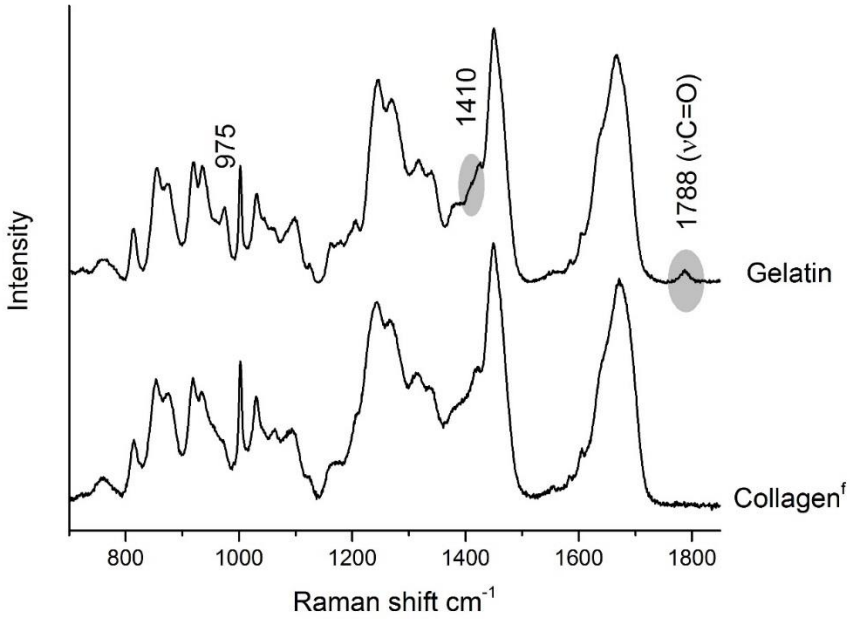

Figure 5.12 Raman spectrum of gelatin and collagen^f. Assignments to the spectrum of gelatin are provided for peaks that differ with those in the spectrum of collagen^f.

The main differences were the presence of the peak at 975 cm^{-1}, a shoulder appearing at 1410 cm^{-1}, and the appearance of the band 1788 cm^{-1}.

The presence of the of the peak at 975 cm^{-1} is unusual because we have not observed a peak in this region of the spectrum of articular cartilage or collagen^f samples throughout these high temperature studies and nor has it been observed in previous studies of collagen or gelatin reported by Frushour and Koenig (1975). We surmise that it is due to the presence of a contaminant from the preparation procedure in this commercially obtained sample. The changes in the peak at around 1410 cm^{-1} are due to symmetric stretch of COO^- and a discussion of this is postponed to the next section. The peak at 1788 cm^{-1} indicates the presence of unionised carboxylic acid. The Raman spectrum of gelatin shown by Frushour *et al.* (1975) did not exhibit the peak at 1788 cm^{-1}. We also note that the Raman spectrum of

gelatin elsewhere has not indicated the presence of this peak (Howell and Badii, 2004). The peak may be absent in those studies because of the dependence of this peak on the pH of the sample.

In summary, we observed the same peak in heated articular cartilage and collagen samples, we also observed a shoulder peak arising at 1410 cm^{-1}. There were no further differences in the spectra, indicating that there are no further markers, which may be attributed to the peptide bond dissociation of collagen.

5.3.6 Quench recovery of heat treated articular cartilage samples

Freeze-dried articular cartilage samples were heated at a rate of 10°C per minute to temperature points 20, 80, 150 and 200°C, and another sample was heated at 200°C for 30 minutes. These samples were subsequently left in water overnight before Raman spectra were obtained (Figure 5.13). We note that hydration of the samples after exposure to high temperature caused the fluorescence background to be attenuated.

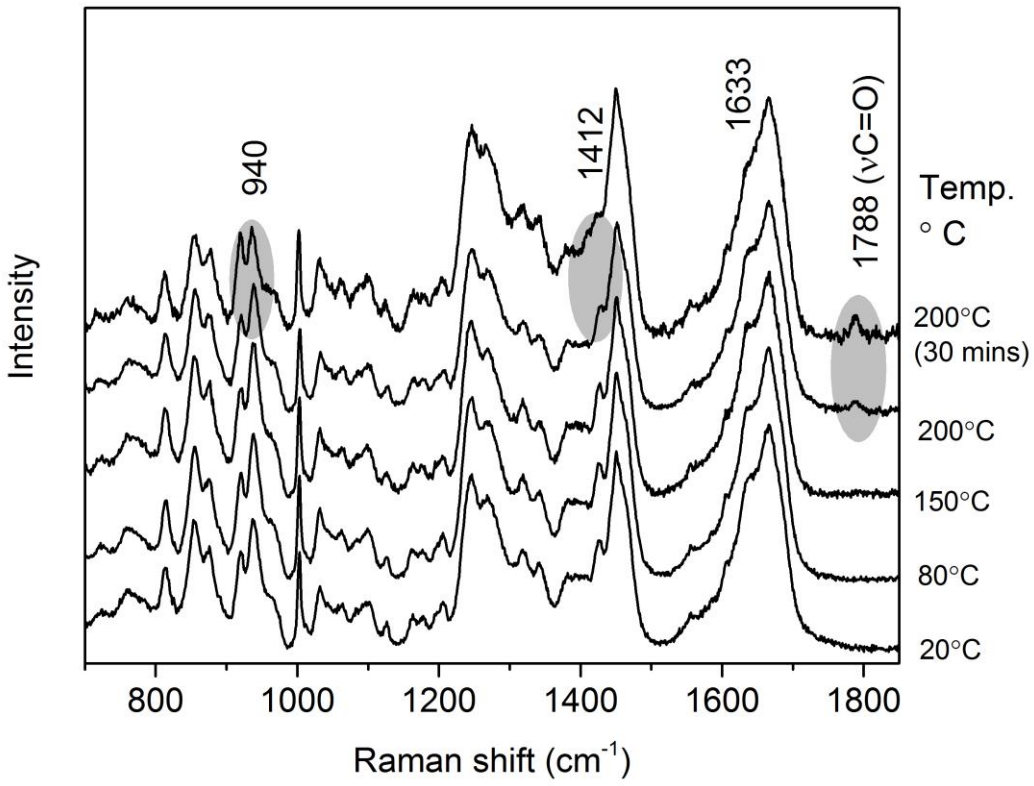

Figure 5.13 Raman spectra of dehydrated articular cartilage samples that were heated to temperatures of 20, 80, 150, 200°C, and 200°C for 30 mins. 200°C - was heated for 30 mins at this temperature. All samples were rehydrated after heat treatment. Bands shaded in grey demonstrate a change in this series of spectra. All spectra were normalised to the phenylalanine peak intensity.*

The spectra show evidence of hydration; compared to the spectra of the freeze-dried samples, the peaks at 940 cm^{-1} and 1633 cm^{-1} are stronger in intensity (due to O-H bending (Walrafen, 1964; Walrafen and Chu, 1995)). Samples heat-treated to 80°C, and 150°C exhibit no changes in the spectra obtained at their surface, which confirmed that heating to these temperatures caused no change in structure. On the other hand, the sample exposed to 200°C exhibits the emergence of the peak at 1788 cm^{-1} and the same goes for the sample exposed to 200°C for 30 minutes, which exhibits the same changes but to a greater degree. It is important

to note that the peak at 1788 cm^{-1} was not observed to shift despite the fact that the samples were placed in water. It is expected that the hydrogen bonding of molecular water with carbonyl would lead to a shift to lower wavenumber (Socrates, 2001), the fact that it does not shift indicates that the carbonyl bonds were not accessible to water in the sample. Furthermore, when the peak at 1788 cm^{-1} becomes apparent there are further changes in the Raman spectrum, which remain post rehydration in water.

These changes were a decrease in the peak at 1420 cm^{-1}, the appearance of a peak at 1412 cm^{-1} (Figure 5.14a), a decrease in intensity in a component of the peak at 934 cm^{-1} (Figure 5.13) and a decrease in the peak at 1633 cm^{-1} (Figure 5.14b).

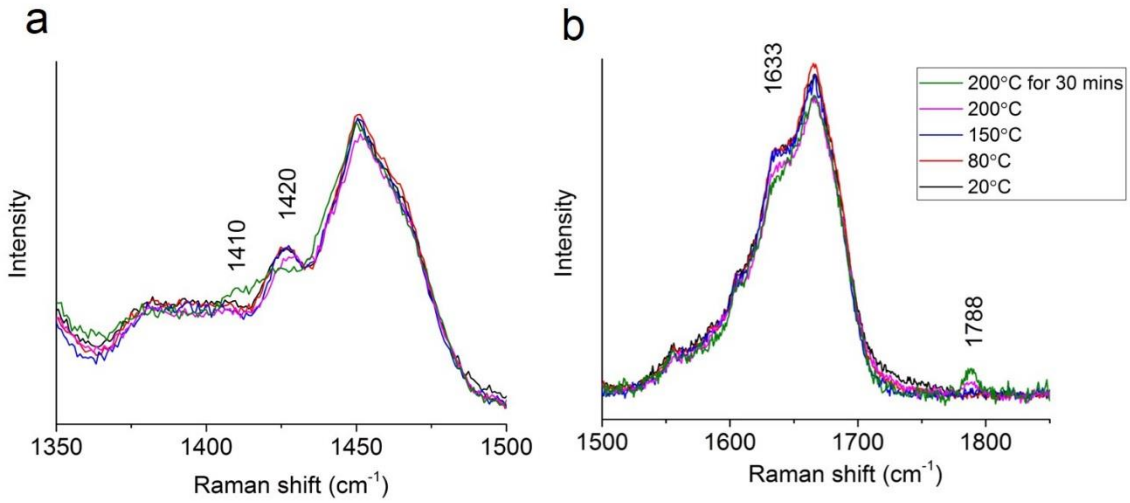

Figure 5.14 Region of spectra for heated cartilage samples, showing decrease in intensity of the peaks at 1420 and 1633 cm^{-1}. All samples were rehydrated after heat treatment.

It is important to note that all of these changes can be attributed to a lower level of hydration in articular cartilage after heat treatment and the concomitant appearance of the peak at 1788 cm^{-1} indicates that these events are associated. Therefore as well as ionisation of COO^- groups in cartilage there is also evidence for a structural change that suggests water was not able to access carbonyl vibrational modes and the water content is also much less for

the samples heated to >150°C.

5.4 Discussion

In the Raman spectra of articular cartilage and collagen samples heated to 120°C, we observed the appearance of a peak at 1788 cm^{-1}. The peak was also observed in the Raman spectrum of a sample of gelatin obtained in our lab. This peak occurs in the range that Tu (1982) proposes for carboxylic acid groups, albeit at a relatively high frequency.

A peak in the same region appears in the spectrum of an amino acid mixture representing the primary sequence of collagen and gelatin in an acidic solution (Frushour and Koenig, 1975). The peak was attributed to COOH and upon exposure of the mixture to alkali environment, the 1788 cm^{-1} peak vanished and a peak appeared at 1412 cm^{-1}, Frushour *et al.* (Frushour and Koenig, 1975) indicated that this shift was due to the ionisation of carboxylic acid. This same change was documented during a Raman study of the di and tri-carboxylic acids upon ionisation; they noted that the peak at around 1400 cm^{-1} was characteristic of the ionised carboxyl group while the peak at >1700 cm^{-1} was characteristic of the unionised group (Edsall, 1937). Monomeric carboxylic acids may appear at such a high frequency (Olbert-Majkut, et al., 2011) and also it has been reported that the presence of NH_3^+ residues in the vicinity of C=O causes the peak to shift to unusually high frequency (Edsall, 1937), which would explain the observation of a carboxylic acid peak appearing with such high frequency.

The appearance of the peak in the spectra of freeze-dried cartilage and collagen samples at >120°C therefore indicated the deionisation of COO^- groups. The most likely possibilities are due to the NH_3^+ or NH_2^+ groups of lysine or arginine or the transfer of protons from water. It also remains a possibility that COOH is formed as a result of peptide bond

dissociation, in support of this, hydrolysed collagen has been shown to exhibit this peak in its spectrum. There is no further spectral evidence that may enable us to identify exchange of protons from other functional groups, such as NH_3^+ (lysine or arginine) and there is no obvious evidence for the formation of NH_2 as a result of peptide bond hydrolysis. Also, the N-H vibrations are known to be discrete in Raman spectra (Socrates, 2001). Therefore we cannot demonstrate or disprove the loss of protons from the NH_2^+ and NH_3^+ groups in the samples.

We obtained further evidence in the Raman spectra pertaining to the structural change related to the formation of COOH during the quench recovery experiment. The heating program in that study was comparable to that for a typical DSC study, and the peak at 1788 cm^{-1} became apparent in the sample heated to 200°C. The degree of change in the spectra appeared to increase upon the exposure of a sample to 200°C for 30 minutes, indicating a kinetic effect. The temperature for the appearance of this peak was different for that at which it appeared in the *in situ* studies (120°C) probably because of the kinetic effect of heating for longer in those experiments. The finding that this peak appeared at 150-200°C means that the changes we observe in the Raman spectrum occur at the same temperature as the endothermic peak for freeze-dried collagen samples (Miles and Ghelashvili, 1999). Miles and Ghelashivili (Miles and Ghelashvili, 1999) also noted that samples rehydrated and scanned by DSC did not exhibit an endothermic peak.

The samples we analysed exhibited evidence for COOH formation, as well as a decrease in the tendency to reabsorb water. This was manifested as a decrease in the O-H bending mode a downwards shift in the peak at 1420 cm^{-1} to 1412 cm^{-1} and a decrease in the peak at 940 cm^{-1}. It is important to note that all samples were hear treated and left in water for 12 hours, therefore the decrease in hydration of the samples were heat-treated to 200°C

demonstrates a structural change which affects their water retention. Furthermore, we note that the peak at 1788 cm^{-1} (due to carboxylic acid groups) was not affected by hydration. It was expected that it would be shifted upon interaction with water therefore it is likely that the COOH groups formed were not accessible to water. Finally, we suggest that the lower uptake of water from the samples heated to 200°C may explain the absence of an endothermic peak upon analysis by DSC, as reported in the study by Miles and Ghelashvili (1999). Furthermore, this is related to the structural change that we suggest is due to either peptide bond hydrolysis or protonation of carboxylate groups in articular cartilage.

The finding of protonation of carboxylic acid groups was not observed previously during studies of collagen denaturation by Raman spectroscopy (Dong, et al., 2004; Polomska, et al., 2010). However, Dong *et al*. (2004) heated collagen to 80°C and Polomska *et al.* (2010) heated collagen to 110°C. We note that ionic interactions are important for the overall stability of collagen (Keshwani, et al., 2013), therefore the protonation of carboxylic acid groups, as observed in this work, may be an important stage in the denaturation of collagen samples of low hydration. These studies do not relate to denaturation of collagen samples of high hydration.

The IR spectra of a sample heated to 190°C exhibited a decrease in the bands at 1526 cm^{-1} and 1238 cm^{-1}. These bands are due to the amide II and amide III modes, and are predominantly due to C-N stretching modes (Miyazawa, et al., 1958). Although these changes were attributed to peptide bond hydrolysis in a study by Lozano *et al*. (Lozano, et al., 2003), we noted that these changes have also been reported in studies where collagen samples were heated in the range where water loss occurs (Pielesz and Weselucha-Birczynska, 2000; Bachmann, et al., 2005).

In the Raman spectra of freeze-dried articular cartilage and collagen[f] heated 20-100°C,

we observed changes that reflect water loss from the collagen component. These changes were reported previously in a hydration-dependent Raman study of collagen (Zhang, *et al.*, 2011). IR spectra also indicated water loss from a sample of freeze-dried articular cartilage after heating to 190°C in the 3300- 3650 cm^{-1} part of the spectrum. We monitored this process during the heating of freeze-dried cartilage by TGA and MS analysis of evolved H_2O and CO_2 to demonstrate that there is a decrease in mass associated with the evolution of water from freeze-dried articular cartilage in the range 20-250°C. This confirmed that water was present in the freeze-dried sample of articular cartilage and was evolved in this temperature range. Further still, above 220°C there was evidence for amino acid decomposition, indicated by the detection of CO_2 from the sample. Previous studies have shown that polypeptides undergo decomposition at this temperature (Qian, et al., 1993), resulting in the evolution of CO_2 during decarboxylation (Li and Brill, 2003).

In this study we set out to investigate the structural changes in freeze-dried articular cartilage and collagen as a function of high temperature. The results we obtained demonstrated that in the samples undergo a process of peptide bond dissociation and also the samples that demonstrate evidence for this also undergo a structural change causes them to retain less water.

Finally, the significant rise in background contribution occurred at >130°C for freeze-dried collagen[f] and of freeze-dried articular cartilage. Also, the onset of increase in the background was at lower temperature for hydrated articular cartilage compared to more dehydrated samples, as found in preliminary studies. We also observed that upon hydration of samples obtained after heating, the background signal was attenuated. In the literature, researchers have assigned the cause of the background signal of collagen samples to elastic light scattering, which causes a broad signal to be observed in the Raman spectra (Bonnier,

et al., 2012). As discussed in the introduction chapter to this thesis it is difficult to ascertain the origin of this fluorescence contribution to the spectra. However, it is important to note that the rise of this background appears is hydration dependent.

6.1 Introduction

In this chapter we demonstrate the changes in the Raman spectrum of articular cartilage tissue that are associated with high and low levels of hydration. The study reported in chapter 5 revealed changes in the Raman spectra of freeze-dried articular cartilage and collagen that related to a decrease in water content upon heating. The hypothesis investigated in this instance was to what degree changes in spectral features reflect the changes in structure brought about by changes in the hydration level of articular cartilage.

6.1.1 Hydration in articular cartilage

It is known from DSC/TGA studies that articular cartilage consists of up to 80 % water (Sohar, et al., 2007). This value has been reported to be 66.2 % for healthy tissue by freeze-drying until the weight was constant (Mankin and Thrasher, 1975). Most of the water in articular cartilage is retained by the presence of numerous anionic groups such as sulphate and carboxylic acid of aggrecan and other proteoglycans (Mow, et al., 1984). The water-ECM interactions can be split broadly into three categories; those that are due to interactions of water with the GAG component of the proteoglycans, those that are due to water interactions with collagen, and bulk water found in between the interstices of the ECM.

Servaty *et al. (2001)* have investigated the hydration of the main components of agggrecan, HA and CS, by IR spectroscopy (Servaty, et al., 2001). At high levels of hydration (above ~80% relative humidity (RH)) these components were found to exhibit changes in the peaks corresponding to vibrational modes of carboxylate, the pyranose ring and sulphate groups as a result of hydration.

For collagen fibres (from human dura mater), different bulk water and protein-water interactions have previously been classified by cryogenic X-ray techniques (Nomura, et al., 1977). The most tightly bound water is expected to be the water that acts as bridges between the hydroxyl groups of hydroxyproline residues and amide bonds of the collagen triple-helices (Kopp, et al., 1989; Bella, et al., 1995). This is known as structural water and, essentially, it is bound to the polar functional groups of the collagen molecule.

Spectroscopy enables the study of bulk water, as well as water-proteoglycan interactions and collagen-water interactions. A detailed Raman spectroscopic study of liquid water was carried out by Walrafen (1964). He assigned the band at 1639 cm^{-1} to O-H bending, the band at 3350 cm^{-1} to the overtone of bending mode, 3450 cm^{-1} to symmetric stretching and 3590 cm^{-1} to asymmetric stretch of water. Recently, a Raman study of collagen type I (from human skin) was carried out at varying relative humidity (Zhang, et al., 2011). The results revealed a hydration sensitive peak at 936 cm^{-1} in the spectrum of collagen and also the dependence of hydration on the shift for the amide vibrational modes.

In this study a similar experimental set-up to that at of Zhang *et al.* (2011) was constructed, see Figure 2.12. A sample of normal articular cartilage was exposed to high versus low levels of hydration and Raman spectra were obtained at its surface.

6.2 Experimental methods

The sample studied was a hydrated biopsy sample of articular cartilage (donor of 49 years, described in chapter 2), taken from the -80°C freezer and thawed at room temperature. Raman spectra were obtained at the surface of one side of an articular cartilage sample, this particular side of the sample exhibited a significant contribution in the sulphate peak, at 1063 cm^{-1}, indicating a significant amount of proteoglycan content at the surface.

The same sample was analysed at high and low hydration. Firstly, the sample of articular cartilage was placed in a closed environment in which liquid water was present for 48 hours (Figure 6.1a below). This represented a humidity level that approached 100 % R.H. At low hydration, the same sample was exposed to previously dehydrated silica gel inside the humidity cell for 48 hours (Figure 6.1b). This was expected to represent a 0% R.H.

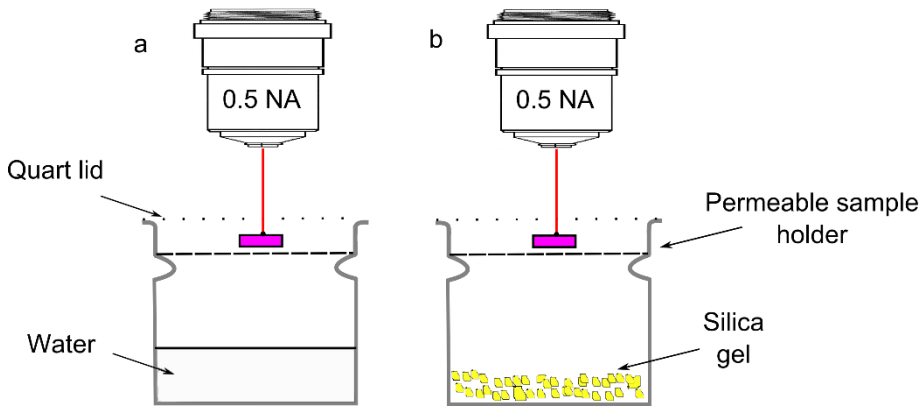

Figure 6.1 Enclosed cell for control of hydration level of cartilage sample. ***a)*** *high level of hydration and* ***b)*** *low level of hydration state, the quartz cell lid was bound to the cell with grease to make it airtight.*

Raman spectra were obtained using a 0.5 N.A. Leica (Germany) objective, a long focal distance was required in order to reach the sample beyond the quartz lid of the enclosed cell. Scans were acquired as two accumulations per acquisition, at different sites on the surface of the sample in each case. Two accumulations per site on the surface of the sample were performed in order to reduce the exposure of the laser to each site scanned, and to obtain an average for the surface of the sample. Ten acquisitions, obtained at ten different sites on the surface of the sample were co-added to make a single spectrum of twenty co-additions per hydration level. The spectrum of distilled water (distilled on site) is shown for comparison.

A separate study followed to investigate unexpected changes in the sulphate vibrational mode (1063 cm^{-1}) in the Raman spectra of articular cartilage at different levels of hydration. We assessed the hydration dependence of this peak in C4S, one of the major contributors to the signal of sulphate in the Raman spectrum of articular cartilage. Chondroitin-4-sulphate was obtained commercially (CSA sodium salt from bovine trachea, C9819 Sigma Aldrich) and one sample was freeze-dried for 24 hours and another was hydrated by mixing 50% water with 50% sample (100 mg : 100 µl).

6.3 Results

6.3.1 Raman spectroscopy of articular cartilage at high and low hydration

The Raman spectrum of liquid water obtained in our lab shows a broad set of bands at ~3202 cm^{-1} and ~3380 cm^{-1}, we note that the band at 3202 cm^{-1} is at higher intensity than the band at 3380 cm^{-1} (Figure 6.2 overleaf). On the other hand, the Raman spectrum of liquid water reported by Walrafen *et al.* (1964), using a photomultiplier detector, shows that the peak at ~3380 cm^{-1} is more intense than that at ~3202 cm^{-1}. Whereas we used a CCD detector,

that was found to have a low efficiency in the high frequency region. This explains the difference in our result with that reported by Walrafen *et al.* (1964). We also note that a study of collagen in water reported a similar profile as the peaks we have shown in this region, they used a 488 nm laser although they did not indicate which type of detector they used (Leikin, et al., 1997).

Figure 6.2 shows the Raman spectra of liquid water and the sample of articular cartilage at high and low level of hydration only for the region of the spectrum (2800 – 3800 cm^{-1}). The Raman spectra were normalised to the intensity of the peak at 1003 cm^{-1} (Phe).

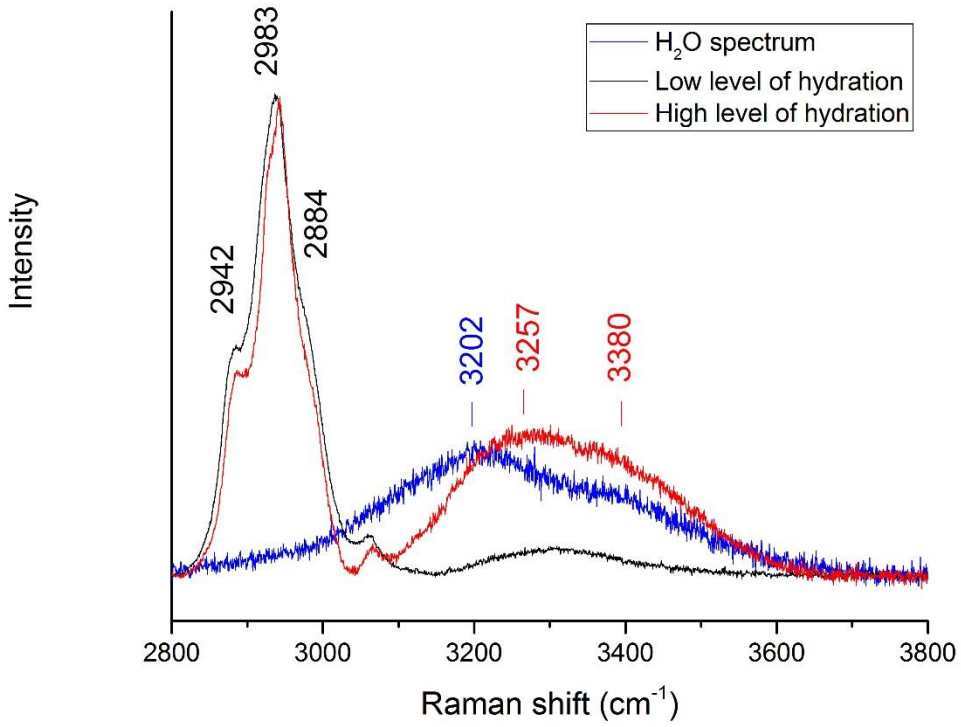

Figure 6.2 Raman spectra in the 2800-3800 cm^{-1} region for articular cartilage at high hydration and low hydration. The spectrum of H_2O is shown for comparison.

It can be seen that the sample at low hydration contains no obvious O-H stretching modes due to water in this region. The spectrum of the articular cartilage in the hydrated condition shows a similar doublet of peaks as the spectrum of H_2O, although the bands are shifted to higher frequency. It is expected that the shift in this case is due to hydrogen bonding interactions of water with the ECM. Most importantly, the results confirmed that the sample was hydrated when exposed to water vapour. Also, in this region of the Raman spectrum are the vibrational modes of the C-H stretch vibrations of the proteins and carbohydrates in cartilage (2800-3100 cm^{-1}). Overlapping of peaks in this region meant that it was difficult to demonstrate any significant changes.

Figure 6.3 overleaf shows the fingerprint regions of the spectra of the articular cartilage sample at low hydration and high levels of hydration and a difference spectrum. A peak in the difference spectrum indicates a greater intensity in the sample of high level of hydration and a trough indicates a greater intensity in the sample of low level of hydration.

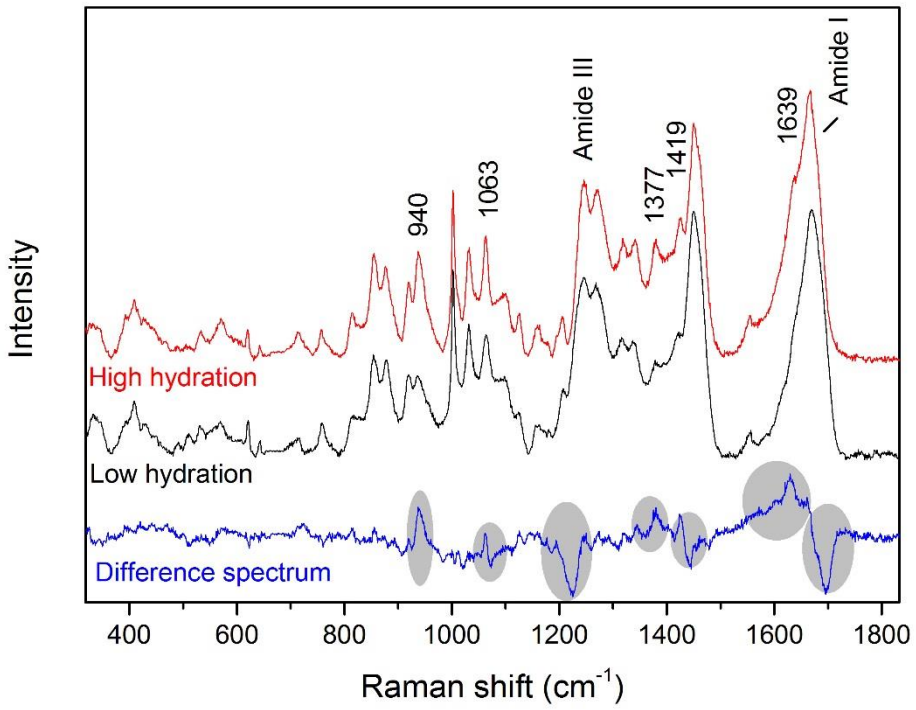

Figure 6.3 Raman spectra of articular cartilage at low and high hydration and difference spectrum of high hydration - low hydration. Shaded in grey are parts of the spectrum that show significant changes.

Upon decreasing the level of hydration from high to low, the following changes were observed. A shift in the amide I band to higher frequency; a lower contribution from the band at 1639 cm^{-1} (bending mode of O-H in water (Walrafen, 1964)), a shift to lower frequency and broadening of the peak at 1419 cm^{-1}, decrease in intensity of the peak at 1377 cm^{-1}, a downwards shift in the amide III band, as well as a decrease in intensity of the band at 940 cm^{-1}. Similar observations were made in the Raman spectra of collagen in states of high and low hydration (Zhang, et al., 2011). The major difference was the presence of the peak at 1063 cm^{-1}, which was absent in the spectrum of collagen as it is due to the sulphate stretching mode of proteoglycan in articular cartilage.

The peak in the region of 1419 cm^{-1} is due to ν_sCOO- stretch (Frushour and Koenig,

1975). The peak centre was at 1418.5 cm^{-1} for the sample in the hydrated state and the corresponding peak was at 1413.7 cm^{-1} in the spectrum of the sample of low hydration. The shift in the peak to lower frequency by around 5 cm^{-1} is in agreement with the decrease of hydrogen bonding with the COO^- groups upon dehydration of the sample. This is due to the lower quantity of molecular water present in the dehydrated sample of articular cartilage. The peak at 1377 cm^{-1} was shown to increase significantly, this is also observed in the sample of collagen at high hydration (Zhang, et al., 2011), this peak has been assigned to C-H (Frushour and Koenig, 1975) and amide II (Tu, 1982).

In Figure 6.4 the region 900–1180 cm^{-1} is shown, which includes the phenylalanine peak at 1003 cm^{-1} and the sulphate peak at 1063 cm^{-1}.

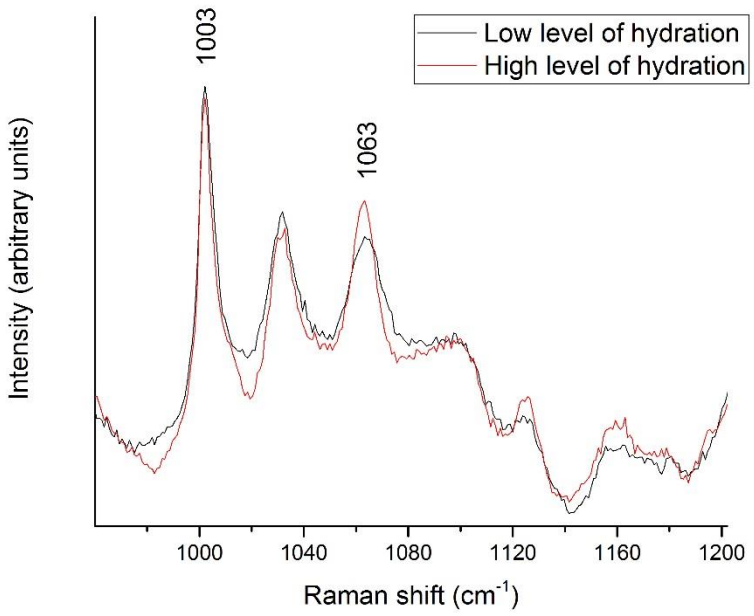

Figure 6.4 Raman spectra of articular cartilage at levels of low and high of hydration in the spectral region 980-1180 cm^{-1}.

The symmetrical stretching mode of sulphate, at 1063 cm^{-1}, appears to be more broad

and the peak centre is at greater frequency by around 1 cm^{-1} in the case where the tissue was in a lower state of hydration. This shift in frequency was expected since greater hydrogen bonding between water and sulphate groups was expected in hydrated cartilage. However, it was not expected that the peak would become more broad when the cartilage was in a lower state of hydration, this observation was investigated further in the following study.

6.3.2 Hydration study of chondroitin-4-sulphate

The result of broadening in the band at 1063 cm^{-1} upon dehydration of the sample of articular cartilage was unexpected. This peak is mainly due to the symmetric stretching mode of sulphate in chondroitin sulphate found in the proteoglycans of articular cartilage. To investigate this result further, Raman spectra were obtained of a sample of chondroitin sulphate in conditions of low and high hydration (Figure 6.5 overleaf). In this case, the low hydration state was a freeze-dried sample of C4S and for the high hydration state a sample of C4S was mixed with deionised water at a 50:50 ratio.

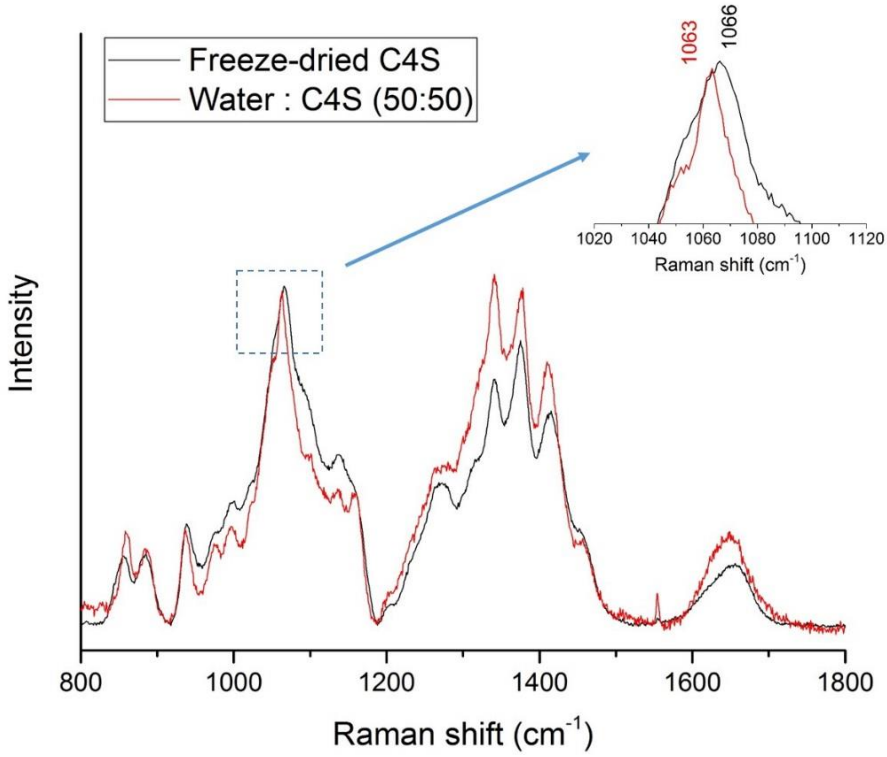

Figure 6.5 The Raman spectra of CS4 upon hydration (50 / 50 % water/ sample by weight) and freeze-dried C4S. Inset, changes in the sulphate peak, spectra obtained with 785 nm laser and 0.5 NA objective.

Inset to the right of the figure, the peak at 1063 cm^{-1} is enlarged. It shows that in the hydrated state, the sample exhibits a sulphate peak of lower frequency, which is also less broad than in the spectrum of the sample at low hydration. This result served to validate the same observation we observed for the sulphate peak in cartilage at high and low levels of hydration. We note that this result had not previously been reported by Bansil *et al.* (1978) and Ellis *et al.* (2009) who also studied CS and aggrecan at low and high levels of hydration; Bansil *et al.* (1978) did not discuss changes in the peak width and Ellis *et al.* (2009) did not mention any changes in the width of the sulphate peak. Therefore, we investigated the literature for Raman studies relating to similar vibrational modes in water. We did not find any studies on sulphate groups at varying hydration but we note that Moran *et al.* (1995)

observe a decrease in the full-width-to-half-maximum (FWHM) of the sulfonate ($-SO_3^-$) vibrations of bis(2-thylhexyl)sulfocuccinate. This was attributed to a reduction in the number of discrete environments of $-SO_3^-$ groups. That is to say that the majority of the population of SO_3^- groups are associated with water in the hydrated form, whereas they are associated with different chemical environments in the non-hydrated form. The former results in a band of lower width compared to the latter. The sulfonate groups differs to sulfate by replacement of an R group with an oxygen atom, meaning that in terms of their interactions with water – the properties would be expected to be similar. Therefore, following the same rationale of their study, we propose that the sulphate vibrational mode is sharper in the spectrum of hydrated C4S and hydrated articular cartilage, because there is a lower amount of discrete environments compared to the less hydrated samples of chondroitin sulphate and articular cartilage.

6.4 Discussion

The Raman spectrum of articular cartilage at high hydration was found to contain much greater amounts of water, as indicated by a greater intensity in the O-H stretching and bending modes of water in the spectrum of the hydrated sample. We focused on differences in the fingerprint region to infer structural changes in the tissue related to water.

In the fingerprint region of the spectra most of the changes could be associated with the hydrogen bonding of water molecules with the amide, carboxylate and sulphate molecules in articular cartilage. These represent the functional groups that are most polar and susceptible to hydrogen bonding with water.

The peak due to sulphate (1063 cm^{-1}) was shifted to higher frequency by 1 cm^{-1} for the hydrated sample and became more broad. This peak is due to the sulphate of the GAGs in

proteoglycan of articular cartilage. We compared the spectra of hydrated and dehydrated chondroitin-4-sulphate (the main sulphate containing GAG of proteoglycan in cartilage) and found the same result. This confirmed the result for the change observed in the articular cartilage in low and high hydration. We noted that a similar observation has been observed for the Raman peak of sulfonate, and that this broadening is caused by such functional groups being in a range of different environments in the dehydrated form, whereas the chemical environment is similar for the hydrated form – the population of groups is bound mainly to water. It is noteworthy to mention that peak broadening did not affect the intensity of the peak, which remained the same despite the change in width.

As for the interactions with the carboxylic acid groups, this is also indicated by a shift in the band at 1419 cm^{-1} ($\nu_s COO^-$ (Frushour and Koenig, 1975)) to lower frequency upon decreasing hydration. This is expected for COO^- groups which were expected to associate with water molecules in articular cartilage. This change was observed for collagen by Zhang *et al.* (Zhang, et al., 2011), indicating that the change in the spectrum is associated with mainly the collagen component of the sample. The broadening in this peak may even be associated with a similar occurrence of the carboxylic acids in the hydrated state occupying different environments. It is likely to be due to the amino acid side chains of aspartate and glutamate that undergo hydrogen bonding with water.

Other significant changes in the spectra were due to the interaction of water with the amide bonds of collagen in the sample. In the state of high hydration, the band at 1240 cm^{-1} (Amide III – N-H bend component) shifted to higher frequency, the band at 1665 cm^{-1} (Amide I – C=O stretch component) was observed to shift to lower frequency. These changes were all observed in the study of collagen by Zhang *et al.* (2011). They also showed a significant increase in intensity of the peak at 1377 cm^{-1} in the hydrated cartilage spectrum, that we

observe however they did not assign that peak in their work. Frushour *et al.* (1975) assign this peak to C-H bending. We note that in the literature this band has also been assigned to the amide II mode (Tu, 1982). Since C-H bending mode would not be expected to increase in intensity upon hydration, it is more likely that this peak is due to an amide II vibrational mode, we also found evidence in deuterium exchange studies of chapter 3 that point towards this assignment.

Finally, the increase in the peak at 940 cm^{-1} was the most significant marker of hydration. The increase in intensity of the band has been attributed to the hydrogen bonding between the in-plane N-C=O stretching mode, which is coupled to the (C-C) stretching mode of proline (Zhang, et al., 2011). As discussed in chapter 3 this mode may also result from C C-C of a helical polypeptides (Carrier and Pézolet, 1984), carboxylate of amino acid residues (Edsall, 1937), or NH_3 rocking (Riauba, et al., 2006). This result and that from the deuteration study point towards the presence of two bands in this region, but importantly, the band that is shifted by hydration here is also shifted upon deuteration. Thus any of the above assignments may fit these two circumstances.

The findings were consistent with those reported by Servaty *et al.* (Servaty, et al., 2001) in the analysis of CS and HA by IR spectroscopy, who observed changes in the carboxylate and sulphate vibrational modes, and also in the analysis of collagen previously where changes in amide modes were detected (Zhang, et al., 2011). The changes in the sulphate vibrational mode also indicate that the water interacts strongly and may even result in organising the sulphate vibrations into one type of discrete environment. We observed broadening of features of sulphate and carboxylate groups upon lower hydration, which are appear to result from changing the chemical environment upon reduction of hydrogen bonding environments with water.

Hydration of polar groups occurs when cartilage is exposed to water. When water is absent salt bridges form. Salt bridges cause bonds to weaken, resulting in the shift of peaks to lower frequency. This is not in agreement with what we observe for the Raman peak for sulphate. However, it is expected that hydration of sulphate groups would be significant. Since the loss of salt bridges and the hydration of sulphate groups occur concomitantly it would be difficult to ascertain which of these events contribute most significantly to the changes in the sulphate peak upon changes in hydration of the sample.

Another important consideration is the binding of cations by CS, it has been reported previously that calcium ions bind most strongly, potassium and sodium bind to some extent (Farber, et al., 1957). Polyanions such as CS are believed to form coils when bound to cations and this results in the polyanion forming a microvolume. The microvolume is considered to be a separate phase from the rest of the solution, and counterions are not believed to be bound to specific sites of the counterion but may be mobile. If this is the case it suggests that upon hydration the CS will be coiled and bound to cations whereas upon dehydration it is not coiled and is extended, meaning the different sulphate groups may be exposed to different micro-environments. This notion seems to fit with the results we obtained, since evidence suggests a restricted number of environments of the sulphate group in hydrated cartilage and a greater number in dehydrated cartilage.

Chapter 7 Conclusions and suggestions for future work

The first goal of this research was to characterise the main components of human articular cartilage tissue. We extracted the soluble (proteolgycan[f]) and insoluble (collagen[f]) components of the tissue, which consisted of mostly proteoglycans and collagen respectively. Since we know that most of the collagen in articular cartilage is collagen type II and most of the proteoglycan is aggrecan, we can suggest that the spectra of these are representative of these substances. Indeed, the Raman spectra of collagen reflect that of the spectrum of collagen type I previously reported (Frushour and Koenig, 1975). The spectrum of collagen type II resembles that of type I and this is expected because the amino acid composition is broadly similar (Leinonen, et al., 2004). The Raman spectrum of the proteoglycan fraction reflects that of aggrecan samples reported in the literature (Ellis, et al., 2009; Gamsjaeger, et al., 2014). We were able to confirm three Raman markers that were useful for detecting the proteoglycan (mainly aggrecan) component in articular cartilage. These markers were due to the sulphate stretching mode (1063 cm^{-1}), glycosidic bonds (940 cm^{-1}) and CH_3 bending mode (1377 cm^{-1}). Raman spectra of collagen type II and collagen type III were found to be similar, with some differences in the peaks present at 1098 cm^{-1} and 1123 cm^{-1}. The peaks have been attributed to glutamic acid and lysine but because of the similarity in the amounts of these amino acids in these types of collagens it cannot be certain that the difference in these peaks are due to those amino acids.

With the main components of the tissue characterised, we assigned peaks in the spectrum of articular cartilage more easily, and peaks could be attributed to either of the major components. Also, this enabled us to identify regions within tissue samples where content was greater in the articular cartilage tissue. This is of significant interest because of

its potential use as a diagnostic of the decrease in GAG content associated with osteoarthritis (Dudhia, et al., 2010). In this work, we used the Raman markers for proteoglycan as the basis of the Raman mapping study carried out in chapter 4. We systematically obtained Raman spectra along the depth (synovial surface to cartilage-bone interface). Micro-beam Raman mapping was carried out on tissue sections of two age groups, a specimen from a young donor (8 years) and a specimen from a mature donor (62 years). In agreement with our results, for the Raman markers of proteoglycan, and the known increase in proteoglycan content as a function of depth in articular cartilage (from cartilage surface to cartilage-bone interface), we observed an increase in the Raman markers of proteoglycan in spectra obtained along the depth. This confirmed our hypothesis that there are detectable changes in the tissue upon different positions in the cartilage tissue along the cross section from the synovial surface to the cartilage bone-interface.

We found an interesting observation when comparing the sulphate peak profile in the spectra obtained from the samples of the two ages. For the young specimen, the increase in intensity in the sulphate peak intensity was associated with an increase in the width in spectra obtained. Whereas the increase in intensity of the sulphate peak in the mature specimen was not associated with an increase in width. The reason for this could be due to a greater amount of C4S in the young specimen compared to the old specimen (Bayliss, et al., 1999). It is known that C4S exhibits a broad band at 1063 cm^{-1} whereas the same peak in the spectrum of C6S is sharper (Bansil, et al., 1978). Further studies would be interesting to compare the proteoglycan component extracted from a young specimen for comparison with that of the mature specimen reported in this thesis.

In terms of the depth-wise analysis of the Raman mapping data, we were also able to demonstrate that there were points along the depth, which showed significant variation in

the trend of increasing proteoglycan content. This was observed at certain positions in samples of both specimens and pointed towards localized regions of high sulphate content. We also revealed distinct zones of low and high sulphate content at the synovial surface (of approximately 400 μm in both cases) and cartilage bone-interface respectively. Although this was only certain for the young specimen scanned for which we had evidence of the section exhibiting a synovial surface and cartilage bone interface. The mature specimen showed signs of thinning and may not have contained a synovial surface. Nevertheless, we were able to delineate the depth of the synovial surface and the cartilage-bone interface regions with this technique. Also, in the mature category it would be important to carry out histology to reveal a synovial surface to enable comparison of samples along the depth from the two age groups. Finally, it would also be advantageous in this work to utilise an objective lens, which exhibits a low Raman signal (as for the studies performed with the 0.5 N.A objective). The limitation of these results are that we only used one sample from each different age group. Further studies would be necessary to confirm that these changes are indeed age-related and not due to sample variation.

In chapter 5 we applied Raman spectroscopy as a probe of freeze-dried articular cartilage and collagen[f] during heating. At 120°C, evidence for protonation of carboxylic acid became apparent in both samples, indicating a structural change. From the observation of this in cartilage and collagen[f] extracted from cartilage, it was clear that the structural change must occur in the collagen component of articular cartilage. We concluded that the appearance of a peak at 1788 cm^{-1} was due to vC=O of unionised bonded carboxylic acid, and its presence may indicate peptide bond hydrolysis or simply protonation of carboxylate residues in collagen. It was difficult from the limited spectral information to conclude on which of these events occurs.

In a quench recovery study we found that the appearance of the peak at 1788 cm^{-1} occurred at higher temperature, the reason for this appears to be due to the difference in the heating protocol. Results showed that a freeze-dried articular cartilage sample heated to 200°C exhibited evidence for protonation of carboxylate / peptide bond hydrolysis, and this is precisely the temperature range where Miles and Ghelashvili (1999) detected an irreversible structural change, which they associated to unfolding of collagen. In samples heated to the point that the peak at 1788 cm^{-1} is apparent, we also note a lower tendency to retain water. It is likely that the lack of water retention is the cause of the absence of the endothermic peak one samples were subsequently studied by DSC reported recently (Miles and Ghelashvili, 1999). Water in collagen samples has been proven to facilitate the onset of the endothermic changes in the samples of collagen (Miles and Bailey, 1999; Miles and Ghelashvili, 1999).

In future work it would be interesting to treat cartilage and collagen samples with proteolytic enzymes such as MMP to induce peptide bond dissociation. Then by obtaining Raman spectra of such samples we may be able to test the hypothesis that proteolytic degradation of collagen may be detectable by Raman spectroscopy.

The presence of water in freeze-dried articular cartilage was confirmed by IR spectroscopy and the process of water loss was monitored as a function of temperature by TGA/MS up until 300°C. This demonstrated also that upon further heating decarboxylation occurs. In chapter 6, articular cartilage (non freeze-dried) was assessed in a controlled environment of high hydration and then low hydration. Most of those features which change in the spectrum are due to the effect of hydrogen bonding with carboxylate and amide vibrational modes of collagen, as well as the sulphate content in proteoglycan of articular cartilage. At low hydration we also noted a broadening in the peak at 1063 cm^{-1} which is due

to -OSO_3H (1063 cm^{-1}). The assessment of chondroitin-4-sulphate, in a hydrated and less hydrated condition also confirmed the finding for the broadening in the sulphate peak upon dehydration in articular cartilage. This is due to the sulphate groups adopting different chemical environments when the water–sulphate interactions are decreased upon desorption of water from the sample. Furthermore, this work and the deuterium exchange study also described in chapter 3 enabled clarification of certain assignments that have been assigned to molecular vibrations in cartilage. These studies were complementary and revealed the possible presence of an amide II band or a NH twisting mode at 1380 cm^{-1}. These studies also revealed that further work to unambiguously assign the peak at 940 cm^{-1} should follow.

References

Altekar, W. (1977) Fluorescence of proteins in aqueous neutral salt-solutions 1. Influence of anions *Biopolymers*, **16**, 341-368.

Anigbogu, A.N.C., *et al.* (1995) Fourier-transform Raman spectroscopy of interaction between the penetration enhancer dimethyl-sulfoxide and human stratum-corneum *International Journal of Pharmaceutics*, **125**, 265-282.

Bachmann, L., Gomes, A.S. and Zezell, D.M. (2005) Collagen absorption bands in heated and rehydrated dentine, *Spectrochimica acta. Part A, Molecular and biomolecular spectroscopy*, **62**, 1045-1049.

Bansil, R., Yannas, I.V. and Stanley, H.E. (1978) Raman spectroscopy - structural probe of glycosaminoglycans, *Biochimica Et Biophysica Acta*, **541**, 535-542.

Barrett, T.W. and Peticolas, W.L. (1979) Laser Raman inelastic light-scattering investigations of hyaluornic acid primary and secondary structure *J. Raman Spectrosc.*, **8**, 35-38.

Barrett, T.W. and Peticolas, W.L. (1979) Laser Raman inelastic light-scattering investigations of hyaluronic-acid primary and secondary structure *J. Raman Spectrosc.*, **8**, 35-38.

Bayliss, M.T., *et al.* (1999) Sulfation of Chondroitin Sulfate in Human Articular Cartilage: The effect of age, topographical position, and zone of cartilage on tissue composition., *Journal of Biological Chemistry*, **274**, 15892-15900.

Bella, J., Brodsky, B. and Berman, H.M. (1995) Hydration structure of a collagen peptide *Structure*, **3**, 893-906.

Bellamy, L.J. (1958) *The infrared spectra of complex molecules*. Wiley, New York.

Bonnier, F., *et al.* (2012) Analysis of human skin tissue by Raman microspectroscopy: Dealing with the background, *Vibrational Spectroscopy*, **61**, 124-132.

Bonnier, F., *et al.* (2011) In vitroanalysis of immersed human tissues by Raman microspectroscopy, *J. Raman Spectrosc.*, **42**, 888-896.

Burjanadze, T.V. and Bezhitadze, M.O. (1992) Presence of thermostable domain in the helical part of the type-I collagen molecule and its role in the mechanism of triple helix folding *Biopolymers*, **32**, 951-956.

Cabassi, F., Casu, B. and Perlin, A.S. (1978) Infrared-absorbtion and Raman-scattering of sulfate groups of heparin and related glycosaminoglycans in aqueous- solution., *Carbohydr. Res.*, **63**, 1-11.

Camacho, N.P., *et al.* (2001) FTIR microscopic imaging of collagen and proteoglycan in bovine cartilage, *Biopolymers*, **62**, 1-8.

Carcamo, J.J., *et al.* (2012) Raman study of the shockwave effect on collagens, *Spectrochimica Acta Part a-Molecular and Biomolecular Spectroscopy*, **86**, 360-365.

Carrier, D. and Pézolet, M. (1984) Raman spectroscopic study of the interaction of poly-L-lysine with dipalmitoylphosphatidylglycerol bilayers, *Biophys. J.*, **46**, 497-506.

Chen, H. and Stimets, R.W. (2014) Fluorescence of trivalent neodymium in various materials excited by a 785 nm laser, *American Mineralogist*, **99**, 332-342.

Collado, J.A. and Ramírez, F.J. (1999) Infrared and Raman spectra of histamine-Nh4 and histamine-Nd4 monohydrochlorides, *J. Raman Spectrosc.*, **30**, 391-397.

D Li-Ven, N.C., WG Flateley (1991) *The handbook of infrared and Raman characteristic frequencies of organic molecules*. Academic Press Inc

Daimay Lin-Vien, N.B.C., William G. Fateley and Jeanette G. Grasselli (1991) The Handbook of Infrared and Raman Characteristic Frequencies of Organic Molecules In. Academic Press Inc, San Diego, pp. 155-178.

De Gelder, J., *et al.* (2007) Reference database of Raman spectra of biological molecules, *J. Raman Spectrosc.*, **38**, 1133-1147.

Dehring, K.A., *et al.* (2006) Correlating changes in collagen secondary structure with aging and defective type II collagen by Raman spectroscopy, *Applied Spectroscopy*, **60**, 366-372.

Dhamelincourt, P. (1979) Étude et réalisation d'une microsonde moléculaire à effet Raman quelques domaines d'application. University of Sciences of Lille, Lille.

Dong, R., *et al.* (2004) Temperature-dependent Raman spectra of collagen and DNA, *Spectrochimica Acta Part A: Molecular and Biomolecular Spectroscopy*, **60**, 557-561.

Donnan, F.G. (1924) The theory of membrane equilibria, *Chemical reviews*, **1**, 73-90.

Draper, E.R.C., Dudhia, J., Mcmillan, P.F., Firth, S. (2009) Tissue assessment. WO2009138738 A1.

Dudhia, J. (2005) Aggrecan, aging and assembly in articular cartilage, *Cellular and molecular life sciences : CMLS*, **62**, 2241-2256.

Dudhia, J., *et al.* (2010) Imaging early molecular alterations in articular cartilage degeneration by Raman spectroscopy: diagnostic applications, *International Journal of Experimental Pathology*, **91**, A32-A33.

E. Draper, J.D., S. Firth, P. McMillan (2009) *Tissue assessment*. WO2009138738 A1.

Edsall, J.T. (1937) Raman Spectra of amino acids and related compounds IV. Ionization of di- and tricarboxylic acids, *Journal of Chemical Physics*, **5**, 508-517.

Edsall, J.T. (1937) Raman spectra of amino acids and related substances III. Ionization and methylation of the amino group, *Journal of Chemical Physics*, **5**, 225-237.

Ellis, R., Green, E. and Winlove, C.P. (2009) Structural analysis of glycosaminoglycans and proteoglycans by means of Raman microspectrometry, *Connect Tissue Res*, **50**, 29-36.

Esmonde-White, K.A., *et al.* (2011) Fiber-optic Raman spectroscopy of joint tissues, *Analyst*, **136**, 1675-1685.

Esmonde-White, K.A., *et al.* (2011) Fiber-optic Raman spectroscopy of joint tissues, *Analyst*, **136**, 1675-1685.

Esmonde-White, K.A., *et al.* (2009) Raman spectroscopy of synovial fluid as a tool for diagnosing osteoarthritis, *J Biomed Opt*, **14**, 034013.

Eyre, D. (2002) Collagen of articular cartilage, *Arthritis Research*, **4**, 30-35.

Farber, S.J., Schubert, M. and Schuster, N. (1957) The binding of cations by chondroitin sulphate, *Journal of Clinical Investigation*, **36**, 1715-1722.

Finch, A. and Ledward, D.A. (1972) Shrinkage of collagen fibres - differential scanning calorimetric study *Biochimica Et Biophysica Acta*, **278**, 433-&.

Frushour, B.G. and Koenig, J.L. (1975) Raman-scattering of collagen, gelatin, and elastin, *Biopolymers*, **14**, 379-391.

Gamsjaeger, S., Klaushofer, K. and Paschalis, E.P. (2014) Raman analysis of proteoglycans simultaneously in bone and cartilage, *J. Raman Spectrosc.*, **45**, 794-800.

Garrett, R.R. and Flory, P.J. (1956) Evidence for a reversible 1st-order phase transition in collagen - diluent mixtures *Nature*, **177**, 176-177.

Ghadially (1983) *Fine structure of synovial joints. A text and atlas of the ultrasturcture of normal and pathological articular tissue*. Butterworths, London.

Haka, A.S., *et al.* (2005) Diagnosing breast cancer by using Raman spectroscopy, *Proc Natl Acad Sci U S A*, **102**, 12371-12376.

Hall, B.K. (2005) Bones and cartilage: developmental and evolutionary skeletal biology. In. Academic press, San Diego, pp. 13-32.

Hanlon, E.B., *et al.* (2000) Prospects for in vivo Raman spectroscopy, *Physics in medicine and biology*, **45**, R1-R59.

Hardingham, T.E., *et al.* (1986) Cartilage proteoglycans, *CIBA Found. Symp.*, **124**, 30-46.

Hascall, V.C. and Sajdera, S.W. (1970) Physical properties and polydispersity of proteoglycan from bovine nasal cartilage, *Journal of Biological Chemistry*, **245**, 4920-&.

Hattrem, M.N., *et al.* (2015) Interfacial and rheological properties of gelatin based solid emulsions prepared with acid or alkali pretreated gelatins, *Food Hydrocolloids*, **43**, 700-707.

Havel, H.A. (1995) Spectroscopic methods for determining protein structure in solution. In. Wiley, pp. 22-50.

Hayashi, T., Curranpatel, S. and Prockop, D.J. (1979) Thermal-stability of the triple helix of type-I procollagen - precautions for minimizing ultraviolet damage to proteins during circular dichroism studies *Biochemistry*, **18**, 4182-4187.

Hill, R.J. and Harper, E. (1984) Quantitation of type I and type III collagens in human tissue samples and cell culture by cyanogen bromide peptide analysis *Analytical biochemistry*, **141**, 83-93.

Hobart H. Willard, L.L.M., Jr., John A. Dean and Frank A. Settle (1988) *Instrumental methods of analysis* Litton Educational Publishing Inc. .

Howell, N.K. and Badii, F. (2004) Fish gelatin: Structure, gelling properties and interactions with other food proteins. In Williams, P.A. and Phillips, G.O. (eds), *Gums and Stabilizers for the Food Industry 12*. pp. 167-178.

Janko, M., *et al.* (2010) Anisotropic Raman scattering in collagen bundles, *Opt. Lett.*, **35**,

2765-2767.

Jeanloz, R.W. (1970) Mucopolysaccharides of higher animals. In Herp, A. (ed), *The carbohydrates*. Academic Press, London, pp. 590-619.

Ji, M., *et al.* (2013) Rapid, Label-Free Detection of Brain Tumors with Stimulated Raman Scattering Microscopy, *Science Translational Medicine*, **5**, 201ra119-201ra119.

Kacurakova, M. and Mathlouthi, M. (1996) FTIR and laser-Raman spectra of oligosaccharides in water: characterization of the glycosidic bond, *Carbohydr Res*, **284**, 145-157.

Kamemoto, L.E., *et al.* (2010) Near-Infrared Micro-Raman Spectroscopy for in Vitro Detection of Cervical Cancer, *Applied spectroscopy*, **64**, 255-261.

Kast, R., *et al.* (2014) Raman molecular imaging of brain frozen tissue sections, *J Neurooncol*, **120**, 55-62.

Kauzmann, W. (1959) Some factors in the interpretation of protein denaturation *Adv. Protein Chem.*, **14**, 1-63.

Keshwani, N., *et al.* (2013) The Role of Cross-Chain Ionic Interactions for the Stability of Collagen Model Peptides, *Biophys. J.*, **105**, 1681-1688.

Khanarian, N.T., *et al.* (2014) FTIR-I compositional mapping of the cartilage-to-bone interface as a function of tissue region and age, *Journal of bone and mineral research : the official journal of the American Society for Bone and Mineral Research*, **29**, 2643-2652.

Kiani, C., *et al.* (2002) Structure and function of aggrecan, *Cell Res*, **12**, 19-32.

Kimura, L.S.L.a.J.H. (1986) Biosynthesis of cartilage proteolgycan In Klaus E. Kuettner, R.S.a.V.C.H. (ed), *Articular cartilage biochemistry*. Raven press, New York.

Kincaid, S.A. and Vansickle, D.C. (1981) Regional histochemical and thickness variations of adult canine articular cartilage, *American Journal of Veterinary Research*, **42**, 428-432.

Kiraly, K., *et al.* (1996) Application of selected cationic dyes for the semiquantitative estimation of glycosaminoglycans in histological sections of articular cartilage by microspectrophotometry, *Histochemical Journal*, **28**, 577-590.

Klimm, K. and Botcharnikov, R.E. (2010) The determination of sulfate and sulfide species in hydrous silicate glasses using Raman spectroscopy, *American Mineralogist*, **95**, 1574-1579.

Kopp, J., Bonnet, M. and Renou, J.P. (1989) Effect of collagen crosslinking on collagen water interactions a DSC investigation, *Matrix*, **9**, 443-450.

Leikin, S., *et al.* (1997) Raman spectral evidence for hydration forces between collagen triple helices, *Proceedings of the National Academy of Sciences of the United States of America*, **94**, 11312-11317.

Leinonen, R., *et al.* (2004) UniProt archive, *Bioinformatics*, **20**, 3236-3237.

Li, J. and Brill, T.B. (2003) Decarboxylation Mechanism of Amino Acids by Density Functional Theory, *The Journal of Physical Chemistry A*, **107**, 5993-5997.

Lozano, L.F., *et al.* (2003) Thermal analysis study of human bone, *Journal of Materials Science*, **38**, 4777-4782.

Mankin, H.J. and Thrasher, A.Z. (1975) Water content and binding in normal and osteoarthritic human cartilage *Journal of Bone and Joint Surgery-American Volume*, **A 57**, 76-80.

Manning, H.B., *et al.* (2013) Detection of cartilage matrix degradation by autofluorescence lifetime, *Matrix Biology*, **32**, 32-38.

Matousek, P., *et al.* (1999) Efficient rejection of fluorescence from Raman spectra using picosecond Kerr gating, *Applied Spectroscopy*, **53**, 1485-1489.

McMillan, P.F., *et al.* (1983) A note on the Raman spectra of water-bearing albite glasses, *Geochimica et Cosmochimica Acta*, **47**, 1937-1943.

Miles, C.A., *et al.* (2005) The increase in denaturation temperature following cross-linking of collagen is caused by dehydration of the fibres, *J Mol Biol*, **346**, 551-556.

Miles, C.A. and Bailey, A.J. (1999) Thermal denaturation of collagen revisited, *Proceedings of the Indian Academy of Sciences-Chemical Sciences*, **111**, 71-80.

Miles, C.A. and Bailey, A.J. (2001) Thermally labile domains in the collagen molecule, *Micron*, **32**, 325-332.

Miles, C.A., Burjanadze, T.V. and Bailey, A.J. (1995) The kinetics of the thermal denaturation of collagen in unrestrained rat tail tendon determined by differential scanning calorimetry, *Journal of Molecular Biology*, **245**, 437-446.

Miles, C.A. and Ghelashvili, M. (1999) Polymer-in-a-box mechanism for the thermal stabilization of collagen molecules in fibers, *Biophys. J.*, **76**, 3243-3252.

Miller, E.J. (1976) Biochemical characteristics and biological significance of genetically-distinct collagens *Molecular and Cellular Biochemistry*, **13**, 165-192.

Miyazawa, T., Shimanouchi, T. and Mizushima, S.I. (1958) Normal vibrations of N-methylacetamide, *Journal of Chemical Physics*, **29**, 611-616.

Moger, C.J., *et al.* (2007) Regional variations of collagen orientation in normal and diseased articular cartilage and subchondral bone determined using small angle X-ray scattering (SAXS), *Osteoarthritis and cartilage / OARS, Osteoarthritis Research Society*, **15**, 682-687.

Mononen, M.E., *et al.* (2011) Alterations in structure and properties of collagen network of osteoarthritic and repaired cartilage modify knee joint stresses, *Biomechanics and modeling in mechanobiology*, **10**, 357-369.

Moran, P.D., *et al.* (1995) Vibrational spectroscopic study of the structure of sodium bis(2-ethylhexyl)sulfosuccinate reverse micelles and water-in-oil microemulsions *Langmuir*, **11**, 738-743.

Morris, P.M.a.M.D. (2010) *Emerging Raman applications and techniques in Biomedical an Pharmaceutical fields*. Springer, London.

Mow, V.C., Holmes, M.H. and Lai, W.M. (1984) Fluid transport and mechanical- properties of articular cartilage - a review, *J. Biomech.*, **17**, 377-394.

Mow, V.C., Ratcliffe, A. and Poole, A.R. (1992) Cartilage and diarthrodial joints as paradigms for hierarchical materials and structures, *Biomaterials*, **13**, 67-97.

Mueller, C., *et al.* (2014) Quantitative proteomics at different depths in human articular cartilage reveals unique patterns of protein distribution, *Matrix Biology*, **40**, 34-45.

Muir, H., Bullough, P. and Maroudas, A. (1970) The distribution of collagen in human articular cartilage with some of its physiological implications, *The Journal of bone and joint surgery. British volume*, **52**, 554-563.

Nguyen, T.T., *et al.* (2012) Characterization of Type I and IV Collagens by Raman Microspectroscopy: Identification of Spectral Markers of the Dermo-Epidermal Junction, *Spectroscopy: An International Journal*, **27**, 7.

Nomura, S., *et al.* (1977) Interaction of water with native collagen, *Biopolymers*, **16**, 231-246.

Nunn, A.D.G., *et al.* (2013) Intra-operative mapping of articular cartilage degeneration with Raman arthrospectroscopy, *International Journal of Experimental Pathology*, **94**, A19-A20.

Olbert-Majkut, A., *et al.* (2011) Raman spectroscopy of acetic acid monomer and dimers isolated in solid argon, *J. Raman Spectrosc.*, **42**, 1670-1681.

Pielesz, A. (2014) Temperature-dependent FTIR spectra of collagen and protective effect of partially hydrolysed fucoidan, *Spectrochimica acta. Part A, Molecular and biomolecular spectroscopy*, **118**, 287-293.

Pielesz, A. and Weselucha-Birczynska, A. (2000) The identification of structural changes in the keratin of wool fibre dyed with an azo dye using the Raman and Fourier transform infrared spectroscopy methods, *J. Mol. Struct.*, **555**, 325-334.

Polomska, M., *et al.* (2010) Fourier Transform Near Infrared Raman Spectroscopy in Studies on Connective Tissue, *Acta Physica Polonica A*, **118**, 136-140.

Poole, C.A., Ayad, S. and Schofield, J.R. (1988) Chondrons from articular cartilage 1. Immunolocalization of type VI collagen in the pericellular capsule of isolated canine tibial chondrons, *Journal of Cell Science*, **90**, 635-643.

Poole, C.A., Flint, M.H. and Beaumont, B.W. (1987) Chondrons in cartilage - ultrastructural analysis of the pericellular microenvironment in adult human articular cartilage *Journal of Orthopaedic Research*, **5**, 509-522.

Privalov, P.L. and Dragan, A.I. (2007) Microcalorimetry of biological macromolecules, *Biophysical chemistry*, **126**, 16-24.

Privalov, P.L. and Tiktopul.Ei (1970) Thermal conformational transformation of tropocollagen. 1. calorimetric study, *Biopolymers*, **9**, 127-&.

Privalov, P.L., Tiktopulo, E.I. and Tischenko, V.M. (1979) Stability and mobility of the collagen structure, *Journal of Molecular Biology*, **127**, 203-216.

Qian, Y.R., *et al.* (1993) Kinetics of peptide hydrolysis and amino-acid decomposition at high-temperature *Geochimica Et Cosmochimica Acta*, **57**, 3281-3293.

Redler, I., *et al.* (1975) Ultrastructure and biomechanical significance of tidemark of articular-cartilage, *Clin. Orthop. Rel. Res.*, 357-362.

Remmele, R.L., McMillan, P. and Bieber, A. (1990) Raman-spectroscopic studies of hen egg-white lysozyme at high-temperatures and pressures, *J. Protein Chem.*, **9**, 475-486.

Riauba, L., *et al.* (2006) A Study of Cysteamine Ionization in Solution by Raman Spectroscopy and Theoretical Modeling, *The Journal of Physical Chemistry A*, **110**, 13394-13404.

Roden, L.B., J.R., Cifonelli, J.A. and Mathews, M.B. (1972) Methods of Enzymology In Ginsberg, V. (ed). Academic Press, New York pp. 73-140.

Roughley, P.J. (2006) The structure and function of cartilage proteoglycans, *European Cells & Materials*, **12**, 92-101.

Schrader, B. (2007) *Infrared and Raman spectroscopy: methods and Applications*. Wiley, Weinheim.

Servaty, R., *et al.* (2001) Hydration of polymeric components of cartilage - an infrared spectroscopic study on hyaluronic acid and chondroitin sulfate, *International Journal of Biological Macromolecules*, **28**, 121-127.

Shurvell, H.F. and Bergin, F.J. (1989) Raman spectra of L(+)-glutamic acid and related compounds, *J. Raman Spectrosc.*, **20**, 163-168.

Socrates, G. (2001) *Infra red and Raman group frequencies*. John Wiley and sons, Chichester.

Sohar, G., *et al.* (2007) New thermogravimetric protocol for the investigation of normal and damaged human hyaline cartilage, *J. Therm. Anal. Calorim.*, **89**, 853-856.

Trebacz, H. and Wojtowicz, K. (2005) Thermal stabilization of collagen molecules in bone tissue, *International Journal of Biological Macromolecules*, **37**, 257-262.

Tu, A.T. (1982) Raman Spectroscopy in Biology: Principles and applications. In. Wiley, pp. 80 - 90.

Ushiki, T. (2002) Collagen Fibers, Reticular Fibers and Elastic Fibers. A Comprehensive Understanding from a Morphological Viewpoint, *Archives of Histology and Cytology*, **65**, 109-126.

Vanderrest, M. and Garrone, R. (1991) Collagen family of proteins, *Faseb J.*, **5**, 2814-2823.

Venyaminov, S.Y. and Prendergast, F.G. (1997) Water (H2O and D2O) molar absorptivity in the 1000-4000 cm(-1) range and quantitative infrared spectroscopy of aqueous solutions, *Analytical biochemistry*, **248**, 234-245.

Verzijl, N., *et al.* (2002) Crosslinking by advanced glycation end products increases the stiffness of the collagen network in human articular cartilage: a possible mechanism through which age is a risk factor for osteoarthritis, *Arthritis and rheumatism*, **46**, 114-123.

Vogel, K.G. and Heinegard, D. (1985) Characterization of proteoglycans from adult bovine tendon *Journal of Biological Chemistry*, **260**, 9298-9306.

Wagnieres, G.A., Star, W.M. and Wilson, B.C. (1998) In vivo fluorescence spectroscopy and imaging for oncological applications, *Photochemistry and Photobiology*, **68**, 603-632.

Walrafen, G.E. (1964) Raman spectral studies of water structure *Journal of Chemical Physics*, **40**, 3249-&.

Walrafen, G.E. and Chu, Y.C. (1995) Linearity between structural correlation length and

correlated proton Raman intensity from amorphous ice and supercooled water up to dense supercritical steam, *J. Phys. Chem.*, **99**, 11225-11229.

Wells, T., *et al.* (2003) Age-related changes in the composition, the molecular stoichiometry and the stability of proteoglycan aggregates extracted from human articular cartilage, *Biochem. J.*, **370**, 69-79.

Williams, R.W., Dunker, A.K. and Peticolas, W.L. (1984) Raman spectroscopy and deuterium-exchange of the filamentous phage FD, *Biochimica Et Biophysica Acta*, **791**, 131-144.

Zhang, Q., *et al.* (2011) Raman microspectroscopic and dynamic vapor sorption characterization of hydration in collagen and dermal tissue, *Biopolymers*, **95**, 607-615.